Novel Functions of the Flippase Drs2 and the Coat Protein COPI in Protein Trafficking

By

Hannah Marcille Hankins

Dissertation

Submitted to the Faculty of the

Graduate School of Vanderbilt University

in partial fulfillment of the requirements

for the degree of

DOCTOR OF PHILOSOPHY

in

Biological Sciences

May, 2016

Nashville, Tennessee

Approved:

Todd R. Graham, Ph.D

Katherine L. Friedman, Ph.D.

Kendal S. Broadie, Ph.D.

Anne K. Kenworthy, Ph.D.

Charles R. Sanders, Ph.D.

ACKNOWLEDGEMENTS

It takes a village to raise a graduate student, and I have many villagers to thank for getting me to this point. I would never have considered doing research if it were not for my professors at Henderson State University, particularly Martin Campbell and Troy Bray, who were very supportive and encouraging throughout my undergraduate studies. I was also fortunate to be able to do full time research during the summers of my sophomore and junior years in the lab of Kevin Raney at the University of Arkansas for Medical Sciences. If it were not for the support system and these wonderful research experiences I had as an undergraduate, I never would have pursued graduate school at Vanderbilt and would not be the scientist I am today.

I would like to thank my graduate school mentor, Todd Graham, for giving me the opportunity to join his lab and for introducing me to the wonderful world of yeast. Todd is an amazing and enthusiastic scientist; his guidance and support throughout my graduate career has been invaluable and I am truly grateful to have such a wonderful mentor. I must also thank Todd for his "constructive" criticism of my wine bottle opening technique (or lack thereof) during my short-lived career as a bartender during the Southeastern Regional Yeast Meeting. I like to think that under Todd's mentorship I have grown both as a scientist and as a normal adult capable of opening bottles of wine.

I thank my committee members Chuck Sanders, Kendal Broadie, Anne Kenworthy, and my chair Kathy Friedman for all of their helpful input and guidance over the years. Kathy is also my lab neighbor and yeast comrade, and I must also thank her for sharing countless reagents and incubator space over the years. My research would not have been possible without my wonderful collaborators Anant Menon and Yves Sere at Cornell University and Howard and Isabelle Riezman at the University of Geneva. I also thank Puck Ohi and Jason MacGurn for generously allowing me to use their microscopes. The people at the BRET office, especially Ashley Brady, have also been an invaluable resource for my career development.

I must also thank all of my labmates for their support and friendship over the years. To my baymate Mehmet Takar, your humor defies all logic and reason, but it is amazing and I hope you never change. Thank you for putting up with me all these years even though I'm a blue-eyed devil and can't be trusted. Peng Xu, thank you for all your help and advice over the years and, most importantly, always reminding us of the two most important phrases in science: "it is what it is" and "let it go." Bart Roland, thanks for being a good friend to me, despite my constant criticism of your "unique" color choices at lab meetings. To the newest member of the Graham lab, Jordan Best, thank you for bringing humor and what I hesitate to call fashion to the lab. I would also like to acknowledge all of the talented visiting students, Lisa Theorin, Susanne Prokop, and Cayetana Arnaiz, and undergraduates, Katie Ivy, Christina Snider, Deanna Tiek, Nick Diab, and Sam Erlinger, we have had come through the lab during my time here.

Funding from the National Institutes of Health supported all of my dissertation research. Funding from the Vanderbilt Graduate School and the Gisela Mosig Travel Fund allowed me to present my research at national conferences in Birmingham and Philadelphia as well as an international conference in Corsica. In particular, the trip to Corsica was my first time traveling abroad (alone, no less!) and it was truly an unforgettable experience with great people and great science.

I am truly fortunate to have a great group of friends in the graduate program. In no particular order, I would like to thank Arwen, Alex, Ushashi, Abigail, Sophia, Jen, Amy, Lehanna, Adrian, Nathan, Joel, Patrick, and Andrew for their friendship over the years. I can't imagine what my graduate school experience would have been like without all of you in it. To my parents, Jim and Gloria, thank you for the support throughout my graduate studies despite you not really knowing what it is I do here and probably wondering why I am just now finishing up college in my 9^{th} year. To my older brothers, Caleb and Noah, thank you for being so wonderful and always so supportive of everything I do. My childhood would not have been nearly as fun without the two of you.

Finally, to my boyfriend, Rubin Baskir, thank you for the unending love and support. You and your family have been a huge part of my life these past three years and I look forward to the years to come.

TABLE OF CONTENTS

LIST OF TABLES

LIST OF FIGURES

LIST OF ABBREVIATIONS

ALP	Alkaline phosphatase
AP	Adaptor protein
COPI	Coat protein complex I
CME	Clathrin-mediated endocytosis
CPY	Carboxypeptidase Y
DHE	Dehydroergosterol
EE	Early endosome
ER	Endoplasmic reticulum
GAP	GTPase-activating protein
GC	Gas chromatography
GEF	Guanine nucleotide exchange factor
GGA	Golgi-localized, gamma-ear-containing, Arf-binding family of proteins
IPC	Inositol-phosphorylceramide
Lat-A	Latrunculin A
LE	Late endosome
MCC	Membrane compartment of Can1
MCP	Membrane compartment of Pma1
MCS	Membrane contact site
MIPC	Mannose-inositol-phosphorylceramide
$M(IP)_2C$	Mannose-(inositol-P)2-ceramide
MS	Mass spectrometry
MVB	Multivesicular body
NBD	7-nitro-2-1,3-benzoxadiazol-4-yl
OSBP	Oxysterol-binding protein
P4-ATPase	Type IV P-type ATPase
PC	Phosphatidylcholine
PCR	Polymerase chain reaction
PE	Phosphatidylethanolamine
PI	Phosphatidylinositol
PI4P	Phosphatidylinositol 4-phosphate
PM	Plasma membrane
PS	Phosphatidylserine
TGN	*trans*-Golgi Network
TM	Transmembrane domain
WT	Wild-type

Chapter I

Introduction*

Overview

Within a eukaryotic cell is a steady stream of vesicles budding from and fusing to different membranes to generate distinct organelles. The formation and movement of these vesicles is a complicated and interconnected process orchestrated by many proteins. Many components of the trafficking machinery have been identified, but there remains much to be elucidated as new proteins and new functions for known proteins are continuously identified. The goal of my dissertation research has been to identify novel roles of two proteins involved in protein trafficking: the flippase Drs2 and the protein coat COPI. The first protein, Drs2, is known to support a variety of coat-dependent trafficking pathways stemming from the *trans*-Golgi network (TGN) and early endosomes. I have determined that Drs2 also has a novel role in coat-independent, domain-mediated protein sorting into exocytic vesicles at the TGN. The primary function of Drs2 in this trafficking pathway appears to be to control the activity of the oxysterol binding protein homologue Kes1/Osh4 to regulate ergosterol homeostasis at the TGN. The second protein, COPI, is known to support retrograde trafficking from the Golgi. However, a small subset of COPI has long been known to localize to early endosomes, but no clear function has been attributed to early endosome-associated COPI. Described in this work is a novel function of COPI in ubiquitin-dependent protein trafficking from early endosomes to the TGN.

*Portions of this chapter have been published as **Hankins, H. M.**, Baldridge, R. D., Xu, P., and Graham, T. R. (2015). Role of flippases, scramblases and transfer proteins in phosphatidylserine subcellular distribution. Traffic *16*, 35–47.

Vesicle-mediated protein transport in *Saccharomyces cerevisiae*

The budding yeast *Saccharomyces cerevisiae* is one of the most extensively studied eukaryotic model systems. The popularity of budding yeast to a great extent stems from its short generation time, ease of genetic manipulation, and its title as the first eukaryote to have a fully sequenced genome. Importantly for this work, many aspects of budding yeast intracellular membrane organization and trafficking pathways are conserved in higher eukaryotes. In fact, much of what is known about the secretory pathway is based on Randy Schekman's isolation of yeast secretory (*sec*) mutants in the 1980s (Novick *et al.*, 1981; Schekman, 2002). For this work, Randy Schekman was awarded the 2013 Nobel Prize in Physiology and Medicine, which he shared with James Rothman and Thomas Südhof, for discoveries of machinery regulating vesicular trafficking. In this section, I provide a brief overview of yeast trafficking pathways beginning with the endoplasmic reticulum (ER), then moving on to the trafficking pathways between the Golgi and the endosomal/vacuolar system, and finishing with trafficking to and from the plasma membrane (Figure 1-1).

Transport between the Endoplasmic Reticulum and the Golgi

The ER serves as the entry point for newly synthesized proteins to enter into the secretory system. These proteins are first translated on the cytosolic surface of the rough ER and are translocated into the ER lumen or inserted into the ER membrane. Vesicle-mediated protein transport between the ER and the Golgi is bidirectional and mediated through mechanisms conserved from yeast to humans. Both involve a protein coat that forms on the donor membrane, selectively incorporates cargo proteins, and then tethers to and fuses with the target organelle, thereby releasing the cargo at the new location (Feyder *et al.*, 2015). The protein coats involved in bidirectional transport between the ER and the Golgi are coat protein complex I (COPI) and II (COPII).

ER to Golgi transport is mediated by the COPII coat, which consists of 5 highly conserved subunits: Sar1, Sec23, Sec24, Sec13, and Sec31 (Barlowe and Miller, 2013). Coat assembly starts when the Sar1 GTPase is activated by the nucleotide exchange factor Sec12. Sar1-GTP then triggers the assembly of

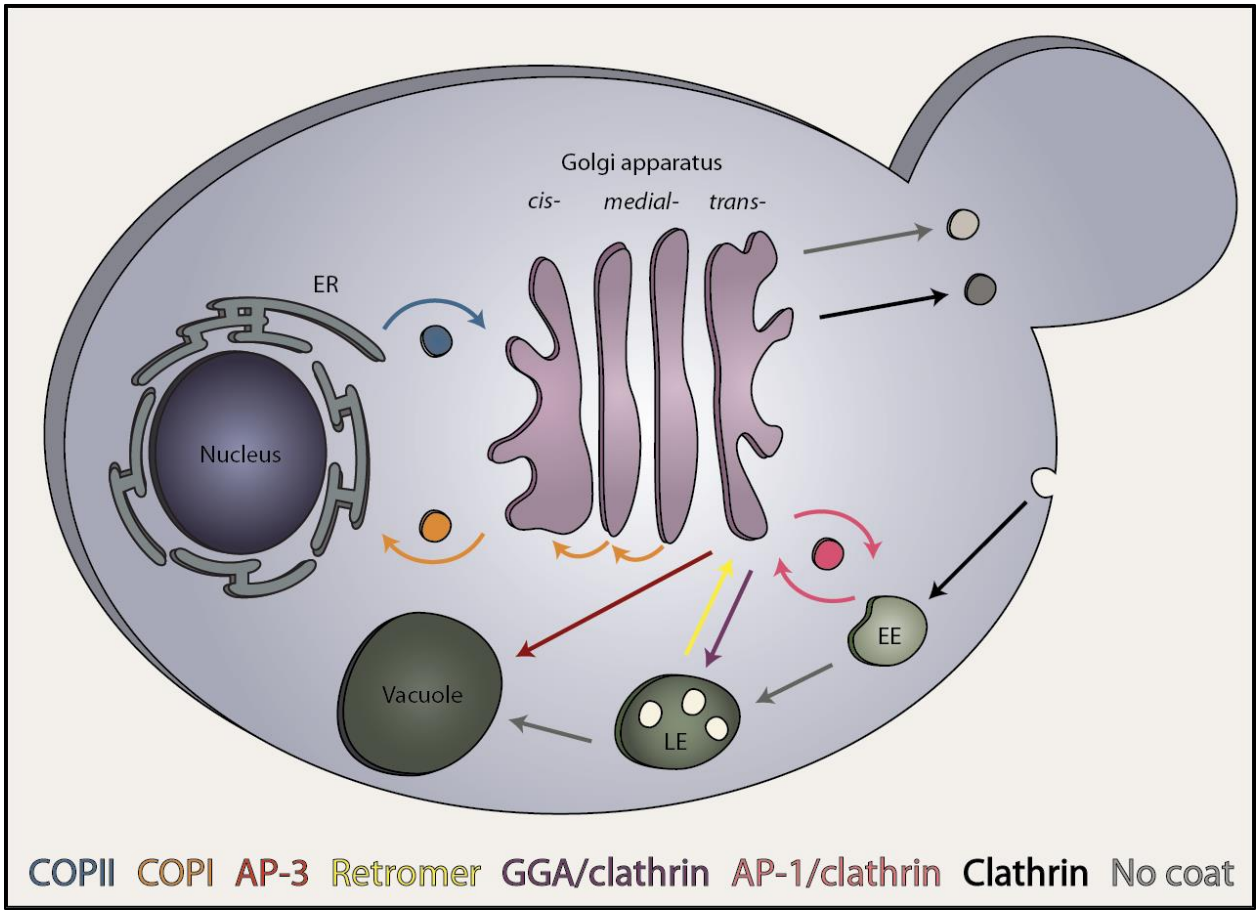

Figure 1-1. Trafficking pathways in *S. cerevisiae* and their associated coat proteins.

the Sec23/24-Sar1 prebudding complex, which recognizes and concentrates cargoes bearing sorting signals (Feyder *et al.*, 2015). The final step of assembly is the recruitment of the outer coat components Sec13/31, which induce coat polymerization and membrane bending to generate the COPII-coated vesicles. COPII vesicles then travel to the Golgi, where cargos are sorted and delivered to different cellular destinations.

In contrast to COPII, COPI mediates retrograde protein trafficking from the Golgi to the ER and also intra-Golgi transport from the *trans*- or *medial*-Golgi to the *cis*-Golgi (Hsu *et al.*, 2009; Popoff *et al.*, 2011). The COPI coat is a heptameric protein complex comprised of an adaptor-like F-subcomplex (β, γ, δ, and ζ) and a clathrin-like B-subcomplex (α, β', and ε) that are proposed to form the inner and outer layers of the COPI coat, respectively (Jackson, 2014). Assembly begins when the soluble small

GTPase Arf1 is activated by Gea1/2 (Peyroche *et al.*, 1996). Upon activation, Arf1-GTP undergoes a conformational change that exposes a myristoylated N-terminus and a short N-terminal amphipathic helix that target Arf1 to the membrane (Liu *et al.*, 2009). Membrane-associated Arf1 then recruits the heptameric COPI coat components, which directly interact with Arf1-GTP and cargo proteins. COPI recognizes retrieval signals in the form of C-terminal dilysine motifs and selectively incorporates the proteins into COPI-coated vesicles for retrograde (Jackson, 2014). Examples of COPI cargo proteins and their dilysine sorting motifs include Emp47 (KxKxx) and Erd2 (KKxSxxx) (Jackson *et al.*, 1990, 1993, 2012; Letourneur *et al.*, 1994a; Eugster *et al.*, 2004).

Transport to the vacuole

Newly synthesized proteins destined for the vacuole (the yeast lysosome) are trafficked by one of two pathways: the carboxypeptidase Y (CPY)/GGA pathway or the alkaline phosphatase (ALP)/AP-3 pathway. The CPY and ALP pathways deliver cargo proteins to the vacuole by an indirect (Golgi → endosome → vacuole) or direct (Golgi → vacuole) route, respectively (Feyder *et al.*, 2015). The majority of proteins targeted to the vacuole follow the CPY pathway. Protein sorting is mediated through cargo interactions with Golgi-localized, gamma-ear-containing, Arf-binding (GGA) adaptor proteins (Gga1 and Gga2), which are monomeric and act redundantly (Bonifacino, 2004). At the Golgi, Gga1/2 interacts with Arf1, clathrin, and cargo proteins to bud vesicles. Cargos include both soluble (e.g. CPY pro-protease) and membrane-bound (e.g. carboxypeptidase S) vacuolar proteins as well as ubiquitinated proteins targeted for degradation (Scott *et al.*, 2004; Feyder *et al.*, 2015). Cargo proteins traveling via the CPY pathway first bud from the Golgi and are then sorted into a multivesicular body (MVB) endosomal intermediate en route to the vacuole.

Vacuolar cargo proteins traveling via the ALP pathway are packaged into vesicles through interactions with the AP-3 adaptor protein complex (Odorizzi *et al.*, 1998b; Pokrzywa *et al.*, 2009). AP-3 is composed of four subunits: Apl5, Apl6, Apm3, and Aps3 (Panek *et al.*, 1997; Odorizzi *et al.*, 1998b). Unlike the CPY pathway, the ALP pathway appears to function in a clathrin-independent manner (Anand *et al.*,

2009). AP-3 recognizes and sorts proteins containing acidic dileucine sorting motifs into Golgi-derived vesicles that traffic to the vacuole without an endosomal intermediate (Darsow *et al.*, 1998). Deletion of any AP-3 subunit results in the mislocalization of ALP and the vacuolar t-SNARE Vam3, but not CPY (Cowles *et al.*, 1997), consistent with the ALP pathway delivering a distinct set of proteins to the vacuole.

Endocytosis

Clathrin-mediated endocytosis (CME) is the major pathway for the internalization of plasma membrane proteins and extracellular materials. Clathrin has long been known to be involved in endocytosis in mammalian cells; however, the role of clathrin in yeast endocytosis has been controversial until relatively recently (Kaksonen *et al.*, 2005, 2006; Newpher *et al.*, 2005; Goode *et al.*, 2015). In yeast, CME is orchestrated by over 50 proteins that assemble at a single site on the plasma membrane in a tightly regulated sequence of recruitment, assembly, and disassembly.

During the process of coat assembly, endocytic adaptor proteins recognize cytosolic sorting signals, such as ubiquitin, on cargo proteins and link the proteins directly to clathrin (Galan and Haguenauer-Tsapis, 1997; Shih *et al.*, 2000; Haglund *et al.*, 2003; Goode *et al.*, 2015). After the early, middle, and late coat proteins are recruited, actin assembly generates the membrane-bending force required for vesicle scission and internalization (Kaksonen *et al.*, 2006). The coat then disassembles and the internalized vesicle fuses with an endosome, where the cargo proteins can then be either recycled back to the plasma membrane or sent to the vacuole for degradation (Goode *et al.*, 2015).

Unlike the yeast AP-1 and AP-3 complexes, which are closely related to and function similarly as their mammalian counterparts, AP-2 is distantly related to mammalian AP-2 (Cowles *et al.*, 1997; Panek *et al.*, 1997; Boehm and Bonifacino, 2002). Mammalian AP-2 interacts with clathrin and is involved in clathrin-mediated endocytosis (Kirchhausen, 1999); in contrast, yeast AP-2 does not appear to bind clathrin and deletion of yeast AP-2 subunits causes no discernible defect in endocytosis (Yeung *et al.*, 1999) except for being required for the internalization of the yeast KS8 “killer” toxin (Carroll *et al.*, 2009).

Recycling pathway

Proteins that are endocytosed enter into the endosomal system where they are either sent to the vacuole for degradation or they are recycled to the TGN (Goode *et al.*, 2015). Retrieved cargos include resident Golgi proteins, plasma membrane receptors, and components of the exocytic trafficking machinery. The best studied cargo of the recycling pathway is the exocytic v-SNARE Snc1, which mediates vesicle fusion at the plasma membrane (Lewis *et al.*, 2000). The v-SNARE Snc1 continuously transits between the TGN, the bud plasma membrane, early endosomes, and back to the TGN. The steady state localization of GFP-Snc1 is primarily at the bud plasma membrane because endocytosis is the rate limiting step of the cycle (Lewis *et al.*, 2000).

Although many of the specifics remain to be elucidated, a variety of proteins involved in distinct retrieval pathways have been identified, including retromer, sorting nexins (Snx4/41/42), AP-1 (which is also involved in TGN to early endosome trafficking), and the F-box protein Rcy1 (Wiederkehr *et al.*, 2000; Hettema *et al.*, 2003; Balderhaar *et al.*, 2010). Retromer and sorting nexins function independently at late endosomes, but only sorting nexins are involved in Snc1 retrieval (Hettema *et al.*, 2003; Balderhaar *et al.*, 2010). Rcy1 functions at early endosomes and appears to be the primary retrieval pathway for Snc1, whereas sorting nexins function at late endosomes and act as a backup retrieval pathway for Snc1 that escaped detection.

This introduction will focus primarily on the Rcy1 pathway as it is the recycling pathway studied in Chapter II. In the absence of Rcy1, GFP-Snc1 accumulates in endosomal structures instead of the plasma membrane (Chen *et al.*, 2005). Rcy1 has been shown to form a Skp1-cullin-F-box (SCF-Rcy1) complex and there is evidence that the v-SNARE Snc1 is ubiquitinated in a Rcy1-dependent manner (Chen *et al.*, 2005, 2011). This addition of ubiquitin is thought to act as a sorting signal for retrieval of Snc1 from the early endosomes to the TGN to restart the cycle. However, there is some debate over whether the SCF-Rcy1 complex is a functional ubiquitin ligase complex (Galan *et al.*, 2001). It is also controversial

because ubiquitin is largely thought to target proteins through the MVB pathway to the vacuole, rather than recycle proteins to the TGN.

A second controversial protein in the recycling pathway is COPI. As mentioned earlier, COPI is best known for its role in retrograde trafficking from the Golgi to the ER. However, a pool of COPI has been shown to localize to early endosomes in mammalian cells (Whitney *et al.*, 1995; Aniento *et al.*, 1996; Daro *et al.*, 1997; Gu *et al.*, 1997). COPI mutants have been previously shown to disrupt Snc1 recycling; however, from these studies it was not clear if this effect is specific to loss of endosome-associated COPI or if the recycling defect is a consequence of disrupting upstream trafficking events between the Golgi and ER (Lewis *et al.*, 2000). The involvement of Snc1 ubiquitination and COPI in the recycling pathway will be discussed in more detail in Chapter IV.

Exocytosis

Exocytosis is the vesicle-mediated process in which proteins are transported from the TGN to the plasma membrane. Although the yeast plasma membrane is not divided into distinct apical and basolateral surfaces, the yeast exocytic pathway is similar to that of highly polarized epithelial cells (Klemm *et al.*, 2009). One exocytic pathway associates with a protein coat and may require an endosomal intermediate, while the other exocytic pathway appears to be "lipid raft"-dependent and is a direct route from the TGN to the plasma membrane (Surma *et al.*, 2012). In yeast, the two distinct classes of exocytic vesicles are known as dense and light vesicles (Harsay and Bretscher, 1995).

Dense vesicles (also known as high density secretory vesicles) appear to be clathrin- and endosome-dependent as deletion of clathrin heavy chain (*CHC1*) or proteins involved in Golgi to prevacuolar endosome transport (*VPS1, VPS4, PEP12*) blocks formation of dense vesicles (Gurunathan *et al.*, 2002; Harsay and Schekman, 2002). Dense vesicles primarily transport soluble secreted enzymes, such as invertase and acid phosphatase (Harsay and Bretscher, 1995); however, when dense vesicle formation is prevented, all secreted cargoes travel to the plasma membrane through rerouting into light vesicles.

Light vesicles (also known as light density secretory vesicles) traffic directly from the TGN to the plasma membrane. Light vesicles transport the plasma membrane ATPase Pma1, GPI-anchored proteins, cell wall proteins, and other putative lipid raft proteins (Harsay and Bretscher, 1995; Klemm *et al.*, 2009; Surma *et al.*, 2012). Unlike dense vesicles, light vesicles do not appear to associate with adaptor proteins or a protein coat (Figure 1-2). Instead, protein sorting and trafficking of light vesicles appear to be dependent on the presence of lipid rafts, which are areas of the membrane highly enriched sphingolipids and sterol (Klemm *et al.*, 2009). Because light vesicles lack adaptor protein and clathrin association, which are thought to be necessary for cargo sorting and membrane curvature generation, the mechanism by which light vesicles form and traffic to the plasma membrane is not well understood.

Because of the content of the cargo proteins (e.g. lipid raft proteins), the Simons lab and others have proposed that a lipid-dependent protein sorting mechanism is involved in the light vesicle branch of the exocytic pathway (Surma *et al.*, 2012). Much of my graduate work has been focused on determining if the budding yeast flippase Drs2, which has previously been implicated in several trafficking pathways, is one of the factors involved in this exocytic pathway.

Role of flippases in membrane asymmetry and protein trafficking

Flippases belong to the P-type ATPase family

Phospholipids are amphipathic molecules that can freely diffuse laterally throughout a single leaflet of a lipid bilayer, but face a significant barrier in flipping between leaflets (flip-flop) due to their hydrophilic headgroups (Daleke, 2003). Phospholipid translocase (flippase) activity was first reported in human erythrocytes by Seignuret and Devaux in 1984 (Seigneuret and Devaux, 1984). Using spin-labeled analogs of phosphatidylcholine (PC), phosphatidylserine (PS), and phosphatidylethanolamine (PE) to study transverse transport and asymmetry, the researchers determined that the labeled PC remained in the extracellular leaflet of the erythrocytes, whereas PS and PE were rapidly translocated to the cytosolic leaflet.

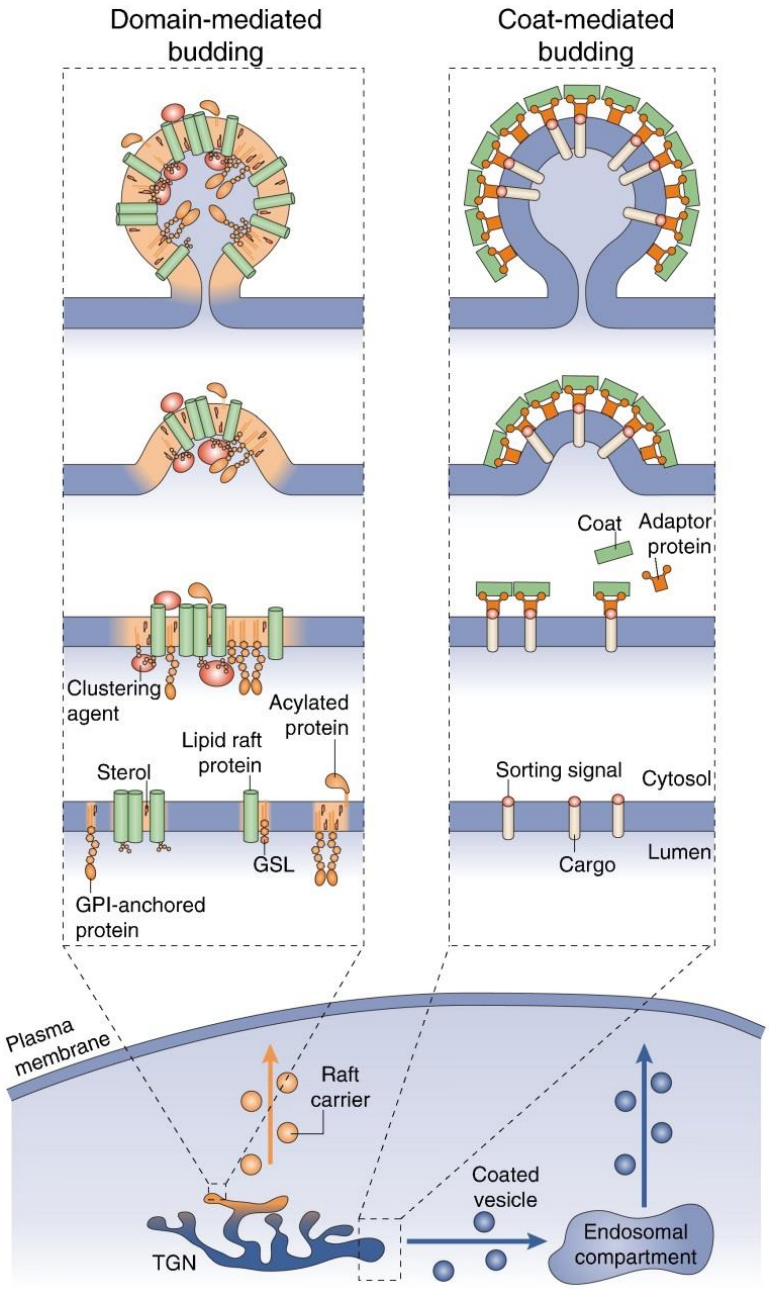

Figure 1-2. Comparison of domain-mediated and coat-mediated vesicle budding from the TGN to the plasma membrane. Image is from (Surma *et al.*, 2012).

The discovery of flippase activity in chromaffin granules led to the cloning of ATPase II, which is now referred to as ATP8A1 (Tang *et al.*, 1996). The mammalian ATP8A1 and its yeast homolog Drs2 are recognized as founding members of the P4-ATPase family. Although proteins capable of flipping lipids were long suspected to exist, definitive proof of flippase activity by a P4-ATPase was not provided until

2009. The Graham lab showed that purified Drs2 reconstituted into proteoliposomes can specifically recognize and flip fluorescently-tagged PS from the outer leaflet to the inner leaflet (Zhou and Graham, 2009). The following month, the Molday lab independently showed that purified Atp8a2 can also flip fluorescently-tagged PS using a similar approach (Coleman *et al.*, 2009). Thus, these two studies were the first to demonstrate a flippase activity by purified P4-ATPases.

P4-ATPases (flippases) are members of the evolutionarily conserved P-type ATPase family of membrane-bound pumps (Axelsen and Palmgren, 1998). P-type ATPases constitute a large superfamily that is divided into five distinct subfamilies based on sequence comparisons (Figure 1-3). P1-ATPases transport heavy metals, P2-ATPases transport Ca^{2+}, Na^{+}/K^{+}, and H^{+}/K^{+}, P3-ATPases transport H^{+}, P4-ATPases transport lipids, and P5-ATPases have an undefined substrate specificity (Palmgren and Nissen, 2011). All P-type ATPases have a similar structural organization that consists of a membrane domain typically comprised of 10 transmembrane (TM) segments, an actuator domain, a phosphorylation domain, and a nucleotide-binding domain (Figure 1-4) (Toyoshima *et al.*, 2000).

Eukaryotes express multiple flippases including the well characterized proteins in budding yeast (Drs2, Dnf1, Dnf2, Dnf3, and Neo1), *Caenorhabditis elegans* (Tat-1 through Tat-6), mammals (ATP8A1 through ATP11C), and *Arabidopsis thaliana* (ALA1 through ALA12) (Sebastian *et al.*, 2012). In yeast, Dnf1 and Dnf2 primarily localize to the bud plasma membrane, Dnf3 and Drs2 primarily localize to the TGN, and Neo1 primarily localizes to the Golgi (Muthusamy *et al.*, 2009a). Although these are the proteins' primary localizations, the Dnf proteins and Drs2 transiently cycle between the TGN, plasma membrane, and early endosomes (Muthusamy *et al.*, 2009a; Sebastian *et al.*, 2012).

Most flippases associate with a noncatalytic beta-subunit from the Cdc50 family, although some flippases appear to function independently, such as Neo1 (Table 1-1; Sebastian *et al.*, 2012). In yeast, the heterodimer pairs include Drs2-Cdc50, Dnf1/2-Lem3, and Dnf3-Crf1 (Sebastian *et al.*, 2012). The beta-subunit consists of two transmembrane segments and a glycosylated ectodomain (Saito *et al.*, 2004; Sebastian *et al.*, 2012).

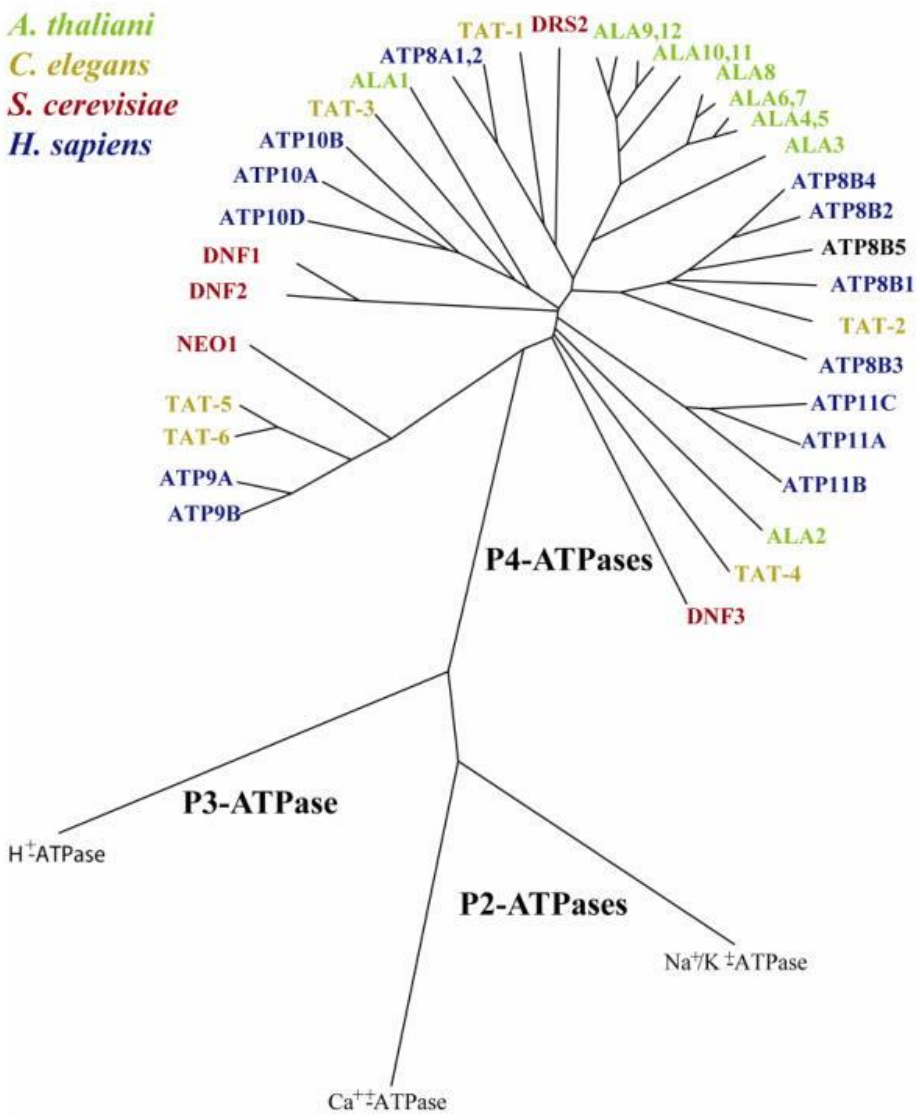

Figure 1-3. Phylogenetic tree of flippases from different species. Image is from (Sebastian *et al.*, 2012).

Formation of the heterodimer is crucial for transport out of the ER and the beta-subunit also influences the catalytic activity of the pump (Chen *et al.*, 1999; Natarajan *et al.*, 2004).

Mechanism of phospholipid translocation

Unlike the ion-transporting P-type ATPases, flippases transport phospholipids from the exofacial/lumenal leaflet to the cytosolic leaflet (Tang *et al.*, 1996; Coleman *et al.*, 2009; Zhou and Graham, 2009). While the mechanism of substrate recognition for cation pumps is well defined, how flippases evolved the

Table 1-1. List of flippases and their beta-subunits. This table is adapted from (Sebastian *et al.*, 2012).

Model organism	Flippase	Beta-subunit	Reference
S. cerevisiae	Drs2	Cdc50	(Saito *et al.*, 2004)
	Dnf1	Lem3	(Saito *et al.*, 2004)
	Dnf2	Lem3	(Furuta *et al.*, 2007)
	Dnf3	Crf1	(Furuta *et al.*, 2007)
	Neo1	None detected	(Saito *et al.*, 2004)
C. elegans	TAT-1	CHAT-1	(Chen *et al.*, 2010)
A. thaliana	ALA2	ALIS1, ALIS3, ALIS5	(López-Marqués *et al.*, 2010)
	ALA3	ALIS1, ALIS3, ALIS5	(Poulsen *et al.*, 2008)
H. sapiens, M. musculus	ATP8A1	CDC50A (CDC50B?)	(Bryde *et al.*, 2010; van der Velden *et al.*, 2010)
	ATP8A2	CDC50A	(van der Velden *et al.*, 2010)
	ATP8B1	CDC50A, CDC50B	(Paulusma *et al.*, 2008)
	ATP8B2	CDC50A, CDC50B	(Bryde *et al.*, 2010; van der Velden *et al.*, 2010)
	ATP8B4	CDC50A (CDC50B?)	(Bryde *et al.*, 2010; van der Velden *et al.*, 2010)
	ATP9A	None detected	(Takatsu *et al.*, 2011)
	ATP9B	None detected	(Takatsu *et al.*, 2011)
	ATP10A	CDC50A	(Takatsu *et al.*, 2011)
	ATP10B	CDC50A	(Takatsu *et al.*, 2011)
	ATP10D	CDC50A	(Takatsu *et al.*, 2011)
	ATP11A	CDC50A	(Takatsu *et al.*, 2011)
	ATP11B	CDC50A	(Takatsu *et al.*, 2011)
	ATP11C	CDC50A	(Takatsu *et al.*, 2011)

ability to recognize and flip phospholipids across the membrane has been a quandary. Crystal structures of P2-ATPases revealed cation-binding sites in a small cavity formed by TM segments 4, 5, 6, and 8 in the Ca^{2+} ATPase (Toyoshima, 2008) and by TM segments 4, 5, 6, 8, and 9 in the Na^{+}/K^{+} ATPase (Shinoda *et al.*, 2009). However, these canonical substrate-binding pockets are likely too small to accommodate a

bulky phospholipid substrate, and flippases lack the polar and charged residues found in the canonical site (Baldridge and Graham, 2013).

This enigma of how P4-ATPases are able to flip phospholipids across the membrane has been termed the "giant substrate problem" (Baldridge and Graham, 2012; Stone and Williamson, 2012). Until recently, the residues involved in recognizing and flipping phospholipid, and even the path the phospholipid travels through the TM region to reach the opposite face of the membrane, were a complete mystery. However, recent work from Baldridge and Graham addressed the P4-ATPase giant substrate problem by identifying residues important for phospholipid substrate specificity (Baldridge and Graham, 2012, 2013; Baldridge *et al.*, 2013).

This work was performed with two divergent flippases in *S. cerevisiae*: Drs2 and Dnf1. Drs2 primarily flips PS and, to a lesser extent, PE (Natarajan *et al.*, 2004; Zhou and Graham, 2009), whereas Dnf1 and Dnf2 primarily flips PC and PE (Kato *et al.*, 2002; Pomorski *et al.*, 2003). However, recent evidence suggests that Dnf1 preferentially flips lysophospholipids that lack the *sn*2 acyl chain (lyso-PC and lyso-PE) (Riekhof *et al.*, 2007; Baldridge *et al.*, 2013). Chimeras were created by transplanting TM segments of Drs2 into Dnf1, with the aim of altering the substrate preference of Dnf1 to that of Drs2 (Baldridge and Graham, 2012). They found that the Dnf1 chimera containing TM 3-4 of Drs2 had an ~8-fold increase in PS transport and decreased PC transport relative to Dnf1, suggesting that these segments are involved in substrate recognition.

Further mapping revealed that the substitution of a single residue, Y618F in TM4, allows Dnf1 to flip 7-nitro-2–1,3-benzoxadiazol-4-yl phospholipid (NBD-PS) without altering NBD-PC/PE recognition (Baldridge and Graham, 2012). The reciprocal change, F511Y in TM4 of Drs2, abrogates PS flip and causes exposure of PS in the plasma membrane extracellular leaflet. In the cation pumps, TM4 forms part of the canonical substrate-binding pocket where a highly conserved helix breaking proline (Pro) is followed by a glutamic acid (Glu) that coordinates ion substrates in both the Na^+/K^+-ATPase and Ca^{2+}-ATPase (Sebastian *et al.*, 2012).

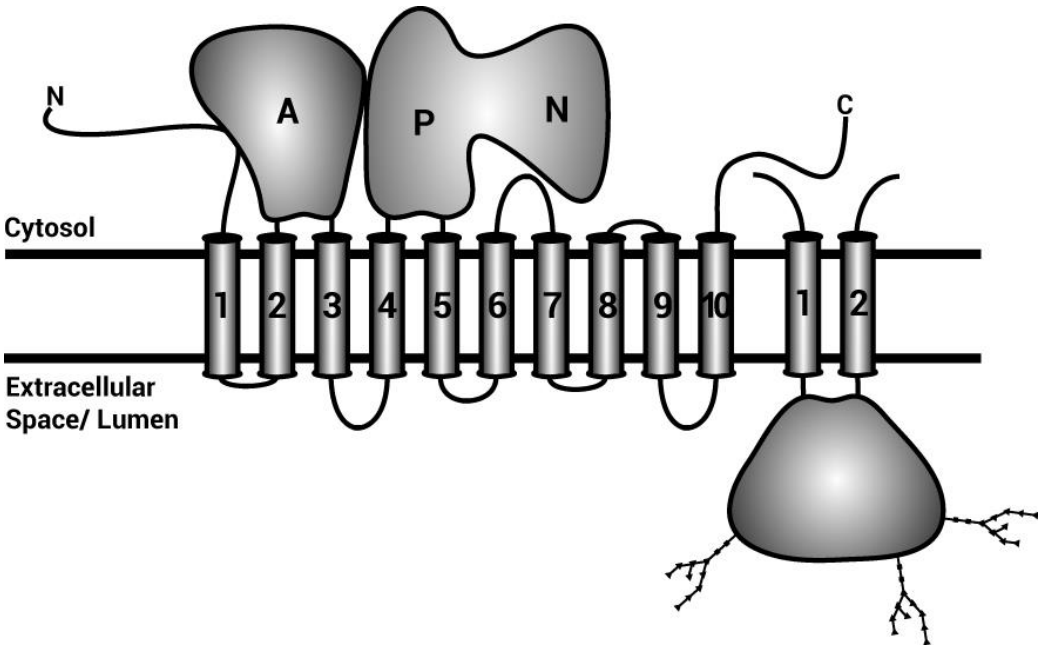

Figure 1-4. Topology diagram of a flippase and its beta-subunit. Image is from (Sebastian *et al.*, 2012).

The TM4 Pro is also conserved in most P-type ATPases, but Drs2 and Dnf1 have a PISLY/F motif rather than the PEGLX motif found in cation pumps (Baldridge and Graham, 2012). Thus, a Tyr or Phe four residues downstream of the Pro (P+4 position), representing the difference of a hydroxyl group, is an important determinant of PS recognition. Importantly, this residue is on the destination side of the membrane, so it was clear from this initial study that more than one residue would be involved in PS recognition and that different Dnf1 residues were selecting PC and PE.

In subsequent work, Baldridge and Graham devised unbiased, genetic strategies for screening thousands of mutations targeted to the TM segments of Dnf1 for those that alter substrate specificity (Baldridge and Graham, 2013). More than 20 residues important for defining headgroup specificity were identified within TM segments 1, 2, 3 and 4, and the exofacial loop between TM3 and 4. These residues cluster in two groups on opposing sides of the membrane, which were termed the entry and exit gates (Baldridge and Graham, 2013). The entry gate is composed of residues on the exofacial side where substrate is selected for transport and loaded into the pump. The exit gate is composed of residues on the cytofacial side and represents a second site of selection prior to substrate release into the cytosolic leaflet. The gates

act cooperatively, but imperfectly, such that neither gate was able to fully restrict PS flip when the opposite gate permitted it.

Importantly, several residues at the exit gate are important for the recognition of lysophospholipids versus diacylated phospholipids (Baldridge *et al.*, 2013). For example, mutation of a conserved asparagine (N550S) in the exit gate allows Dnf1 to flip endogenous diacylated PS and restore PS asymmetry in *drs2*Δ cells. Most notably, the residues that are important for phospholipid selection do not correspond to the canonical substrate binding pocket of P2-type ATPases. For example, the first 3 TM segments of the cation pumps are not involved in substrate selection (Toyoshima, 2008; Shinoda *et al.*, 2009). Baldridge and Graham proposed a noncanonical pathway by which the phospholipid headgroup is translocated along a groove at the protein/membrane interface formed by TM segments 1, 3, and 4, while the acyl chains reorient within the surrounding lipid environment (Baldridge and Graham, 2013). This model provides a solution to the giant substrate problem because the entire phospholipid does not have to be accommodated within a binding pocket in the middle of the membrane domain.

The P-type ATPases are characterized by the autocatalyzed formation of an aspartyl-phosphate intermediate within the P domain and subsequent hydrolysis of this bond during the ATPase cycle (Skou, 1957; Post *et al.*, 1969; Palmgren and Nissen, 2011). These events are coupled to conformational changes (E1 → E1~P → E2~P → E2 → E1) that drive substrate transport against the prevailing concentration gradient. For the Na^+/K^+-ATPase, Na+ stimulates autophosphorylation and is pumped out of the cell during the E1 → E2~P transition. K^+ then binds from the outside, stimulates dephosphorylation and is pumped into the cell during the E2~P → E1 transition. In contrast, the P4-ATPases autophosphorylate in the apparent absence of any substrate (E1 → E2~P), and phospholipid substrate stimulates dephosphorylation (E2~P → E1) (Ding *et al.*, 2000; Coleman *et al.*, 2009; Jacquot *et al.*, 2012). These observations suggest a model in which phospholipid substrate binds the entry gate in either the E1 or E1~P conformation, but this interaction is not coupled to ATP binding or phosphorylation. TM1-2 are drawn up towards the cytosolic leaflet during the E1 to E2~P transition, presumably pulling the substrate

headgroup with it, creating a path for migration of the headgroup into the exit gate. Exit gate binding is specific not only to the lipid headgroup, but also to the glycerol backbone (sphingolipids are not flipped) and to the acyl chain occupancy at the *sn2* position (Baldridge and Graham, 2013; Baldridge *et al.*, 2013). This binding event would stimulate dephosphorylation, release of substrate to the cytosolic leaflet, and resetting of the pump for another round of transport.

This model potentially provides insight into how flippases evolved the ability to transport phospholipid substrate. The Ca^{2+}-ATPase crystal structure in the E2 conformation (Protein Data Bank ID code 2AGV) has a bound PE in a position homologous to the exit gate in flippases (Obara *et al.*, 2005). This binding pocket closes in the E1 conformation, implying that the PE is a boundary lipid that enters and exits this site from the cytosolic leaflet with each round of ATP hydrolysis. Flippases may have evolved from a primordial cation pump through gene duplication and by acquiring the ability to load this phospholipid binding site from the opposite side of the membrane, thus flipping the phospholipid (Axelsen and Palmgren, 1998). Armed with a new substrate and a selective advantage, flippases would have gradually lost the ability to pump cations.

However, an alternative model for phospholipid translocation has recently been proposed by the Molday and Andersen labs. Vestergaard, *et al*. investigated the consequences of mutating a highly conserved P+1 isoleucine (I364) in TM4 of the mammalian flippase ATP8A2 (Vestergaard *et al.*, 2014). This isoleucine residue corresponds to a glutamate in P2-ATPases that is crucial for cation transport (Vilsen and Andersen, 1998; Olesen *et al.*, 2007). A missense mutation at the I364 position (I364M) was recently identified as the cause of cerebellar ataxia, mental retardation, and dysequilibrium syndrome (CAMRQ) in a Turkish family (Emre Onat *et al.*, 2013). *Wabbler-lethal* mice, which also have mutations in Atp8a2, have severe axonal degeneration (Zhu *et al.*, 2012; van der Mark *et al.*, 2013), indicating that ATP8A2 is important in the maintenance of the nervous system. Vestergaard, *et al*. found that mutations of I364 and N359, another TM4 residue, strongly perturbed flippase activity and the ability of PS to stimulate ATPase activity (Vestergaard *et al.*, 2014).

In lieu of a P4-ATPase crystal structure, the researchers created two homology models of ATP8A2 based on the related P2-ATPase sarco(endo)plasmic reticulum Ca^{2+} ATPase (SERCA) in two conformational states (E_2P and E_2) (Vestergaard *et al.*, 2014). Molecular dynamic refinements of the models opened a groove bordered by TM1, TM2, TM4, and TM6 that allowed substantial water penetration. The groove is divided into two distinct pockets at the exoplasmic and cytoplasmic faces by a central cluster of hydrophobic residues, including I364. Vestergaard, *et al*. proposed that the hydrophobic cluster divides the hydrated groove into phospholipid entry and exit sites (Vestergaard *et al.*, 2014). Movement of the hydrophobic residues during the reaction cycle may cause the sequential formation and dissolution of the two sites to enable translocation of the phospholipid headgroup in an aqueous environment, while the acyl chains follow passively in the lipid phase of the surrounding membrane (Vestergaard *et al.*, 2014).

The proposed route of translocation suggested by Vestergaard and colleagues differs from the one suggested by Baldridge and Graham, although it is consistent with the view that flippases use a noncanonical transport mechanism driven primarily by substrate interactions with the first four TM segments (Baldridge and Graham, 2013; Vestergaard *et al.*, 2014). The entry and exit gate residues that define substrate specificity could be accessible from the TM2-4-6 groove, depending on their actual side chain orientations and how deeply the phospholipid headgroup can enter the membrane domain. Limited sequence similarity between several membrane segments of P2-ATPases and flippases creates uncertainties in alignments and homology models. Ultimately, multiple flippase structures with substrate bound will be needed to assess the validity of the proposed models.

Flippases as regulators of membrane asymmetry

Although the mechanism of phospholipid translocation requires further study, there is a wealth of data supporting the role of flippases as generators of membrane asymmetry (Daleke, 2007; Hankins *et al.*, 2015a). Phospholipid synthesis occurs primarily in the cytosolic leaflet of the ER, and to preserve membrane stability of the ER, there must be a mechanism by which newly synthesized lipids are redistributed from the cytosolic leaflet to the lumenal leaflet. A number of labs have proposed that ER

lipids are bidirectionally scrambled across the bilayer in an energy-independent fashion, presumably forming a symmetric membrane, although the mechanism remains unclear (Bell *et al.*, 1981; Bishop and Bell, 1985; Herrmann *et al.*, 1990; Buton *et al.*, 1996; Sanyal *et al.*, 2008). In contrast, Higgins and Dawson reported that PS is enriched in the lumenal leaflet of the ER (Higgins and Dawson, 1977).

A recent finding by Fairn, *et al*. supports the hypothesis of a non-symmetric ER (Fairn *et al.*, 2011). The Grinstein lab has developed a novel probe containing the C2 domain of lactadherin (Lact-C2) that specifically binds the biologically relevant PS isomer phosphatidyl-L-serine and no other lipids in a Ca^{2+}-independent manner (Yeung *et al.*, 2008). Genetically encoded Lact-C2 labels the cytosolic surface of membranes with the highest concentration of the probe at the PM and with very little ER labeling. To provide access to the entire pool of PS, ultrathin sections of fast-frozen samples were overlaid with Lact-C2. A substantial increase in labeling of ER, Golgi, and mitochondria, was observed, indicating that PS is preferentially localized to the lumenal leaflet of the ER (Fairn *et al.*, 2011).

The eukaryotic PM is organized such that the two leaflets have distinct lipid environments. The outer (extracellular) leaflet is primarily composed of PC and sphingolipids, whereas PS, PE, and phosphatidylinositol (PI) are primarily restricted to the inner (cytosolic) leaflet (Daleke, 2003; Sebastian *et al.*, 2012). If PS is primarily enriched in the lumenal leaflet of the ER and cytosolic leaflet of the PM, PS must change sidedness somewhere along its journey. Colocalization experiments show little overlap between Lact-C2 and a *trans*-Golgi cisternae marker, indicating that PS at the *trans*-Golgi is still largely constrained to the lumenal leaflet (Fairn *et al.*, 2011). However, significant colocalization occurs between Lact-C2 and a TGN marker, suggesting the TGN is the site of PS translocation. This observation is consistent with TGN localization of yeast flippase Drs2 (Chen *et al.*, 1999; Hua *et al.*, 2002; Natarajan *et al.*, 2004; Alder-Baerens *et al.*, 2006) and indicates that mammals likely have one or more TGN-localized PS flippases (Fairn *et al.*, 2011). PS translocation at the TGN plays a crucial role in the budding of transport vesicles from this organelle (Xu *et al.*, 2013), in addition to helping generate the asymmetric organization of the plasma membrane (Alder-Baerens *et al.*, 2006).

Along with flippases, two other classes of membrane proteins are involved in the formation or dissolution of membrane asymmetry: floppases and scramblases. Floppases are ABC-transporters that mediate the movement of phospholipids from the cytosolic leaflet to the lumenal/extracellular leaflet (in the opposite direction of flippases) (Daleke, 2003, 2007). However, an exception to this categorization is the ABC-transporter ABCA4, which acts as a PE and retinylidene-PE flippase in outer segment membranes of rod and cone cells (Quazi *et al.*, 2012; Quazi and Molday, 2013). Flippases are clearly linked to the establishment of membrane asymmetry in multiple cell types and organisms, but the ABC transporters appear to play more specialized roles, such as the excretion of the lipid components of bile (Daleke, 2003). Phospholipid transport mediated by both flippases and floppases is unidirectional and ATP-dependent. In contrast, scramblases are ATP-independent and disrupt membrane asymmetry by bidirectionally translocating lipids between leaflets (Sahu *et al.*, 2007).

PS in the cytosolic leaflet plays an important role in the recruitment of a variety of signaling proteins (Sigal *et al.*, 1994; Lemmon, 2008). There are also proteins that interact with PS in the extracellular leaflet; however, these interactions are limited as they occur only under specific conditions where PS asymmetry is disrupted. PS exposure on red blood cells and platelets substantially accelerates clotting reactions and is therefore crucial for controlling thrombosis (Bevers *et al.*, 1983; Lentz, 2003). Regulated exposure of PS in the outer leaflet of the plasma membrane is an early event in apoptosis and serves as an "eat me" signal important for the orderly removal of cell corpses (Fadok *et al.*, 1992; Bratton *et al.*, 1997; 2001). In addition to scramblase activity being turned on during apoptosis, flippase activity must also be turned off such that the disordering of lipid asymmetry is not corrected (Suzuki *et al.*, 2013).

In addition to PS exposure being a mediator of certain biological processes, loss of membrane asymmetry through disruption of flippase activity also has implications in a number of diseases. For example, mutations in the flippase gene ATP8A2 have been linked to neurodegenerative diseases in both humans and mice (Zhu *et al.*, 2012; Emre Onat *et al.*, 2013). Mutations in ATP8B1 may cause hearing loss or disrupt asymmetry in the canalicular membrane of hepatocytes, resulting in the severe liver disease

progressive familial intrahepatic cholestasis (PFIC1) (Pawlikowska *et al.*, 2004; Paulusma *et al.*, 2006; Cai *et al.*, 2009; Stapelbroek *et al.*, 2009). A genome-wide association study of single-nucleotide polymorphisms (SNPs) associated with Alzheimer's disease suggested that mutations in ATP8B4 may predispose individuals to the condition (Li *et al.*, 2008). Diet-induced obesity and type II diabetes have been linked to mutations in the ATP10A and ATP10D genes (Flamant *et al.*, 2003; Dhar *et al.*, 2004; Dupuis *et al.*, 2010; Milagro *et al.*, 2011). B cell generation in mice is severely diminished in mice with mutations in ATP11C (Siggs *et al.*, 2011a; Yabas *et al.*, 2011). It is clear from the diversity in phenotypes described above and summarized in Table 1-2 that flippases are important players in a wide variety of physiological functions. However, the relationship between defective flippase activity and diseases remains to be fully elucidated.

Importance of flippase activity in protein trafficking

In addition to their role in maintaining membrane asymmetry, flippases are also involved in multiple protein trafficking pathways (Figure 1-5). Although the precise function flippases have in protein trafficking remains to be elucidated, there are several hypotheses to explain their role. One hypothesis is based on the bilayer couple hypothesis, which states that when one leaflet of the membrane expands, the other leaflet contracts so that the two leaflets remain in contact (Sheetz and Singer, 1974). Through the coordination of membrane expansion in one leaflet and contraction in the other, membrane curvature is generated. Thus, one hypothesis for the role of flippases in protein trafficking is that, by unidirectionally flipping lipids from the lumenal/extracellular leaflet, flippases generate the membrane curvature required to bud vesicles. A second hypothesis is that flippases enrich specific lipids (e.g. PS) in the cytosolic leaflet to recruit protein machinery involved in the budding process (Xu *et al.*, 2013). There is evidence to support both of these hypotheses, and it is likely that they are not mutually exclusive.

Table 1-2. Mammalian flippases associated with disease phenotypes (van der Mark *et al.*, 2013).

Flippase	Disease in mice	Disease in humans	Reference
ATP8A1	impaired learning, increased physical activity		(Levano *et al.*, 2012)
ATP8A2	neurodegenerative disease, axonal degeneration, growth retardation	mental retardation, hypotonia, CAMRQ	(Zhu *et al.*, 2012; Onat *et al.*, 2013)
ATP8B1	intrahepatic cholestasis, hearing loss	PFIC1, BRIC1	(Pawlikowska *et al.*, 2004; Paulusma *et al.*, 2006, 2010; Cai *et al.*, 2009; Stapelbroek *et al.*, 2009)
ATP8B3	Sperm capacitation anomalies		(Wang *et al.*, 2004; Gong *et al.*, 2009)
ATP8B4		Alzheimer's disease	(Li *et al.*, 2008)
ATP10A	insulin resistance, diet-induced obesity, hyperlipidemia, hyperinsulinemia	type 2 diabetes, insulin resistance in African Americans, diet-induced obesity	(Dhar *et al.*, 2004, 2006; Dupuis *et al.*, 2010; Irvin *et al.*, 2011; Milagro *et al.*, 2011)
ATP10D	diet-induced obesity, hyperinsulinemia, hyperglycemia		(Flamant *et al.*, 2003)
ATP11A		metastasis in colorectal cancer	(Miyoshi *et al.*, 2010)
ATP11C	arrested B cell development, dystocia, anemia, hepatocellular carcinoma, conjugated hyperbilirubinemia, unconjugated hypercholanemia		(Siggs *et al.*, 2011a, 2011b; Yabas *et al.*, 2011)

The first connection between flippases and protein trafficking was established by the Graham lab using a genetic screen to identify proteins that functionally interact with ADP-ribosylation factor 1 (Arf1) (Chen and Graham, 1998). GTP-bound Arf1 facilitates the recruitment of adaptor and coat proteins, such as COPI and clathrin, to sites of vesicle budding at the Golgi. The researchers identified seven genes that were synthetically lethal with *arf1*Δ (*SWA1-7*). Notably, the screen identified proteins involved in clathrin function, such clathrin heavy chain (*SWA5*) and auxilin (*SWA2*), as well as the flippase Drs2 (*SWA3*) and its beta-subunit Cdc50 (*SWA4*) (Chen *et al.*, 1999, 2006; Gall *et al.*, 2000).

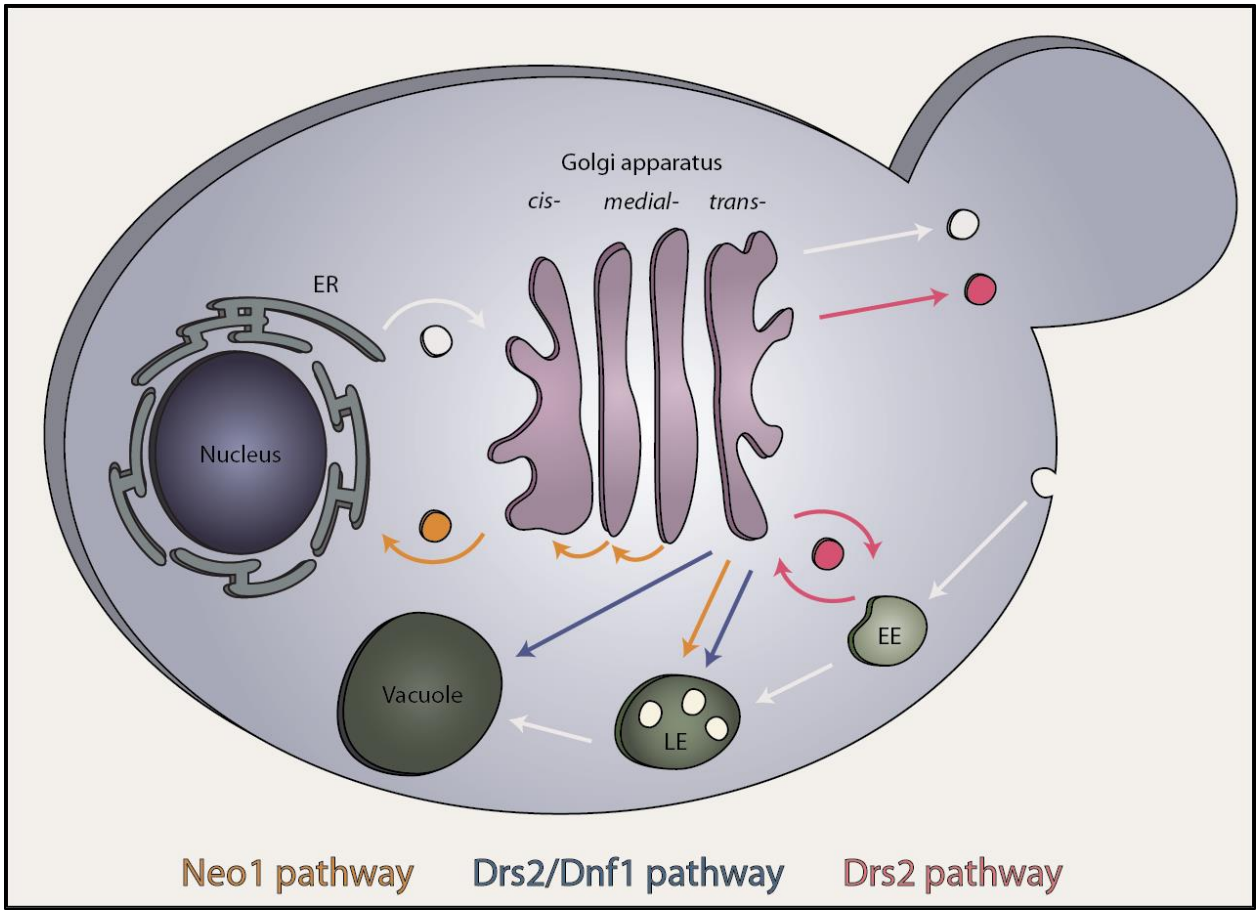

Figure 1-5. Influence of flippases on vesicle-mediated trafficking pathways in *S. cerevisiae*.

Drs2 and Cdc50 also have a synthetic lethal interaction with clathrin temperature-sensitive mutants, but not COPI or COPII mutants. This pattern of genetic interactions is consistent with loss of Drs2 perturbing clathrin-dependent trafficking pathways but not affecting COPI- and COPII-dependent trafficking pathways (Chen *et al.*, 1999; Hua *et al.*, 2002; Liu *et al.*, 2008). Morphologically, *drs2*Δ cells are similar to clathrin temperature-sensitive mutants in that they both accumulate large (200-250 nm in diameter) cup-shaped Golgi membranes, which suggest defective vesicle budding (Chen *et al.*, 1999).

Drs2 also localizes to early endosomes and is both a mediator and cargo of bidirectional trafficking pathways between the TGN and early endosomes (Furuta *et al.*, 2007; Liu *et al.*, 2008). The trafficking pathways between these two organelles that Drs2 is involved in are facilitated by AP-1/clathrin (TGN ↔ early endosomes) and the F-box protein Rcy1 (early endosomes → TGN). Because both AP-1/clathrin

and Rcy1 trafficking pathways are severely compromised in *drs2*Δ cells, it suggests that Drs2 is a shared and essential regulator of the two pathways.

The integrity of the AP-1/clathrin pathway can be assessed by observing the trafficking of the cargo protein chitin synthase III (Chs3) (Shaw *et al.*, 1991). Chs3 normally cycles between the Golgi and early endosomes, but also localizes to the bud plasma membrane during the G1 phase of the cell cycle. However, disruption of the AP-1 complex shifts Chs3 localization to the plasma membrane and late endosomes (Valdivia *et al.*, 2002). This same defect is observed in *drs2*Δ cells, suggesting Drs2 is required for AP-1/clathrin trafficking (Liu *et al.*, 2008).

Notably, AP-1/clathrin-coated vesicles do not form in *drs2*Δ cells even though AP-1 and clathrin are recruited normally to the membrane in the absence of Drs2 (Liu *et al.*, 2008). This finding suggests that AP-1, clathrin, and other components of the budding machinery may be insufficient to generate the membrane curvature required to bud the vesicles in the absence of Drs2 (Muthusamy *et al.*, 2009a). Yeast cells tolerate the loss of the AP-1/clathrin trafficking pathways, and there is no further defect when Drs2 activity is concomitantly disrupted (Liu *et al.*, 2008). However, there is a severe growth defect when the GGA pathway (TGN → late endosomes) is also blocked in AP-1 or Drs2 mutant backgrounds (Costaguta *et al.*, 2001; Liu *et al.*, 2008). These observations suggest that AP-1/clathrin and GGA mediate parallel pathways, and yeast must have at least one functional transport pathway between the TGN and endosomal system to remain viable.

Retrieval of proteins from early endosomes to the TGN via the Rcy1 recycling pathway is strongly dependent on the presence of Drs2 (Furuta *et al.*, 2007). GFP-Snc1 accumulates in early endosomes in both *rcy1*Δ and *drs2*Δ cells (Furuta *et al.*, 2007), suggesting the pathway is disrupted when either is lost. Rcy1 physically interacts with the C-terminal regulatory domain of Drs2, where Drs2 also interacts with the ArfGEF Gea2 and PI4P (Furuta *et al.*, 2007; Natarajan *et al.*, 2009; Zhou *et al.*, 2013). The C-terminus of Drs2 is autoinhibitory for flippase activity in the absence of regulator binding, so it is possible that Rcy1 binding activates flippase activity in early endosomes.

There is some degree of functional overlap between the yeast flippases for protein transport from the TGN to the vacuole via the CPY/GGA and ALP/AP-3 pathways (Hua *et al.*, 2002). CPY is a vacuolar protein that is processed into its mature form once it reaches the vacuole. When the GGA pathway is blocked, there is a severe delay in CPY processing and the cells accumulate and partially secrete the CPY precursor (Hirst *et al.*, 2000). CPY is processed normally at 30°C in *drs2*Δ and *dnf1*Δ single mutants, but transport is delayed in the *drs2*Δ*dnf1*Δ double mutant (Hua *et al.*, 2002). Likewise, transport of ALP to the vacuole via the AP-3 pathway occurs normally in *drs2*Δ and *dnf1*Δ single mutants, but transport is disrupted in the *drs2*Δ*dnf1*Δ double mutant (Hua *et al.*, 2002). These observations suggest that the roles of Drs2 and Dnf1 are functionally redundant in trafficking pathways leading to the vacuole.

Neo1 has also been linked to the GGA pathway. Temperature sensitive *neo1* alleles (*neo1*-ts) have delayed CPY transport to the vacuole (Hua and Graham, 2003). The *drs2*Δ *dnf1*Δ and *neo1-ts* defects are not as severe as the defects observed in *gga1,2*Δ cells, suggesting all three flippases contribute to vesicle budding in the GGA pathway. Neo1 is also involved in COPI-dependent retrograde trafficking of the Golgi protein Rer1. When Neo1 is inactivated, Rer1 mislocalizes to the vacuole, which is similar to the phenotype observed in COPI mutants (Hua and Graham, 2003). Consistent with a role in COPI trafficking, Neo1 shows a genetic interaction with COPI, but not COPII or components of downstream trafficking pathways.

Unlike protein transport between the TGN and endosomal/vacuolar system in which there appears to be some degree of contribution or functional overlap between Drs2 and Dnf1, Drs2 appears to be the only flippase involved in the AP-1 pathway, the Rcy1 pathway, and exocytosis. As mentioned previously, proteins destined for the plasma membrane are packaged into either dense or light vesicles, which are distinguished based on their density and cargo (Harsay and Bretscher, 1995). The Graham lab demonstrated that loss of Drs2 prevents the formation of clathrin-coated dense vesicles, which accumulate intracellularly when actin assembly is blocked (Gall *et al.*, 2002). However, cargo proteins that normally travel via dense vesicles (e.g. invertase and acid phosphatase) still reach the plasma membrane in *drs2*Δ

cells, as they are rerouted into light vesicles (Chen *et al.*, 1999; Hua *et al.*, 2002). Drs2 has not previously been implicated in the light vesicle branch of exocytosis; however, my results summarized in Chapter II suggest that Drs2 also functions in protein sorting into these vesicles.

Influence of Drs2 and Kes1 on sterol homeostasis

The basis for my research project that would later become Chapter II is that Drs2 has a role in sterol homeostasis (Muthusamy *et al.*, 2009b). Exocytic light vesicles are coat-independent and are proposed to be lipid-raft dependent, as they are highly enriched in sterol and sphingolipids. Mutations that disrupt ergosterol (*erg* mutants) or sphingolipid synthesis (*lcb1-100*) cause light vesicle cargo proteins, such as GPI-anchored proteins, Tat2, Fur4, and Pma1, to lose their detergent resistant membrane (DRM) association and/or mislocalize to the vacuole (Umebayashi and Nakano, 2003; Proszynski *et al.*, 2005; Daicho *et al.*, 2009; Surma *et al.*, 2012). In this thesis work, I set forth to determine if the sterol defects of *drs2*Δ cells affect the exocytic trafficking of these proteins or their lateral organization at the plasma membrane.

Budding yeast lateral membrane organization

While the role of flippases in the transverse segregation of phospholipids has been well established, their role in the lateral segregation of phospholipids has yet to be studied. In 1972, Singer and Nicolson proposed the fluid mosaic model which stipulated that membranes are composed of a homogenous lipid bilayer in which proteins are attached or embedded in (Singer and Nicolson, 1972). According to this model, proteins are able to freely float in the sea of lipids. However, it has since become apparent that not all proteins and lipids at the yeast TGN and plasma membrane are homogenously dispersed throughout one leaflet; rather, the membranes are a heterogeneous landscape composed of distinct patches and networks with unique protein-lipid microenvironments (Ziółkowska *et al.*, 2012). This compartmentalization is proposed to enable for spatiotemporal regulation of processes such as cell polarity, signal transduction, and membrane protein turnover (Malínská *et al.*, 2003; Spira *et al.*, 2012; Ziółkowska *et al.*, 2012).

S. cerevisiae is an attractive model for studying lateral membrane organization. Unlike higher eukaryotes, yeast forms stable, large domains that can be easily visualized (Malínská *et al.*, 2003; Olivera-Couto and Aguilar, 2012). Although putative lipid raft proteins travel to the plasma membrane in light vesicles, once at the plasma membrane the proteins localize to distinct membrane compartments. To date, three membrane compartments have been described in *S. cerevisiae*: the membrane compartments of Can1 (MCC), Pma1 (MCP), and TORC2 (MCT) (Figure 1-6) (Olivera-Couto and Aguilar, 2012). MCC was the first compartment described in yeast and is characterized as having a punctate distribution with each domain forming a 50 nm x 300 nm furrow (Malinska *et al.*, 2004). MCC patches are enriched in sterol and a variety of proteins (24 currently identified) including several nutrient symporters, such as transporters of arginine (Can1), uracil (Fur4), and tryptophan (Tat2) (Olivera-Couto and Aguilar, 2012).

In 2009, Stradalova et al. reported colocalization of the MCC marker Sur7 and the eisosome core component Pil1 at the characteristic furrows, indicating that both are part of the same microdomain (Strádalová *et al.*, 2009). Eisosomes were first speculated to be static complexes involved in endocytic events (Moreira *et al.*, 2009), but it was later shown that endocytic machinery assembles in the MCP and that MCC/eisosomes are devoid of endocytic events (Grossmann *et al.*, 2008). MCP was defined based on the localization of the membrane ATPase Pma1, the most abundant yeast plasma membrane protein (Malínská *et al.*, 2003). MCP appears as a meshwork that percolates between the other domains. MCT, the most recently characterized compartment, houses TORC2, which functions in the regulation of sphingolipid metabolism (Berchtold and Walther, 2009; Berchtold *et al.*, 2012). Unlike MCC and MCP, which are thought to be enriched in ergosterol and sphingolipids, MCT might represent a disorganized portion of the yeast PM, as it is enriched in phospholipids and is ergosterol/sphingolipid poor (Berchtold and Walther, 2009).

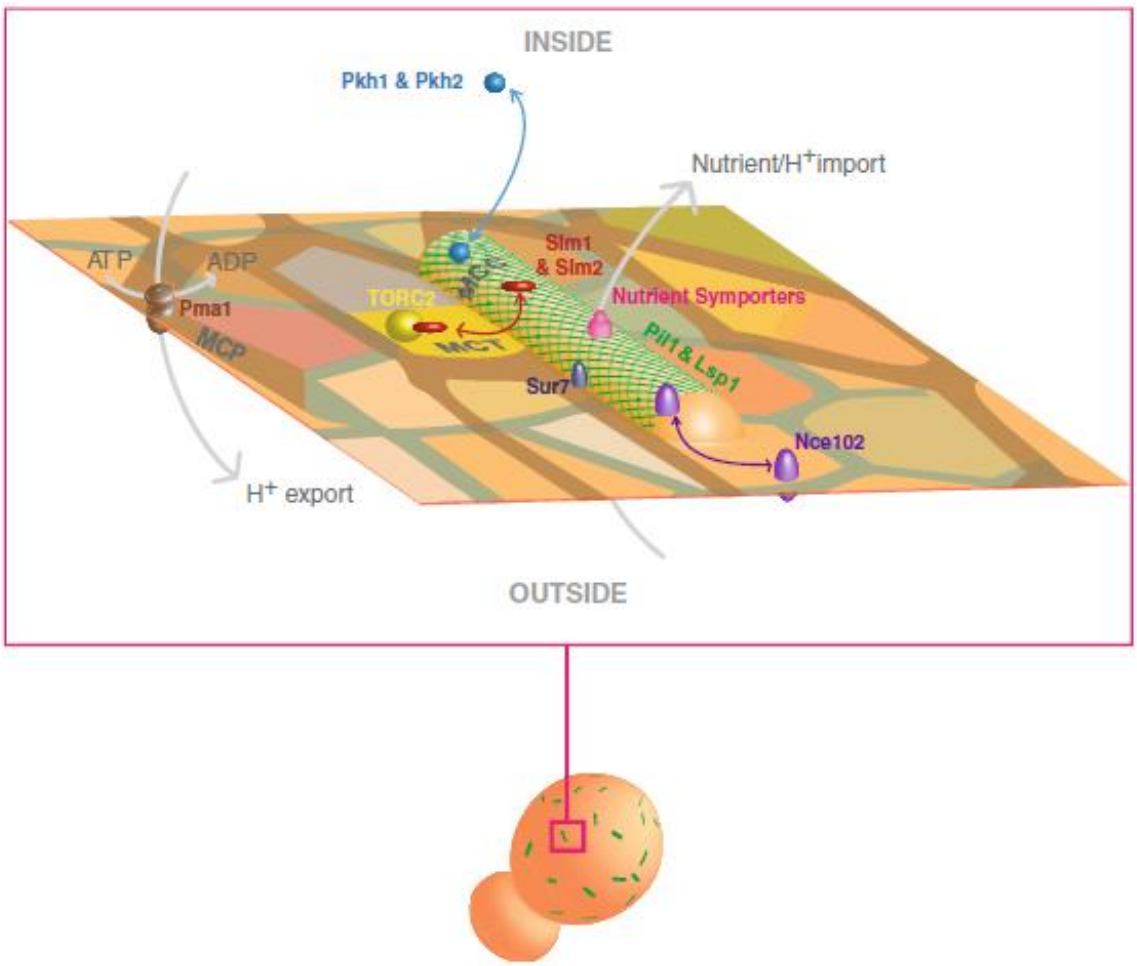

Figure 1-6. The yeast plasma membrane is composed of various membrane compartments that appear as distinct patches or as continuous networks. Image is from (Olivera-Couto and Aguilar, 2012).

Non-vesicular sterol transport by Kes1

A well-conserved feature of the eukaryotic plasma membrane is an enrichment of sterol relative to internal membranes, but how this lipid gradient is generated and maintained is not well understood (Alvarez *et al.*, 2007). Large amounts of lipids are exchanged between membranes during the processes of vesicle budding and fusion in yeast; however, lipid transport is still detectable when vesicular trafficking is blocked by ATP depletion, by a reduction in temperature, or in *sec18* mutants (Saraste *et al.*, 1986; Kuismanen and Saraste, 1989; Voelker, 1990; Orcl *et al.*, 1991; Funato and Riezman, 2001; Baumann *et al.*, 2005). Furthermore, lipid transport occurs between organelles that are not connected by any known

vesicular transport systems (e.g. mitochondria and peroxisomes) (Voelker, 2003; Holthuis and Levine, 2005). Together, these findings suggest that a non-vesicular mode of lipid transport exists.

Lipid transfer proteins (LTPs) have been identified that are capable of catalyzing non-vesicular transport of lipids between membranes. However, there has been significant controversy if LTPs mediate bulk transfer of lipids and contribute to compositional differences between organelle membranes *in vivo* (Zilversmit, 1983; Helmkamp, 1986; Georgiev *et al.*, 2011). An LTP extracts a specific lipid species from the donor membrane and then transports the lipid, concealed within a hydrophobic tunnel, to the acceptor membrane (Lev, 2010). The size and shape of this tunnel determine the lipid specificity of the LTP.

LTPs that specifically bind to and transport sterol are members of the oxysterol-binding protein (OSBP)-related proteins (ORP) family in mammals or the oxysterol-binding homologue (Osh) family in yeast (Fang *et al.*, 1996). However, not all ORP/Osh proteins actually interact with sterol. For example, Osh6 and Osh7 specifically recognize PS (Maeda *et al.*, 2013). This section will focus on OSBP and Osh4/Kes1 (hereafter referred to as Kes1), which have separate but overlapping binding pockets for sterol and PI4P (Saint-Jean *et al.*, 2011).

Recent work from the Antonny and Drin labs have addressed how these LTPs differentiate donor from acceptor membranes to give directional sterol/PI4P lipid transport between the TGN and ER (Mesmin *et al.*, 2013; Moser von Filseck *et al.*, 2015). OSBP resides at ER-Golgi membrane contact sites (MCSs) along with a number of other lipid transporters such as CERT (Hanada *et al.*, 2003) and FAPP2 (D'Angelo *et al.*, 2012). These proteins contain a PH domain that interacts with Golgi PI4P (Levine and Munro, 2002; Godi *et al.*, 2004), a FFAT motif that interacts with the ER protein VAP-A (Loewen *et al.*, 2003; Kaiser *et al.*, 2005; Furuita *et al.*, 2010; Mikitova and Levine, 2012) and a lipid transfer domain (Levine, 2004; Lev, 2010). This combination of interaction sites suggests that these lipid transport proteins may be able to tether ER and Golgi membranes and transfer lipids between them.

Mesmin *et al.* tested if OSBP has an effect on PI4P and cholesterol cellular distributions (Mesmin *et al.*, 2013). In wild-type cells, the PI4P probe (GFP fused to PH domain of OSBP) primarily stains the Golgi

(Levine and Munro, 2002); however, overexpression of OSBP caused a 3.5-fold decrease in Golgi PI4P staining (Mesmin *et al.*, 2013). Addition of 25-hydroxycholesterol (25-OH) also caused the PI4P probe to relocalize to the Golgi, indicating that OSBP extraction of PI4P cannot occur when OSBP is blocked by 25-OH. Mutations which prevent OSBP from interacting with VAP-A/PI4P or disrupt lipid transfer ability (Saint-Jean *et al.*, 2011) also hindered OSBP extraction of PI4P from the Golgi (Mesmin *et al.*, 2013). These results suggest that OSBP regulates Golgi PI4P turnover in a manner which involves all three (PH, FFAT, and lipid transfer) domains.

OSBP-dependent transfer of DHE and PI4P between liposomes significantly slows after a few cycles of transfer, suggesting a negative feedback loop (Mesmin *et al.*, 2013). However, this conflicts with OSBP overexpression depleting PI4P at the Golgi instead of shutting down exchange after PI4P begins accumulating at the ER. This discrepancy is resolved by taking into account the involvement of SacI, an integral ER protein that hydrolyzes PI4P to PI (Foti *et al.*, 2001; Kim *et al.*, 2013). By preventing PI4P accumulation at the ER, SacI gives directionality to OSBP lipid transport. Lipid transfer by OSBP can thus be summarized as a four-step cycle (Mesmin *et al.*, 2013). OSBP first tethers the ER and Golgi membranes through its FFAT motif and PH domain. OSBP transports cholesterol from the ER to Golgi, and then transports PI4P from the Golgi to ER. SacI then hydrolyzes PI4P *in cis,* making the cycle irreversible and thus giving directionality to the lipid exchange.

A more recent study by the Antonny and Drin labs examined Kes1 lipid transfer activity between liposomes that mimic the ER and Golgi (Moser von Filseck *et al.*, 2015). Their results suggest that Kes1 mediates the exchange of sterol/PI4P using the same four-step cycle as OSBP (Figure 1-7). Consistent with this model, Kes1 has been previously shown to bind PI lipids (Li *et al.*, 2002) and regulate the level of PI4P at the Golgi (Fairn *et al.*, 2007). Additionally, *KES1* has been implicated as a negative regulator of TGN function in exocytosis (Jiang *et al.*, 1994; Fang *et al.*, 1996; Li *et al.*, 2002; Alfaro *et al.*, 2011). Unlike OSBP, however, Kes1 lacks FFAT and PH domains (Stefan *et al.*, 2011), so it is still unclear how Kes1 communicates with the ER to mediate efficient exchange between the two organelles.

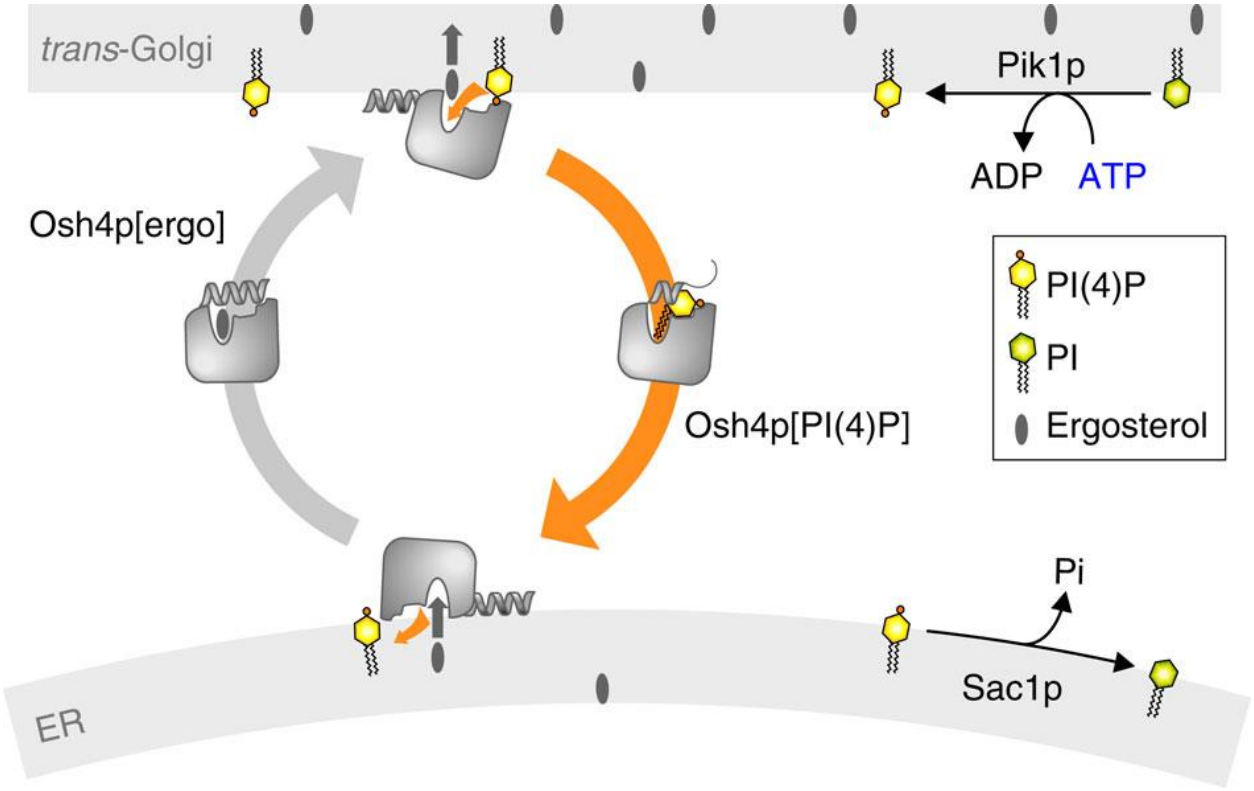

Figure 1-7. Kes1/Osh4 exchanges ergosterol from the ER for PI4P from the TGN. Sac1 hydrolyzes PI4P at the ER, preventing its accumulation and allowing the cycle to continue. Image is from (Moser von Filseck *et al.*, 2015).

Antagonistic relationship between Drs2 and Kes1 in sterol homeostasis

A previous graduate student in the Graham lab, Baby-Periyanayaki Muthusamy, found that Drs2 and the Kes1 work antagonistically to regulate ergosterol distribution in the cell (Muthusamy *et al.*, 2009b). Although the joint regulation of ergosterol by Drs2 and Kes1 was a novel finding, some links between flippases and ergosterol had been established prior to this study. Loss of Drs2 or Cdc50 is synthetically lethal with *erg* mutants, which disrupt the late steps of ergosterol synthesis (Kishimoto *et al.*, 2005). Relative to wild-type cells, *cdc50*Δ cells accumulate more lipid droplets, which also stain with a higher intensity with Nile Red (Fei *et al.*, 2008). Additionally, the *C. elegans* flippases *tat-1* through *tat-3* are essential for reproduction during sterol starvation (Lyssenko *et al.*, 2008).

Muthusamy *et al.* initially sought to determine the mechanistic basis for the *drs2*Δ cold sensitivity phenotype that occurs at ≤ 20°C (wild-type yeast are able to grow at 10-40°C) (Muthusamy *et al.*, 2009b).

To do this, the researchers selected for spontaneous extragenic suppressors that allowed *drs2*Δ colonies to grow at 17°C. The mutant alleles that were able to suppress *drs2*Δ cold sensitivity fell into two complementation groups, which were named suppressor of *drs2* knockout 1 (*SDK1*) and 2 (*SDK2*) and composed of 12 and 4 suppressors, respectively. While the attempts to clone *SDK2* were unsuccessful, the *SDK1* strains were determined to be loss of function *kes1* alleles, indicating loss of Kes1 activity was responsible for suppression.

The researchers next purified TGN membranes purified from wild-type, *drs2*Δ, *kes1*Δ, and *drs2*Δ*kes1*Δ cells and assayed for flippase activity (as measured by the ability to flip NBD-PS to the TGN lumenal leaflet) (Muthusamy *et al.*, 2009b). Relative to wild-type, NBD-PS flippase activity was nearly 2-fold higher for *kes1*Δ and severely reduced in *drs2*Δ and *drs2*Δ*kes1*Δ TGN membrane preparations, suggesting Drs2 is hyperactive when Kes1 is absent. In fact, addition of recombinant Kes1 to membranes isolated from *kes1*Δ cells potently inhibited Drs2 flippase activity (Muthusamy *et al.*, 2009b).

Because Kes1 was previously implicated in sterol transport, the researchers next tested if *kes1*Δ could suppress sterol-related *drs2*Δ defects (Muthusamy *et al.*, 2009b). Deletion of *KES1* suppresses the *drs2*Δ*erg6*Δ synthetic lethality that was previously reported. Additionally, *drs2*Δ cells are hypersensitive to the ergosterol synthesis inhibitor mevastatin, but *drs2*Δ*kes1*Δ cells show resistance similar to wild-type. Deletion of *KES1* also suppresses the *drs2*Δ hypersensitivity to nystatin, a polyene antifungal compound that binds to ergosterol in the plasma membrane (Muthusamy *et al.*, 2009b). Taken together, these results may suggest *drs2*Δ causes an ergosterol synthesis defect that is suppressed by *kes1*Δ; however, *drs2*Δ cells appear to have an ergosterol concentration similar to wild-type cells (Fei *et al.*, 2008).

Although the total amount of ergosterol appears to be unaffected in *drs2*Δ cells, there is a change in how ergosterol is distributed throughout the cell. The researchers treated the strains with the fluorescent compound filipin that binds to ergosterol. Filipin primarily localizes to the plasma membrane in wild-type cells but accumulated in intracellular membranes in the *drs2*Δ and *kes1*Δ single mutants (Muthusamy *et*

al., 2009b). However, plasma membrane filipin localization was restored in the *drs2*Δ*kes1*Δ double mutant, indicating co-suppression. The researchers also found that Kes1-dependent transport of sterol was significantly increased in *drs2*Δ cells, whereas the transport rate for *drs2*Δ*kes1*Δ was similar to wild-type, consistent with Kes1 hyperactivity in the absence of Drs2 and vice versa. However, *KES1* suppression is not consistent for all known *drs2*Δ defects. Deletion of *KES1* does not suppress loss of asymmetry at the plasma membrane, the trafficking defect of the v-SNARE Snc1, or hypersensitivity to calcofluor white (Muthusamy *et al.*, 2009b).

My thesis work was based on this antagonistic relationship between Drs2 and Kes1 in sterol homeostasis. I hypothesized that the redistribution of ergosterol to intracellular membranes in *drs2*Δ and *kes1*Δ single mutants would affect the trafficking of exocytic proteins that associate with ergosterol-enriched lateral membrane domains ("lipid rafts") for their trafficking from the TGN to the plasma membrane.

Chapter II

Phosphatidylserine translocation at the yeast *trans*-Golgi network regulates protein sorting into exocytic vesicles*

ABSTRACT

Sorting of plasma membrane proteins into exocytic vesicles at the yeast *trans*-Golgi network (TGN) is thought to be mediated by their coalescence with specific lipids, but how these membrane remodeling events are regulated is poorly understood. Here we show that the ATP-dependent phospholipid flippase Drs2 is required for efficient segregation of cargo into exocytic vesicles. The plasma membrane proteins Pma1 and Can1 are missorted from the TGN to the vacuole in *drs2*Δ cells. We have also used a combination of flippase mutants that either gain or lose the ability to flip phosphatidylserine (PS) to determine that PS flip by Drs2 is its critical function in this sorting event. The primary role of PS flip at the TGN appears to be to control the oxysterol binding protein (OSBP) homologue Kes1/Osh4 and regulation of ergosterol subcellular distribution. Deletion of *KES1* suppresses plasma membrane missorting defects and the accumulation of intracellular ergosterol in *drs2* mutants. We propose that PS flip is part of a homeostatic mechanism that controls sterol loading and lateral segregation of protein and lipid domains at the TGN.

*This chapter has been published as Hankins, H. M., Sere, Y. Y., Diab, N. S., Menon, A. K., and Graham, T. R. (2015). Phosphatidylserine translocation at the yeast trans-Golgi network regulates protein sorting into exocytic vesicles. Mol. Biol. Cell *26*, 4674–4685.

INTRODUCTION

The TGN serves as a major sorting station for the delivery of post-Golgi cargo to different subcellular locations (Gu *et al.*, 2001; Papanikou and Glick, 2014). Cargo proteins travelling through the TGN are sorted into exocytic vesicles destined for the plasma membrane or are sorted into vesicles targeted to the endosomal system. Sphingolipid synthesis occurs in the Golgi, and lipids are also sorted at the TGN to produce exocytic vesicles enriched in sphingolipid and sterol relative to the TGN donor membrane (Klemm *et al.*, 2009). While many of the cargos leaving the TGN for endosomes are sorted by coat-dependent mechanisms (Robinson, 2004), exocytic vesicles enriched in sterol and sphingolipids do not associate with any known coat (Klemm *et al.*, 2009; Surma *et al.*, 2012). Lipid-dependent protein sorting ("lipid raft"-based sorting) has been proposed to explain how specific cargos are sorted into these vesicles; however, the mechanisms and proteins involved in this sorting process are not well understood (Simons and van Meer, 1988; Simons and Ikonen, 1997; Ikonen and Simons, 1998; Graham and Burd, 2011; Surma *et al.*, 2012). Several candidate proteins have been proposed to be involved in the sorting of cargo into exocytic vesicles, including the budding yeast oxysterol binding protein (OSBP) homologue Kes1/Osh4 (hereinafter referred to as Kes1), which has been previously identified in a screen for proteins involved in efficient exocytosis of plasma membrane proteins (Proszynski *et al.*, 2005).

OSBP and Kes1 have been proposed to mediate the unidirectional transport of ER sterol to the TGN where it is exchanged for Golgi phosphatidylinositol-4-phosphate (PI4P), thereby enriching sterol at the TGN (or directly at exocytic vesicles) (Im *et al.*, 2005; Mesmin *et al.*, 2013; Moser von Filseck *et al.*, 2015). The cycle is completed by delivery of PI4P to the ER where it is converted to phosphatidylinositol (PI) by the phosphatase Sac1 (Mesmin *et al.*, 2013). Genetic studies have implicated *KES1* as a negative regulator of TGN function in exocytosis (Jiang *et al.*, 1994; Fang *et al.*, 1996; Li *et al.*, 2002; Alfaro *et al.*, 2011), and that Kes1 acts in a mutually antagonistic manner with the phospholipid flippase Drs2 (Muthusamy *et al.*, 2009b). However, what impact the relationship between the OSBP homologue Kes1

and the flippase Drs2 has on the sorting of proteins into exocytic vesicles, in which ergosterol is highly enriched, is unclear.

There are five yeast flippases in the type IV P-type ATPase family: Neo1, Dnf1, Dnf2, Dnf3, and Drs2. This essential group of flippases generate and maintain plasma membrane asymmetry with PS and phosphatidylethanolamine (PE) primarily in the cytosolic leaflet and phosphatidylcholine (PC) and sphingolipids primarily in the outer (extracellular) leaflet (Kato *et al.*, 2002; Pomorski *et al.*, 2003; Saito *et al.*, 2004; Chen *et al.*, 2006). The mechanism of phospholipid recognition and translocation has been studied extensively with Drs2 and Dnf1 (Baldridge and Graham, 2012, 2013; Baldridge *et al.*, 2013), which are heterodimers with their beta subunits Cdc50 and Lem3, respectively (Saito *et al.*, 2004; Chen *et al.*, 2006; Furuta *et al.*, 2007; Takahashi *et al.*, 2011). Drs2 localizes to the TGN and appears to be the primary PS flippase in the cell but is also capable of flipping PE (Chen *et al.*, 1999; Hua *et al.*, 2002; Natarajan *et al.*, 2004; Liu *et al.*, 2008; Baldridge *et al.*, 2013). In contrast, Dnf1 dynamically traffics between the plasma membrane, endosomes, and TGN and preferentially flips lysophosphatidylcholine and lysophosphatidylethanolamine (Hua *et al.*, 2002; Pomorski *et al.*, 2003; Riekhof *et al.*, 2007; Baldridge *et al.*, 2013).

Residues defining these differences in substrate specificity have been mapped in Drs2 and Dnf1, and it is possible to tune their substrate preference through targeted mutagenesis. For example, substitution of QQ in the first transmembrane segment of Drs2 for GA (Dnf1 residues) disrupts the ability of Drs2 to flip PS without altering its ability to flip PE (Baldridge and Graham, 2013). Conversely, a N550S point mutation in Dnf1 allows it to flip PS in addition to its normal substrates (Baldridge and Graham, 2013; Baldridge *et al.*, 2013). Surprisingly, Dnf1-N550S, but not wild-type (WT) Dnf1, can replace the function of Drs2 *in vivo*, indicating that PS flip is the crucial function of Drs2 (Baldridge *et al.*, 2013; Xu *et al.*, 2013).

PS flip by Drs2 has been previously shown to be critical for TGN-associated trafficking pathways (Natarajan *et al.*, 2004; Xu *et al.*, 2013). Drs2 is required for bidirectional transport between the TGN and early endosomes as well as the formation of one class of exocytic vesicle; however, loss of Drs2 does not

appear to perturb the rate of protein secretion (Chen *et al.*, 1999; Gall *et al.*, 2002; Hua *et al.*, 2002; Liu *et al.*, 2008). Consistent with Drs2's TGN localization, studies by the Grinstein lab using the PS probe Lact-C2 in mammalian cells suggest that PS remains primarily in the lumenal leaflet of the ER and Golgi, but gets flipped to the cytosolic leaflet at the TGN (Fairn *et al.*, 2011; Hankins *et al.*, 2015a). This change in PS sidedness to the cytosolic leaflet is maintained when TGN-derived vesicles fuse with the plasma membrane, where PS is highly enriched. This finding suggests that the TGN is a major site of PS translocation and also that mammalian cells have PS flippase(s) at the TGN that function similarly to Drs2.

In this study, we investigated how the TGN-localized flippase Drs2 and the OSBP homologue Kes1 are involved in the lipid-based sorting of plasma membrane proteins into exocytic vesicles. To do this, we looked at the distribution of two plasma membrane proteins: the plasma membrane ATPase Pma1 and the arginine transporter Can1. Pma1 and Can1 have been proposed to traffic from the Golgi to the plasma membrane through a lipid-based (coat-independent) mechanism (Bagnat *et al.*, 2000, 2001; Opekarová *et al.*, 2005; Surma *et al.*, 2012). However, once at the plasma membrane, these proteins partition into distinct membrane compartments called the Membrane Compartments of Pma1 (MCP) and Can1 (MCC) (Malínská *et al.*, 2003; Grossmann *et al.*, 2007; Spira *et al.*, 2012; Ziółkowska *et al.*, 2012). We examined the distribution of these proteins both at the plasma membrane and throughout the cell to study the influence of transverse PS asymmetry on exocytic trafficking and lateral compartmentalization of the plasma membrane.

RESULTS

Compartmentalization of the plasma membrane is significantly perturbed in cho1Δ cells but not drs2Δ cells

To first determine if plasma membrane organization is perturbed in *drs2*Δ cells, we examined the segregation of Pma1-RFP and Can1-GFP into their respective compartments at the cell surface (Figure 2-1). In WT cells, Pma1-RFP and Can1-GFP colocalized little (Pearson's coefficient: -0.0044 ± 0.023) as

previously reported (Malínská *et al.*, 2003; Spira *et al.*, 2012). There was a small increase in colocalization of these proteins in *drs2*Δ cells (Pearson's coefficient: 0.030 ± 0.025), but not significantly so. This result suggests that PS asymmetry is not critical for the normal segregation of MCP and MCC at the plasma membrane. Because we did not see a strong defect when PS asymmetry was disrupted, we also tested if the absence of PS would have an effect on compartmentalization. To do this, we also imaged *cho1*Δ cells, which are unable to synthesize PS because they lack the PS synthase and must be supplemented with choline to be viable (Atkinson *et al.*, 1980). There was a significant increase in colocalization between Pma1-RFP and Can1-GFP in *cho1*Δ cells (Pearson's coefficient: 0.32 ± 0.047), suggesting that the absence of PS has a stronger disrupting effect on distinct membrane compartments at the plasma membrane than loss of PS asymmetry.

Pma1 and Can1 mislocalize to the vacuole when PS flippase activity is disrupted

Although there was not a significant defect in plasma membrane compartmentalization in *drs2*Δ cells (Figure 2-1), we did observe that the markers were accumulating internally. Pma1-GFP primarily localized to the plasma membrane in WT cells. However, a significant amount of Pma1-GFP mislocalized in *drs2Δ* cells (~25% reduction in plasma membrane fluorescence relative to WT cells) (Figure 2-2A, B). We determined that the internal Pma1-GFP was accumulating in the vacuole lumen by labeling the cells with FM4-64, which labels the vacuole limiting membrane (Figure 2-2D). When missorted to the vacuole, Pma1 has been found to enter the vacuole lumen where it is degraded by vacuolar proteases (Chang and Fink, 1995; Luo and Chang, 2000; Gaigg *et al.*, 2006). In addition, several GFP-tagged membrane proteins have been observed to sort to the vacuolar lumen through the multivesicular body pathway where GFP remains stable as the remainder of the fusion protein is degraded (Odorizzi *et al.*, 1998a; Prosser *et al.*, 2010). Consistent with these observations, the increased Pma1-GFP fluorescence in the vacuole lumen of *drs2*Δ relative to WT cells corresponds to a reduction in the full-length fusion protein and an increase in soluble GFP. In WT cells, 26.0% ± 4.7% of Pma1-GFP is degraded into soluble GFP, whereas

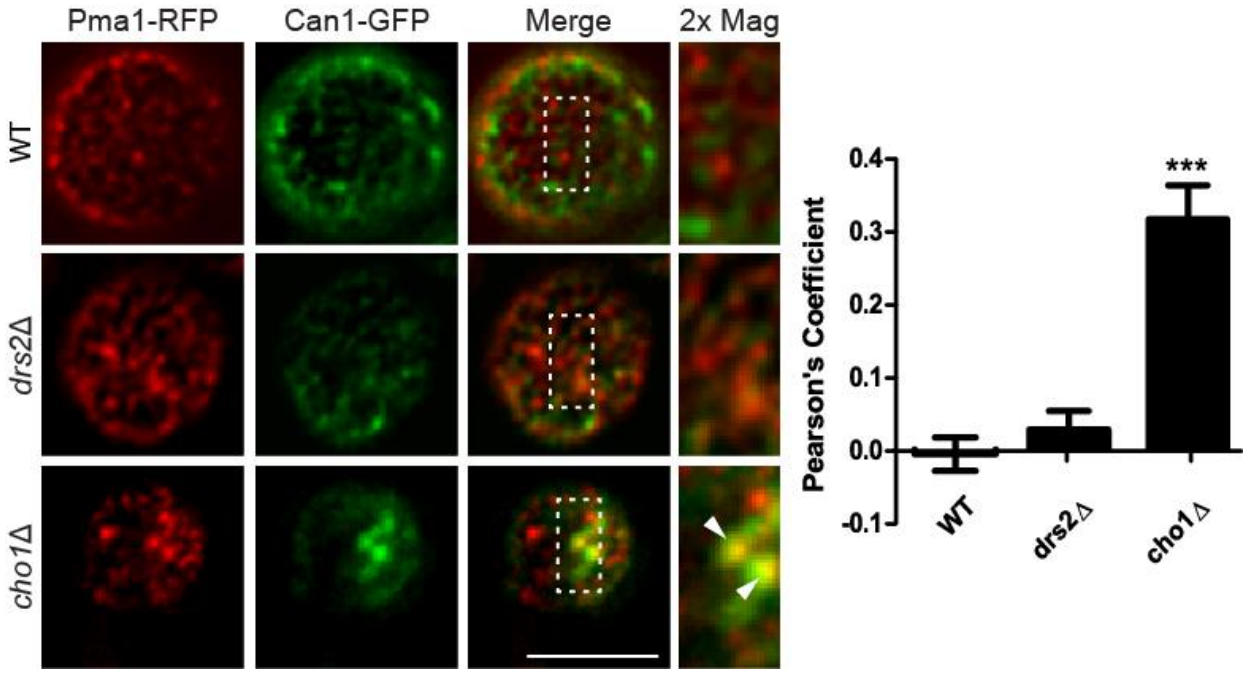

Figure 2-1. Plasma membrane compartmentalization is significantly perturbed in *cho1*Δ cells but not *drs2*Δ cells. Cells expressing Pma1-RFP and Can1-GFP and were grown to mid-log and imaged on a DeltaVision Elite Imaging system. Optical sections were collected every 200 nm. Images were deconvolved using the Deltavision software SoftWoRx. Arrowheads denote regions of colocalization. Colocalization of the two markers was determined using the ImageJ plugin Colocalization Finder on deconvolved images. Values represent mean ± SEM (n = 10 cells, one-way ANOVA, ***p<0.001). Scale bar, 5 µm.

44.5% ± 4.0% of Pma1-GFP is degraded in *drs2Δ* cells as detected by Western blotting with anti-GFP antibody (Figure 2-2C).

Drs2 primarily flips PS and to a lesser extent PE, so to distinguish which substrate is important for Pma1-GFP trafficking we used two flippase mutants that specifically lose (Drs2-[QQ->GA]) or gain (Dnf1-N550S) the ability to flip PS (Baldridge and Graham, 2013). Dnf1-N550S, but not Drs2-[QQ->GA], was able to restore WT-like Pma1 localization to the plasma membrane in *drs2Δ* cells (Figure 2-2A, B). This restoration was not due to adding an extra copy of *DNF1* as *drs2*Δ *DNF1* cells mislocalized Pma1-GFP comparably to *drs2*Δ cells. This finding suggests that PS flip is critical for normal localization of Pma1 at the plasma membrane. Consistently, Pma1 also mislocalized to the vacuole in *cho1*Δ cells (~30% reduction in plasma membrane fluorescence), which are unable to synthesize PS. The same results were

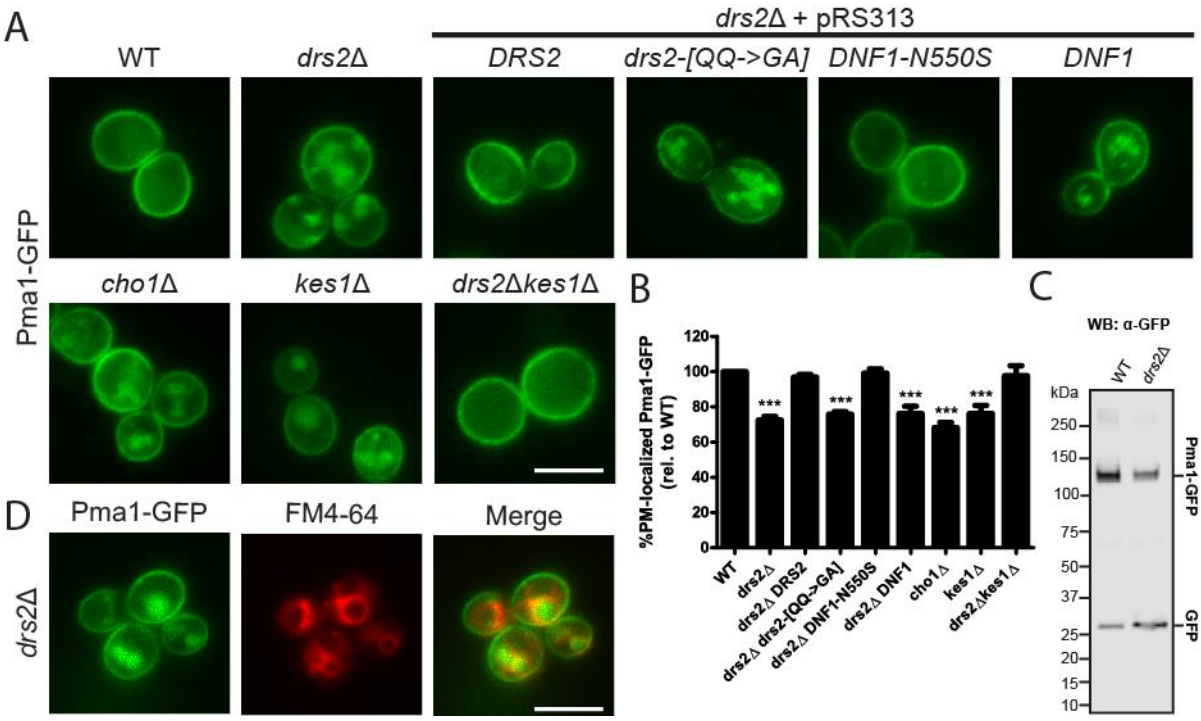

Figure 2-2. Pma1-GFP mislocalizes to the vacuole when TGN PS flippase activity or sterol loading is disrupted. (A) Cells expressing Pma1-GFP were grown to mid-log phase at 30°C and imaged. (B) %PM-localized Pma1-GFP was calculated by dividing plasma membrane fluorescence by total fluorescence with WT set to 100%. Values represent mean ± SEM (n = 3, total of 150 cells, one-way ANOVA, ***p<0.001). (C) WT and *drs2*Δ cells expressing Pma1-GFP were probed with anti-GFP antibody. Bands corresponding to full length Pma1-GFP (127 kDa) and soluble GFP (27 kDa) are indicated on the right. (D) To confirm vacuolar localization, mid-log phase cells were labeled with FM4-64 for 20 minutes. Scale bar, 5 µm.

observed for Can1 (Figure 2-3A-C), although the vacuolar mislocalization defect was stronger for Can1-GFP (~40% reduction in plasma membrane fluorescence) (Figure 2-3A, B) than Pma1-GFP (~25% reduction in plasma membrane fluorescence) (Figure 2-2A, B). These observations suggest that PS translocation across the TGN membrane is required for efficient sorting of Pma1-GFP and Can1-GFP to the plasma membrane.

Drs2 and Kes1 work antagonistically in the sorting of Pma1 and Can1

We observed the same antagonistic relationship between *drs2*Δ and *kes1*Δ in sorting plasma membrane proteins that has been described previously for ergosterol homeostasis (Muthusamy *et al.*, 2009b). Pma1 and Can1 mislocalized to the vacuole in both *drs2*Δ and *kes1*Δ single mutants but had a WT-like

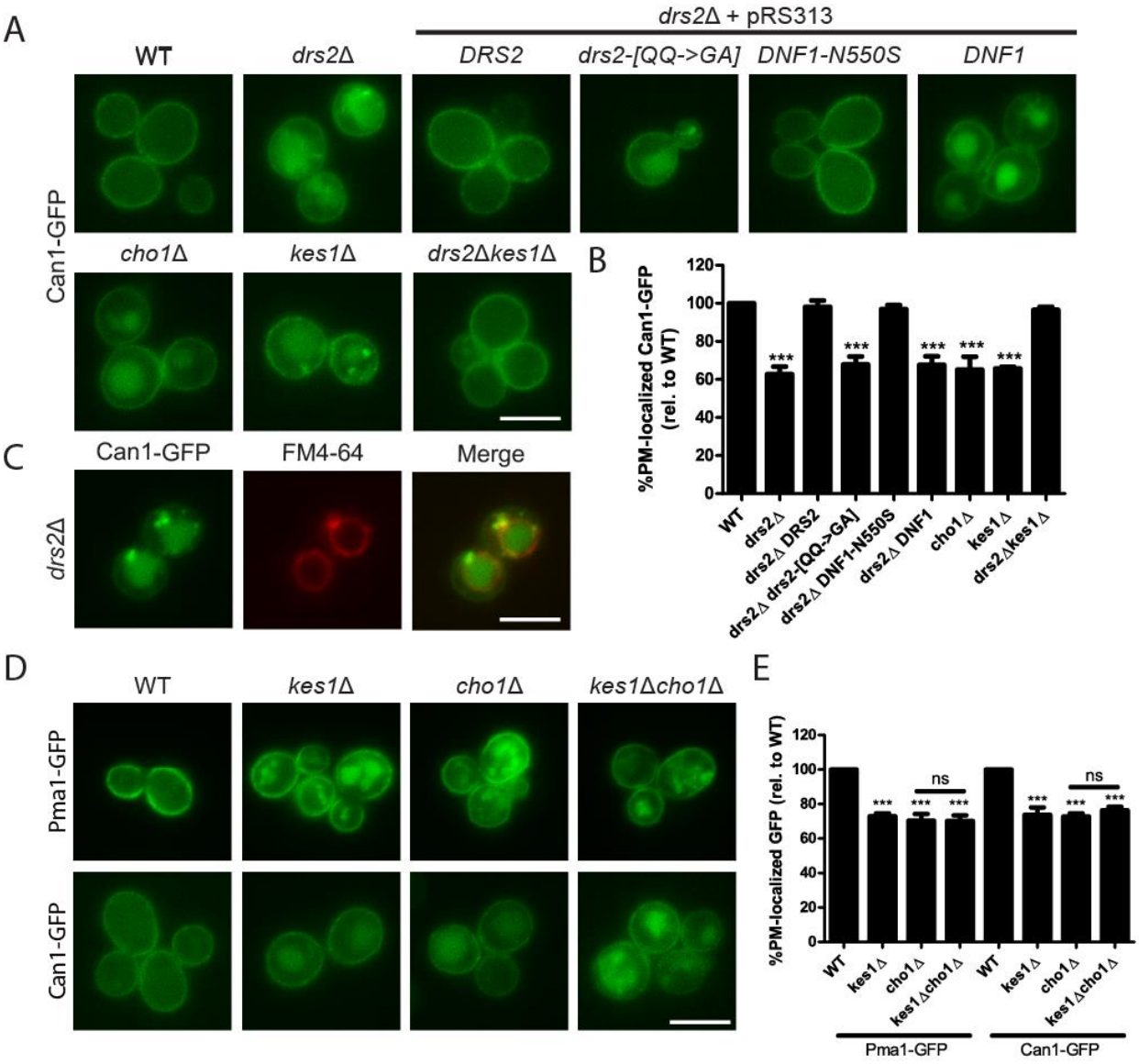

Figure 2-3. Can1-GFP mislocalizes to the vacuole when TGN PS flippase activity or Kes1 activity is disrupted. (A) Cells expressing Can1-GFP were grown to mid-log phase at 30°C and imaged. (C) To confirm vacuolar localization, mid-log phase cells were labeled with FM4-64. Scale bar, 5 µm. (D) Deletion of *kes1*Δ does not suppress *cho1*Δ defects in Pma1-GFP or Can1-GFP trafficking. (B and E) %PM-localized GFP was calculated by dividing PM fluorescence by total fluorescence with WT set to 100%. Values represent mean ± SEM (n =3, total of 150 cells, one-way ANOVA, ***p<0.001). Scale bar, 5 µm.

distribution in *drs2*Δ*kes1*Δ cells (Figure 2-2A-C and Figure 2-3A-C). These results indicate that the activities (or lack of activities) of these two proteins must be matched to facilitate normal trafficking of Pma1 and Can1 to the plasma membrane. Interestingly, *kes1*Δ cells did not suppress the *cho1*Δ defect in

Pma1 and Can1 mislocalization (Figure 2-3D, E), indicating that the presence of PS is required for their efficient plasma membrane localization and this deficiency cannot be overcome by disrupting *KES1*.

Role of PS in ergosterol enrichment at the plasma membrane

Previously, our lab showed that Drs2 and Kes1 act antagonistically to regulate sterol distribution between the plasma membrane and internal membranes (Muthusamy *et al.*, 2009b). Ergosterol is enriched at the plasma membrane, particularly in the MCC and is required for correct sorting of Can1 and other plasma membrane permeases (Umebayashi and Nakano, 2003; Malinska *et al.*, 2004; Grossmann *et al.*, 2006, 2007). Therefore, we next tested the influence of PS flippases on the cellular distribution of ergosterol to determine if PS flip is Drs2's critical role in sterol homeostasis.

We first used the fluorescent sterol-binding compound filipin, a polyene antibiotic (Norman *et al.*, 1972; Drabikowski *et al.*, 1973), to observe sterol distribution throughout the cell. Filipin primarily stains the plasma membrane of WT and *drs2*Δ*kes1*Δ cells, but we observed a ~20% reduction in filipin staining at the plasma membrane in *drs2*Δ *and kes1*Δ single mutants (Figure 2-4A, B), consistent with previous findings (Muthusamy *et al.*, 2009b). Transformation of *drs2*Δ with the *drs2-[QQ->GA]* mutant or WT *DNF1*, which do not recognize PS, failed to correct this defect, and the cells displayed an equivalent 20% reduction in plasma membrane ergosterol. In contrast, WT *DRS2* or *DNF1-N550S*, which can flip PS, completely restored plasma membrane ergosterol in *drs2*Δ cells. The sterol content of *drs2*Δ cells is similar to WT cells (Fei *et al.*, 2008) so these results suggest that PS translocation at the Golgi is required for normal sterol enrichment at the plasma membrane.

Interestingly, *cho1*Δ cells had highly variable filipin staining patterns ranging from a more severe defect than *drs2*Δ to WT-like, even within the same culture. On average, filipin staining of the plasma membrane was reduced in *cho1*Δ cells, but it was not statistically different from WT cells (Figure 2-4A, B). The *cho1*Δ cells were cultured and imaged under a variety of different conditions, but we were unable to pinpoint the source of variability in the filipin staining pattern. Another potential issue with using

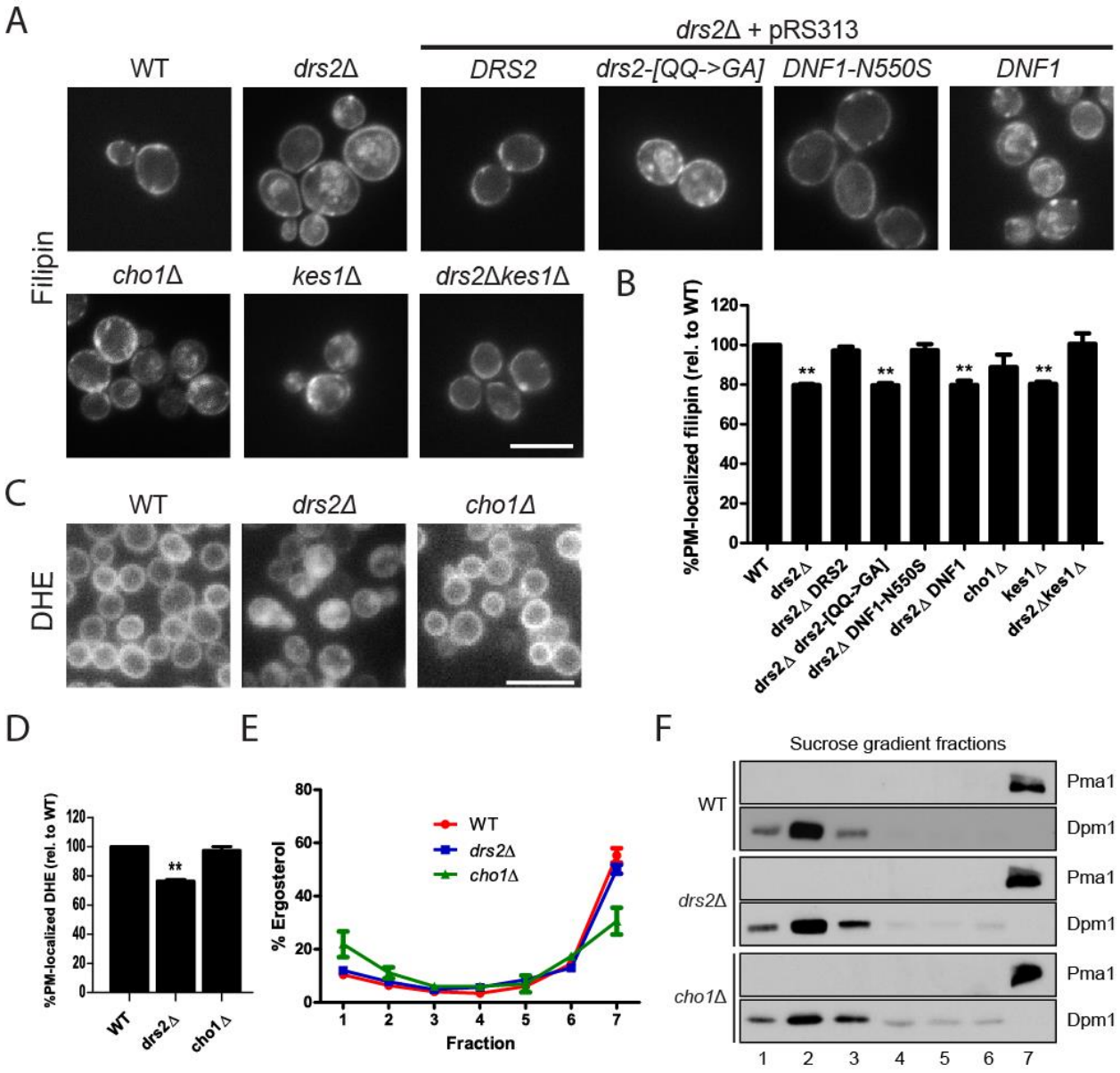

Figure 2-4. Observation of ergosterol distribution in cells using filipin staining, DHE uptake, and sucrose gradient fractionation. (A) Strains were grown at 30°C under aerobic conditions to mid-log phase and then fixed with 4% formaldehyde prior to staining with filipin. (B) %PM-localized filipin was calculated by dividing PM fluorescence by total fluorescence with WT set to 100%. Values represent mean ± SEM (n = 3, total of 150 cells, one-way ANOVA, **p< 0.01). Scale bar, 5 µm. (C) Strains were incubated at 30°C under hypoxic conditions for 36 hours in the presence of DHE. Scale bar, 10 µm. (D) %PM-localized DHE was calculated by dividing PM fluorescence by total fluorescence with WT set to 100%. Values represent mean ± SEM (n = 2, total of 100 cells, one-way ANOVA, **p< 0.01) (E) Strains grown at 30°C under aerobic conditions were subjected to sucrose gradient fractionation with the lower fractions corresponding to the ER and internal organelles and fraction 7 corresponding to the plasma membrane. (F) Western blots of sucrose gradient fractions from (E) with Pma1 used as a plasma membrane marker and Dpm1 as an ER marker to verify successful fractionation.

filipin staining as a readout for ergosterol localization is that filipin and other sterol-binding toxins may bind to other molecules or have nonlinear responses to sterol level (Maxfield and Wüstner, 2012).

To try to resolve the variability issues with the *cho1*Δ cells and potential issues intrinsic to filipin staining, we used a second approach to monitor subcellular sterol distribution. We examined cells containing dehydroergosterol (DHE), a fluorescent, naturally occurring sterol that closely mimics ergosterol and is able to functionally replace ergosterol in yeast (Georgiev *et al.*, 2011). Cells were grown under hypoxic conditions for 36 hours in medium supplemented with DHE to allow for sterol uptake, which effectively replaces >95% of the ergosterol with DHE (Georgiev *et al.*, 2011). Consistent with the filipin staining, DHE was primarily at the plasma membrane in WT but displayed increased localization to internal structures in *drs2*Δ cells (Figure 2-4C, D). Quantitatively, filipin and DHE both indicate a ~20% reduction in plasma membrane-localized sterol in *drs2*Δ relative to WT. Therefore, filipin appears to provide an accurate measure of ergosterol distribution in *drs2* mutants. Unlike the filipin staining, *cho1*Δ cells were uniformly WT-like, which may be due to differences in growth conditions between the two assays (i.e. growth under aerobic conditions for the filipin stain versus hypoxic conditions for DHE uptake).

For a third approach to further investigate changes in ergosterol distribution in *cho1*Δ cells, cells grown under aerobic conditions were lysed, and the plasma membrane was separated from the ER and other internal organelles by fractionation through a sucrose gradient. Ergosterol was quantified in each membrane fraction, and by this assay 55% of ergosterol in WT cells is at the plasma membrane (fraction 7). Plasma membrane ergosterol of *drs2*Δ cells was reduced to 50%, although this was not statistically different from WT. This lack of statistical significance may be due to the sucrose gradient assay not being sensitive enough to pick up on the relatively small defect observed by filipin staining and DHE fluorescence (the expected result was ~45% ergosterol in the *drs2*Δ plasma membrane fraction). Surprisingly, c*ho1*Δ cells displayed a significant depletion of plasma membrane ergosterol (30% of

ergosterol in plasma membrane fraction) relative to WT with a concomitant increase in fractions 1 and 2 corresponding to ER and internal organelles (Figure 2-4E, F).

The reason for these discrepancies in the three approaches is not clear but may reflect differences in sterol distribution under different growth conditions or the ability of different assays to reproducibly detect small differences in sterol distribution. However, we can conclude that PS is not absolutely required to enrich ergosterol at the plasma membrane because all *cho1*Δ cells lack PS and there are always cells in the population that are indistinguishable from WT when imaged with filipin or DHE. The PS and phosphatidylinositol synthases compete for the same precursor (CDP-diacylglycerol) (Kelley *et al.*, 1988) and perhaps increased synthesis of phosphatidylinositol in *cho1*Δ cells can partially compensate for the complete lack of PS. Disruption of *DRS2* does not substantially alter total cellular PS or PI levels (Chen *et al.*, 2006) but rather more subtly perturbs transbilayer PS distribution. In contrast to *cho1*Δ, the *drs2* mutants display a fairly uniform reduction of PM ergosterol as assayed by filipin or DHE and clearly perturb sterol homeostasis.

Pma1 and Can1 are missorted from the TGN to the vacuole in drs2Δ and cho1Δ cells

We next wanted to determine the route by which Pma1 and Can1 travel to the vacuole in the *drs2*Δ and *cho1*Δ mutants. The observed vacuolar mislocalization phenotype could either be due to increased endocytosis at the plasma membrane or due to misrouting of newly synthesized Pma1 and Can1 from the TGN to the vacuole through the endosomal system. To differentiate these two possibilities for Pma1, we used the actin polymerization inhibitor Lat-A to block endocytosis (Huang and Chang, 2011). As a positive control, we also imaged GFP-Snc1, an exocytic v-SNARE that constantly cycles between the TGN, plasma membrane, and early endosomes (Lewis *et al.*, 2000; Galan *et al.*, 2001).

In WT cells, Snc1 localizes to the bud plasma membrane because endocytosis is the slowest step of Snc1 recycling. In contrast, Snc1 accumulates intracellularly in the early endosomes of *drs2*Δ and *cho1*Δ cells, which have defects in Snc1 recycling (Hua *et al.*, 2002; Furuta *et al.*, 2007; Xu *et al.*, 2013). However, since newly synthesized Snc1 travels to the plasma membrane prior to arrival in the early endosomes, it

will accumulate at the plasma membrane when endocytosis is blocked. After 3 hours of Lat-A treatment, we found that GFP-Snc1 accumulated significantly more at the plasma membrane in all of the strains, indicating that Lat-A was effectively blocking endocytosis (Figure 2-5A, B). In contrast, Lat-A treatment did not shift the distribution of Pma1-GFP to the plasma membrane in *drs2*Δ and *cho1*Δ cells (Figure 2-5A, C). This observation suggests that Pma1-GFP is missorted directly from the TGN rather than being endocytosed from the plasma membrane.

To determine if Can1 was missorted at the level of the TGN or plasma membrane, we used an endocytosis-resistant Can1-GFP mutant (Can1^{end}-GFP). Can1^{end}-GFP has 3 N-terminal lysine residues that have been mutated to arginines (K42R/K45R/K47R). These mutations prevent the protein from undergoing ubiquitin-mediated endocytosis such that once Can1^{end}-GFP reaches the plasma membrane it should remain there (Charles Lin and Scott Emr, unpublished observations). Can1-GFP and Can1^{end}-GFP were both mislocalized in *drs2*Δ and *cho1*Δ to the same extent, indicating that Can1 is missorted from the TGN to the vacuole (Figure 2-5D,E). To ensure that Can1^{end}-GFP is indeed endocytosis-resistant, we induced Can1 endocytosis with 5 mM arginine (Figure 2-S1). There was a stark decrease in Can1-GFP, but not Can1^{end}-GFP, fluorescence at the plasma membrane in the presence of the high arginine concentration, confirming that Can1^{end}-GFP is endocytosis-resistant. These results indicate that TGN missorting, not endocytosis, is the route by which Can1-GFP is mislocalized to the vacuole in *drs2*Δ and *cho1*Δ cells.

Missorting of Pma1 and Can1 is not due to drs2Δ AP-1/Rcy1 trafficking defects

We next tested if the missorting of Pma1 and Can1 is due to previously described trafficking defects caused by disruption of Drs2 flippase activity. Drs2 is required for AP-1/clathrin trafficking between the TGN and early endosomes (Chen *et al.*, 1999; Liu *et al.*, 2008) and the Rcy1 recycling pathway from the early endosomes to TGN (Hua *et al.*, 2002; Furuta *et al.*, 2007). However, disrupting these two pathways by deleting an AP-1 subunit (*apl4*Δ) or *rcy1*Δ had no effect on Pma1 localization (Figure 2-6A, C). Can1 localized normally in *apl4*Δ cells, but there was a small increase in Can1 localization to puncta in *rcy1*Δ

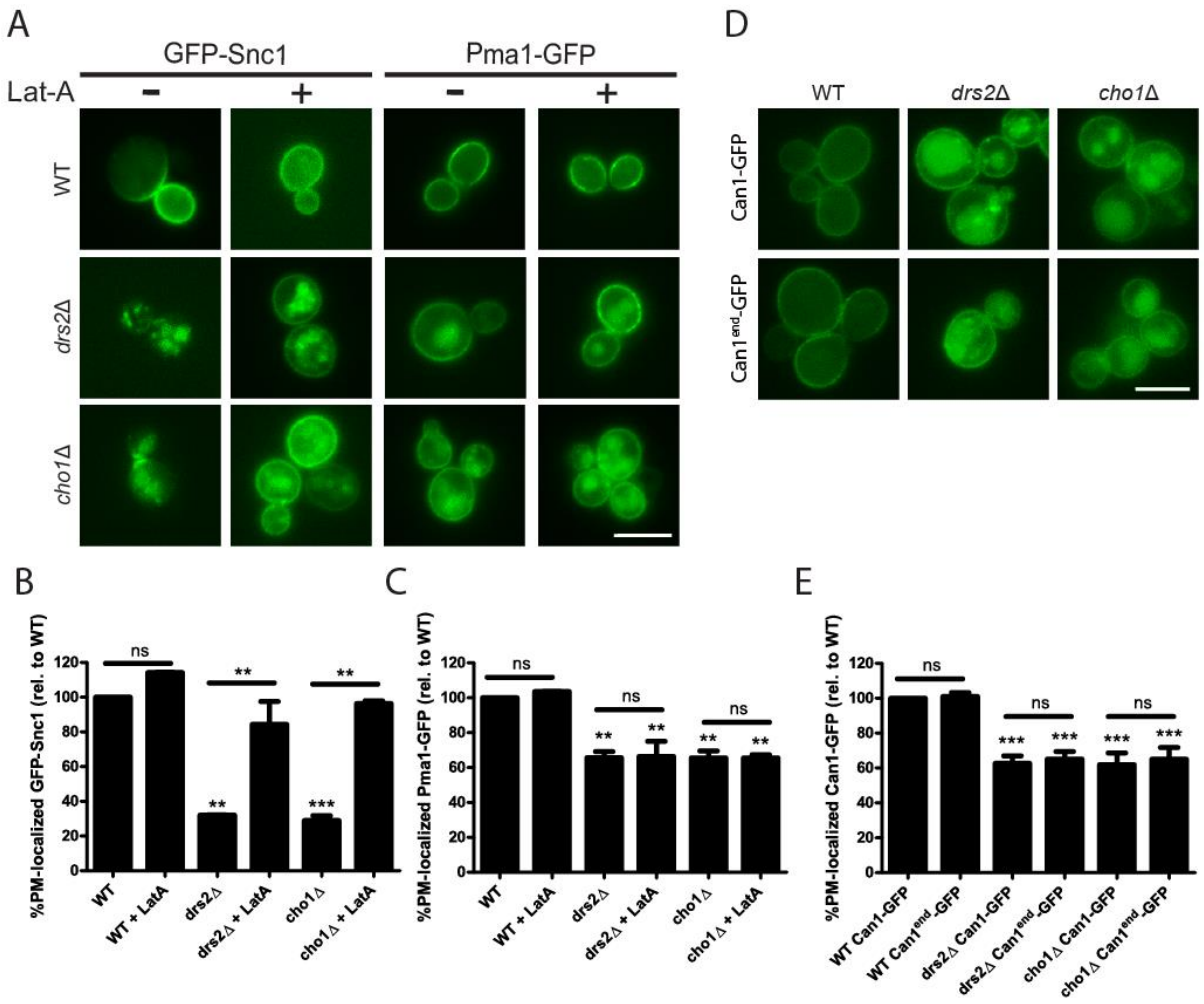

Figure 2-5. Pma1-GFP and Can1-GFP are missorted from the TGN to the vacuole in *drs2*Δ and *cho1*Δ cells. (A) Cells expressing GFP-Snc1 or Pma1-GFP were grown to mid-log phase before switching to medium containing 10 µM Lat-A and incubated for 3 hours at 30°C. (D) Cells expressing Can1-GFP or endocytosis-resistant Can1^{end}-GFP were grown to mid-log phase at 30°C and imaged. (B and C) Values represent mean ± SEM (n = 2, total of 100 cells). (E) Values represent mean ± SEM (n = 3, total of 150 cells). (B, C, and E) %PM-localized GFP of the mother cell was calculated by dividing plasma membrane fluorescence by total fluorescence with WT set to 100% (one-way ANOVA, **p<0.01, ***p<0.001). Scale bar, 5 µm.

cells (Figure 2-6B, D). However, the Can1 trafficking defect was very mild in comparison to *drs2*Δ (Figure 2-3A, B) and was phenotypically distinct. Therefore, it is unlikely that disruption of the Rcy1 recycling pathway is the cause of Pma1 and Can1 missorting to the vacuole in *drs2*Δ cells. In addition, we tested if disrupting other TGN-associated trafficking pathways would affect Pma1 and Can1 sorting. We

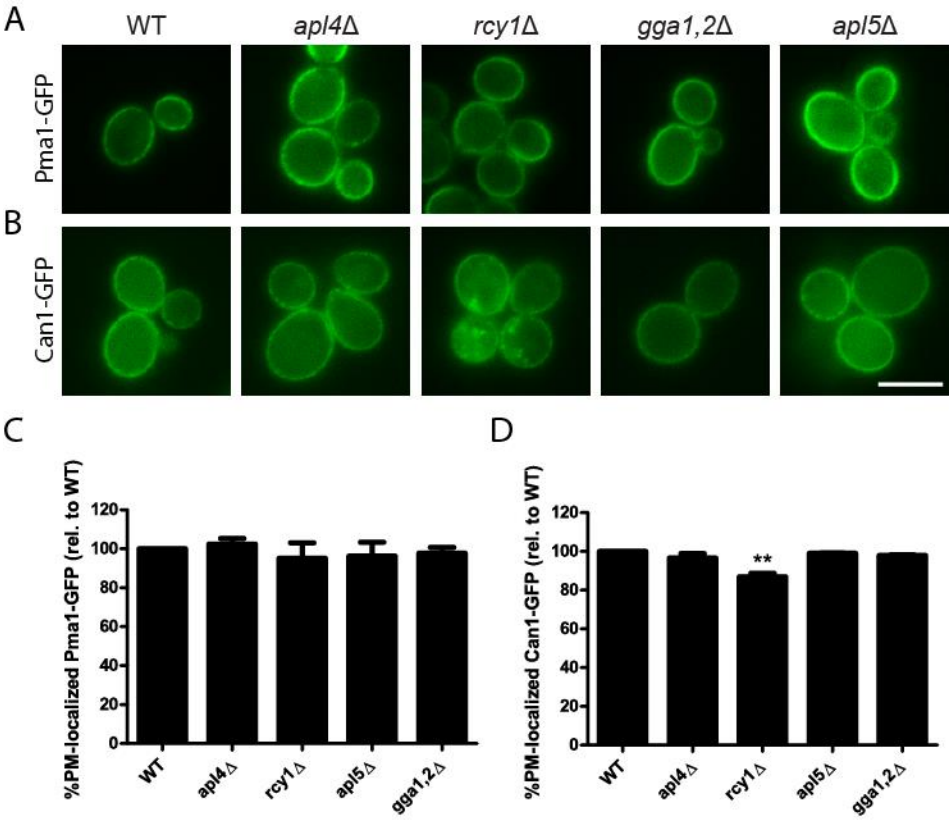

Figure 2-6. Missorting of Pma1 and Can1 is not due to disrupting other TGN-associated trafficking pathways. Cells expressing (A) Pma1-GFP or (B) Can1-GFP were grown to mid-log phase at 30°C and imaged. %PM-localized (C) Pma1-GFP and (D) Can1-GFP were calculated by dividing plasma membrane fluorescence by total fluorescence with WT set to 100%. Values represent mean ± SEM (n = 2, total of 100 cells, one-way ANOVA, **p<0.01). Scale bar, 5 µm.

disrupted the GGA pathway (*gga1,2*Δ) from the TGN to late endosomes and the AP-3 pathway (*apl5*Δ) from the TGN to the vacuole but observed no effect on Pma1 and Can1 sorting (Figure 2-6), further suggesting the *drs2*Δ missorting defect is not an indirect consequence of disrupting unrelated TGN trafficking pathways.

DISCUSSION

The experiments presented here show that PS flip by Drs2 at the yeast TGN is regulating the lipid-based sorting of proteins into exocytic vesicles. Pma1 and Can1 populate non-overlapping compartments of the plasma membrane, but partitioning into microdomains rich in ergosterol and sphingolipids is thought to concentrate both proteins into exocytic vesicles at the TGN (Klemm *et al.*, 2009; Surma *et al.*, 2012).

Evidence of Drs2's involvement as a sorting factor in this pathway is that disrupting *DRS2* causes 25 and 40% of Pma1 and Can1 to missort to the vacuole (Figure 2-2A, B and Figure 2-3A, B), respectively. Additionally, 20% of ergosterol appears to mislocalize to internal membranes in *drs2*Δ cells as assessed by filipin staining and DHE fluorescence (Figure 2-4A-D). These defects are specific to loss of PS flip because Drs2-[QQ->GA], which loses the ability to flip PS without altering the ability to flip PE (Baldridge and Graham, 2013), causes mislocalization of Pma1-GFP, Can1-GFP, and ergosterol to the same extent as *drs2*Δ. In contrast, Dnf1-N550S, which gains the ability to flip PS without altering transport of its normal substrates, fully restores efficient sorting of Pma1-GFP, Can1-GFP, and ergosterol localization to the plasma membrane in *drs2*Δ cells. However, Pma1-RFP and Can1-GFP that arrive at the plasma membrane of *drs2*Δ cells segregate normally into distinct membrane compartments, despite aberrantly exposing PS in the outer (extracellular) leaflet (Figure 2-1 and (Chen *et al.*, 2006)). Thus, lateral compartmentalization of the plasma membrane does not depend on PS transverse asymmetry.

Consistent with plasma membrane compartmentalization being unperturbed, the mislocalization of Pma1-GFP and Can1-GFP in *drs2*Δ cells is due to a defect in sorting at the TGN rather than an increased rate of endocytosis. Blocking endocytosis had no effect on Pma1-GFP and Can1-GFP delivery to the vacuole (Figure 2-5), which would be expected if *drs2*Δ destabilized the residence of these proteins within separate plasma membrane compartments. Missorting of Pma1-GFP and Can1-GFP is also independent of known *drs2*Δ defects in bidirectional trafficking between the TGN and early endosomes (AP-1/clathrin and Rcy1 recycling pathways) (Furuta *et al.*, 2007; Liu *et al.*, 2008) as disrupting these pathways had little to no impact on Pma1 and Can1 localization (Figure 2-6). We also observed no effect when we disrupted other TGN-associated trafficking pathways mediated by GGA and AP-3. These findings suggest that the Pma1-GFP and Can1-GFP missorting defects are not an indirect consequence of disrupting other coat-dependent TGN trafficking pathways but rather are a specific consequence of perturbing PS flip.

It is possible that failure to remove PS from the lumenal leaflet of the *drs2*Δ TGN disrupts the lipid-based segregation of plasma membrane proteins into regions of the membrane that are released from the TGN to become exocytic vesicles. This explanation is unlikely because *cho1*Δ cells, which lack PS, have the same degree of Can1-GFP and Pma1-GFP missorting as observed in *drs2* mutants (Figure 2-2A, B and Figure 2-3A, B). Moreover, deletion of *CHO1* has previously been shown to exacerbate, rather than suppress, *drs2* phenotypes (Natarajan *et al.*, 2004). These results suggest a positive role for PS in the formation of microdomains in the TGN, rather than a poisoning of microdomain organization in the lumenal leaflet when PS is present in the flippase mutant. While *cho1*Δ displayed substantial variability in ergosterol subcellular localization (Figure 2-4), these cells were uniformly defective in sorting Pma1 and Can1 (Figure 2-2A, B and Figure 2-3A, B). This observation again implies a positive role for PS in exocytic protein sorting that may be independent of sterol homeostasis. Therefore, we suggest it is either the physical displacement of PS across the TGN membrane or its appearance in the cytosolic leaflet that is crucial for concentrating Pma1 and Can1 into exocytic vesicles.

Translocation of PS across the TGN bilayer should have a number of effects on the biophysical properties of the membrane. The unidirectional movement of PS reduces the surface area of the inner (lumenal) leaflet while simultaneously expanding the outer (cytosolic) leaflet. This imbalance places stress on the membrane that can be relieved by membrane bending and budding of small diameter vesicles (Sheetz and Singer, 1974; Graham, 2004). Additionally, the PS head group carries a negative charge and also has an intrinsic positive curvature due to its conical shape that should accentuate membrane bending toward the cytosol (Fuller *et al.*, 2003). Consistent with this prediction, localization of a biosensor for membrane curvature and charge (+ALPS-GFP) to TGN and early endosomal membranes requires PS flip by Drs2 (Xu *et al.*, 2013). The induction of curvature by PS flip may be sufficient to facilitate sorting of lipids or proteins into subdomains of the TGN that give rise to exocytic vesicles (Roux *et al.*, 2005; Sorre *et al.*, 2009; Ryu *et al.*, 2014).

Another potential effect of unidirectional PS flip is that overcrowding the cytosolic leaflet could provide a driving force to push lipids that can spontaneously flip-flop, such as ergosterol, to the lumenal leaflet. Freeze-fracture electron microscopy studies of filipin-stained mammalian cells indicate that cholesterol moves in bulk across the bilayer to the lumenal leaflet during secretory granule formation (Orci *et al.*, 1980, 1981a, 1981b). This movement of cholesterol may coincide with the bulk movement of PS from the lumenal to cytosolic leaflet at the TGN (Fairn *et al.*, 2011). In yeast, this interleaflet exchange of PS for ergosterol may sufficiently concentrate ergosterol and sphingolipid in the lumenal leaflet to induce domain formation and partitioning of plasma membrane proteins into these domains. Once nucleated from the lumenal leaflet, the preference of the Pma1 and Can1 membrane domains for ergosterol and saturated phospholipid may propagate the microdomain organization to the cytosolic leaflet. Exocytic vesicles in budding yeast are significantly enriched for ergosterol relative to the TGN membrane from which they were formed (Zinser *et al.*, 1991, 1993; Klemm *et al.*, 2009). The source of this additional ergosterol may be the OSBP homologue Kes1, which is capable of loading the TGN membrane (or newly budded vesicle) with ergosterol in exchange for PI4P (Mesmin *et al.*, 2013; Moser von Filseck *et al.*, 2015).

Based on our current study, Drs2 and Kes1 are required for efficient sorting of Pma1 and Can1 to the plasma membrane. In the absence of PS flip or Kes1 activity, the TGN still buds exocytic vesicles that are delivered normally to the plasma membrane; however, Pma1 and Can1 are not efficiently concentrated into these exocytic vesicles and likely spill into vesicles targeted to the endosomal system. Genetically, *DRS2* and *KES1* appear to antagonize each other's activity (Muthusamy *et al.*, 2009b). Single mutants carrying *drs2*Δ or *kes1*Δ mutations display the same defect in Pma1 and Can1 localization, but the *drs2*Δ *kes1*Δ double mutant is indistinguishable from WT cells. This observation may seem to diminish the significance of flippases and OSBP homologues in this pathway, as they are dispensable; however, Drs2 and Kes1 are both members of large protein families with some degree of functional redundancy (7 OSBP homologs and 5 flippases are expressed in budding yeast). For instance, *kes1*Δ will suppress *drs2*Δ

phenotypes, but it does not suppress the lethality caused by deletion of *DRS2* and the *DNF* genes (*drs2*Δ*dnf1,2,3*Δ) (Muthusamy *et al.*, 2009b).

Our data suggest that it is critical to balance the activity of Drs2 and Kes1 during TGN membrane remodeling events to ensure correct sorting of proteins and lipids. Biochemical experiments support this idea: Drs2 PS flippase activity is two-fold higher in Golgi membranes purified from *kes1*Δ cells relative to WT cells (Muthusamy *et al.*, 2009b). Addition of recombinant Kes1 to *kes1*Δ Golgi membranes inhibited Drs2 to WT levels with an IC_{50} of ~100 fM (Muthusamy *et al.*, 2009b). Inhibition was likely caused by the ability of Kes1 to extract PI4P from the TGN, which is a stimulator of Drs2 activity (Natarajan *et al.*, 2009; Zhou *et al.*, 2013). Conversely, high concentrations of PS inhibit the ability of Kes1 to exchange sterol for PI4P in transfer assays with liposomes, potentially by trapping Kes1 on the membrane and causing a futile cycle of exchange with the same membrane (Saint-Jean *et al.*, 2011). Thus, Drs2-catalyzed PS translocation at the TGN may attenuate Kes1's ability to load ergosterol into the TGN. Therefore, we suggest that Kes1 overloads the TGN with ergosterol in situations when Drs2 is absent, when Drs2 cannot recognize PS (Drs2-[QQ->GA]), or when Drs2 cannot flip PS because PS is absent (*cho1*Δ cells). The similar phenotypes of *kes1*Δ and *drs2*Δ single mutants imply that overloading or underloading the TGN with ergosterol disrupts the balance required for concentrating Pma1 and Can1 into microdomains for their selective incorporation into exocytic vesicles.

MATERIALS AND METHODS

Media, strains, and plasmids

Yeast strains were grown in synthetic minimal medium (SD) containing required nutrients and 2% glucose. For experiments involving *cho1*Δ, the SD medium was supplemented with 1 mM choline (Sigma-Aldrich, St. Louis, MO). All yeast transformations were performed by the lithium acetate method (Gietz and Schiestl, 2007). PCR-based genomic integration of fluorescent tags was carried out according to the method described by Janke *et al.* (Janke *et al.*, 2004). The strains and plasmids used in this study are listed in Table 2-1 and Table 2-2, respectively.

Western Blot

Samples were prepared using a protocol modified from Chang and Slayman (Chang and Slayman, 1991). Cell pellets were resuspended in lysis buffer (10 mM Tris, pH 7.4, 0.3 M sorbitol, 0.1 M NaCl, and 5 mM $MgCl_2$) containing 1 mM phenylmethylsulfonyl fluoride and 1x protease inhibitor cocktail (ThermoFisher Scientific, San Jose, CA). The cells were then lysed by vortexing for 6 minutes with 1 minute pulses at 4°C. The beads were allowed to settle without centrifugation for 10 minutes at 4°C before removing the lysate supernatant. The lysates were then added 1:1 to Laemmli buffer and incubated at 37°C for 5 minutes. The samples were then subjected to SDS-PAGE and transferred to a PVDF membrane. For the anti-GFP western blot, an IR800CW secondary antibody was used and the bands were imaged and quantified using an LI-COR Odyssey CLx infrared imager and its software (LI-COR Biosciences, Lincoln, NE).

Vacuolar labeling with FM4-64

To confirm vacuolar localization of GFP-tagged Pma1 and Can1, mid-log phase (OD_{600} 0.5-0.8) cells were labeled with the lipophilic dye FM4-64 (Life Technologies, Grand Island, NY) as described previously (Babu *et al.*, 2012). Cells were labeled with 32 µM FM4-64 for 20 minutes in the dark at 30°C. The cells were then washed with 1x phosphate buffered saline (PBS) and resuspended in SD medium for 30 minutes at 30°C. The cells were washed twice in 1x PBS before imaging.

Filipin staining

To examine the distribution of ergosterol, cells were stained with filipin (Sigma-Aldrich, St. Louis, MO) using a protocol similar to the one described by Beh and Rine (Beh and Rine, 2004). 5 mL of mid-log phase (OD_{600} 0.5-0.8) cells grown in SD medium were fixed with 4% formaldehyde for 10 minutes at 30°C with shaking. The cells were then harvested and washed twice with 10 mL sterile water. The cells were resuspended in 1 mL sterile water, 0.2 mL of which was mixed with 3 µL of freshly prepared, ice

cold 5 mg/mL filipin in ethanol. The cells were then incubated with filipin for 15 minutes at 30°C in the dark prior to harvesting the cells and imaging.

Dehydroergosterol uptake assay

Dehydroergosterol (DHE) (Sigma-Aldrich, St. Louis, MO), a naturally occurring fluorescent sterol (McIntosh *et al.*, 2008), was used to visualize the distribution of ergosterol in living cells. Yeast strains were incubated with DHE under hypoxic conditions to allow for sterol uptake and imaged as described previously (Georgiev *et al.*, 2011; Gatta *et al.*, 2015). Briefly, yeast strains were inoculated from an overnight saturated liquid culture to OD_{600}~ 0.005 in 10 mL synthetic medium supplemented with 20 µg/mL DHE, 0.5% ethanol, and 0.5% Tween-80. The cultures, together with BD GasPak* EZ Anaerobe carbon sachets (BD Diagnostics), were placed inside an anaerobe incubation chamber, the chamber was then sealed and incubated at 30°C for 36 hours. The sachets reduce oxygen levels to 0.7% (v/v), yielding hypoxic conditions. At the end of the hypoxic incubation, the chamber was opened, and cells were energy-poisoned with ice-cold NaN3/NaF (10 mm/10mM) prior to imaging.

Sucrose gradient fractionation

Cell homogenates were analyzed by sucrose gradient fractionation as previously described (Georgiev *et al.*, 2011; Gatta *et al.*, 2015). A total of 7 fractions were collected from the top of the gradient, and each fraction was immunoblotted against Dpm1 (ER marker) and Pma1 (plasma membrane marker) to verify that the fractionation was successful.

Actin depolymerization

Latrunculin A (Lat-A) (Cayman Chemical Co., Ann Arbor, MI) was used to block endocytosis through inhibition of actin polymerization. Mid-log phase (OD_{600} 0.5-0.8) cells were harvested, resuspended in SD medium containing 10 µM Lat-A, and incubated for 3 hours at 30°C as described previously (Huang and Chang, 2011). Control cells were treated with an equal volume of ethanol.

Induction of Can1 endocytosis with arginine

Can1 endocytosis was triggered by the addition of arginine as described by Brach *et al*. (Brach *et al.*, 2011). Cells were grown to an OD of 0.4, harvested and resuspended in SD medium supplemented with 5 mM arginine. Cells were incubated for 3 hours at 30°C prior to imaging.

Fluorescence microscopy

Images of Pma1-RFP and Can1-GFP distribution at the plasma membrane were taken with a DeltaVision Elite Imaging system (Applied Precision, Issaquah, WA). A Z-stack was acquired with 200 nm intervals, and the images were deconvolved in SoftWoRx (Applied Precision, Issaquah, WA). Images of DHE were taken with an inverted microscope (Leica, Deerfield, IL) equipped with a cooled CCD camera (Princeton Instruments, Trenton, NJ) and MetaMorph software (Universal Imaging, West Chester, PA). To visualize DHE, a specially designed filter cube (Chroma Technology Corp., Brattleboro, VT) was used with a 355-nm (20-nm bandpass) excitation filter, a 365-nm longpass dichromatic filter, and a 405-nm (40-nm bandpass) emission filter. All other images were taken with an Axioplan microscope (Carl Zeiss, Thornwood, NY) equipped with a Zyla sCMOS 5.5 megapixel camera (Andor, Belfast, Northern Ireland) and micro-manager software (University of California, San Francisco, CA). Filipin was imaged using a DAPI filter set; GFP-tagged proteins were imaged using a GFP filter set; RFP-tagged proteins and FM4-64 were imaged using an RFP filter set. Images were merged and pseudocolored in ImageJ (National Institutes of Health, Bethesda, MD).

Data analysis

The percentage of filipin/Pma1/Can1/Snc1 localized to the plasma membrane (%PM-localized) was calculated by first outlining the outside of each cell using the freehand selection tool in ImageJ and measuring the total fluorescence of the cell ($Fluor_{Total}$). Next, the area just within the plasma membrane was outlined using the freehand selection tool to give the total internal fluorescence excluding the plasma membrane ($Fluor_{int}$). Next, the internal fluorescence was subtracted from the total to determine the

fluorescence at the plasma membrane ($Fluor_{Total} - Fluor_{int} = Fluor_{PM}$). Finally, the fluorescence at the plasma membrane was divided by the total fluorescence of the cell to give %PM-localized fluorescence ($Fluor_{PM}/Fluor_{Total}$ = %PM-localized). All quantification was performed using raw images. To determine the degree of colocalization between Pma1-RFP and Can1-GFP at the plasma membrane, individual cells taken from one slice of a deconvolved Z-stack were outlined using the freehand selection tool in ImageJ and copied into new images to produce two images, one in the GFP channel and one in the RFP channel. The ImageJ plugin Colocalization Finder (http://rsb.info.nih.gov/ij/plugins/colocalization-finder.html) was then used to calculate the Pearson's coefficient for each cell.

ACKNOWLEDGEMENTS

We thank Jason MacGurn, Scott Emr, Christopher Burd, and Roland Wedlich-Söldner for generously gifting us plasmids used in this study. We thank Fred Maxfield for the use of a fluorescence microscope to visualize DHE. We also thank Barbara O'Brien of the Vanderbilt University Medical Center Editors' Club for assistance with editing. Support for this project in the Menon lab was provided by the Qatar National Research Fund (NPRP 7-082-1-014). Research in the Graham lab is supported by a grant from the National Institutes of Health (1R01GM107978).

Table 2-1. Yeast strains used in this study.

Strain	Genotype	Plasmid	Source
BY4741	MATa *his3Δ1 leu2Δ0 ura3Δ0 met15Δ0*		Invitrogen
BY4742	MATα *his3Δ1 leu2Δ0 ura3Δ0 lys2Δ0*		Invitrogen
ZHY615M2D	MATα *his3Δ1 leu2Δ0 ura3Δ0 lys2Δ0 drs2Δ*		(Hua, et al. 2002)
RBY8700	MATa *his3Δ1 leu2Δ0 ura3Δ0 met15Δ0 cho1Δ::natNT2*		(Baldridge et al., 2013)
BMY02	BY4742 *kes1Δ::HIS3*		(Muthusamy *et al.*, 2009)
BMY01	ZHY615M2D *kes1Δ::HIS3*		(Muthusamy *et al.*, 2009)
HHY101	BY4742	pRS313	This study
RBY3901	ZHY615M2D	pRS313	(Baldridge and Graham, 2012)
RBY3904	ZHY615M2D	pRS313-DRS2	(Baldridge and Graham, 2012)
RBY3934	ZHY615M2D	pRS313-Drs2 [QQ->GA]	(Baldridge and Graham, 2013)
RBY3952	ZHY615M2D	pRS313-DNF1 N550S	(Baldridge and Graham, 2013)
RBY3946	ZHY615M2D	pRS313-DNF1	(Baldridge and Graham, 2012)
HHY102	RBY8700	pRS313	This study
HHY103	BY4742 *Pma1-GFP::hphNT1*		This study
HHY104	ZHY615M2D *Pma1-GFP::hphNT1*		This study
HHY105	RBY8700 *Pma1-GFP::hphNT1*		This study
HHY106	BMY02 *Pma1-GFP::hphNT1*		This study
HHY107	BMY01 *Pma1-GFP::hphNT1*		This study
HHY108	HH103	pRS313	This study
HHY109	HH104	pRS313	This study
HHY110	HH104	pRS313-DRS2	This study
HHY111	HH104	pRS313-Drs2 [QQ->GA]	This study
HHY112	HH104	pRS313-DNF1 N550S	This study
HHY113	HH104	pRS313-DNF1	This study
HHY114	HH105	pRS313	This study
HHY115	BY4742	pCHL571	This study
HHY116	HH101	pCHL571	This study
HHY117	ZHY615M2D	pCHL571	This study
HHY118	RBY3901	pCHL571	This study
HHY119	RBY3904	pCHL571	This study
HHY120	RBY3934	pCHL571	This study
HHY121	RBY3952	pCHL571	This study
HHY122	RBY3946	pCHL571	This study
HHY123	RBY8700	pCHL571	This study
HHY124	HH102	pCHL571	This study
HHY125	BMY02	pCHL571	This study
HHY126	BMY01	pCHL571	This study
HHY127	MATα *his3Δ1 leu2Δ0 ura3Δ0 kes1Δ::KanMX4 cho1Δ::natNT2*		This study
HHY128	HH127 *Pma1-GFP::HIS3MX6*		This study
HHY129	HH127	pRS313	This study
HHY130	HH127	pCHL571	This study
HHY131	HH115	pFS008	This study
HHY132	HH117	pFS008	This study
HHY133	HH123	pFS008	This study
HHY134	BY4742	pRS416-GFP-SNC1	This study
HHY135	ZHY615M2D	pRS416-GFP-SNC1	This study
HHY136	RBY8700	pRS416-GFP-SNC1	This study
HHY137	BY4742	pCHL572	This study
HHY138	ZHY615M2D	pCHL572	This study

HHY139	RBY8700	pCHL572	This study
BY4741 YPR029C	BY4741 *apl4Δ::KanMX6*		Invitrogen
BY4741 YJL204C	BY4741 *rcy1Δ::KanMX6*		Invitrogen
BY4741 YPL195W	BY4741 *apl5Δ::KanMX6*		Invitrogen
KLY691	*MATa his3Δ1 leu2Δ0 ura3Δ0 gga1Δ::KanMX6 gga2Δ::KanMX6*		(Liu *et al.*, 2008)
HHY140	BY4741 YPR029C *Pma1-GFP::hphNT1*		This study
HHY141	BY4741 YJL204C *Pma1-GFP::hphNT1*		This study
HHY142	BY4741 YPL195W *Pma1-GFP::hphNT1*		This study
HHY143	KLY691 *Pma1-GFP::hphNT1*		This study
HHY144	BY4741 YPR029C	pCHL571	This study
HHY145	BY4741 YJL204C	pCHL571	This study
HHY146	BY4741 YPL195W	pCHL571	This study
HHY147	KLY691	pCHL571	This study

Table 2-2. Plasmids used in this study.

Plasmid	Description	Source
pRS313		(Sikorski and Hieter, 1989)
pRS313-DRS2		(Natarajan and Graham, 2006)
pRS313-Drs2 [QQ->GA]	PS loss of flip flippase mutant	(Baldridge and Graham, 2013)
pRS313-Dnf1 N550S	PS gain of flip flippase mutant	(Baldridge and Graham, 2013)
pRS313-DNF1		(Liu *et al.*, 2007)
pCHL571	pRS416-pCAN1-CAN1-GFP	(Lin *et al.*, 2008)
pCHL572	Endocytosis-resistant pCHL571	(C. Lin and S. Emr, unpublished)
pFS008	pRS315-pPma1-Pma1-RFP	(Spira *et al.*, 2012)
pRS416-GFP-SNC1	GFP-tagged Snc1	(Lewis *et al.*, 2000)
pYM44	For integration of *GFP::hphNT1*at C-terminus	(Janke *et al.*, 2004)
pYM25	For integration of *Pma1-GFP::HIS3MX6* at C-terminus	(Janke *et al.*, 2004)

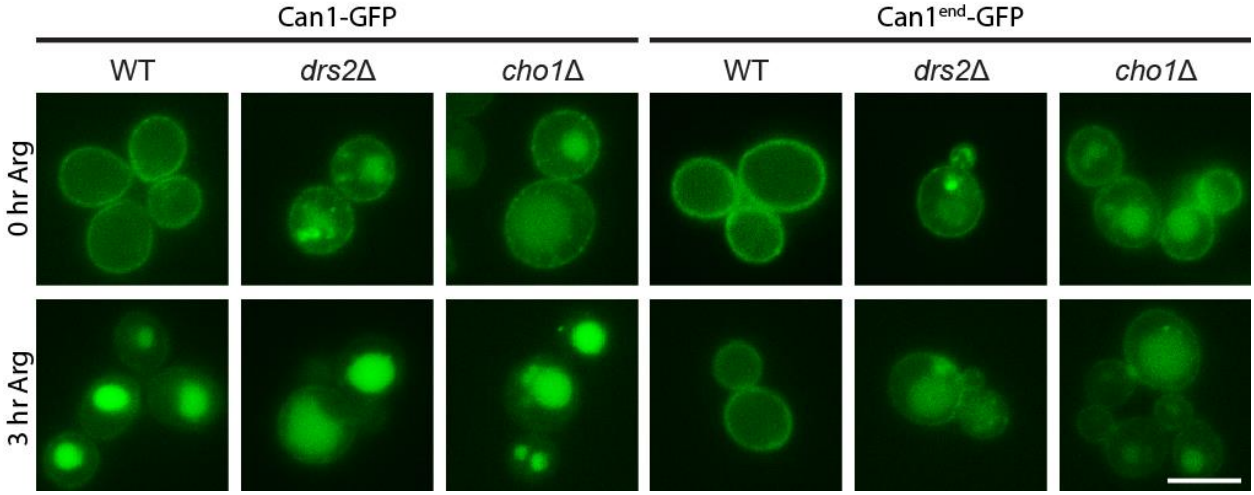

Figure 2-S1. Can1^{end}-GFP is resistant to arginine-induced endocytosis. Cells expressing Can1-GFP or endocytosis-resistant Can1^{end}-GFP were grown to an OD of 0.4 before shifting to SD medium containing 5 mM arginine. Cells were incubated at 30°C for 3 hours prior to imaging.

Chapter III

Lipidomic analysis of yeast flippase mutants

ABSTRACT

Drs2 is a TGN-localized flippase that translocates PS and, to a lesser extent, PE from the lumenal to the cytosolic leaflet. We have previously shown that loss of PS flip by Drs2 results in reduced cold tolerance at or below 20°C and defects in protein sorting into cholesterol- and sphingolipid-enriched exocytic vesicles at the TGN. Drs2 is thought to have a direct function in exocytic trafficking given its localization at the TGN; however, it is also possible that loss of membrane asymmetry in *drs2*Δ cells alters lipid homeostasis and that the defects are an indirect consequence of alteration in the cellular lipid composition. In this study, we performed a lipidomic analysis of flippase mutants to determine the impact loss of membrane asymmetry and changes in temperature have on the yeast lipidome and how these changes correlate with the *drs2*Δ defects in cold tolerance and exocytic trafficking. We found that sterol concentration is slightly, but likely not significantly, elevated in *drs2*Δ cells. There are also changes in how sphingolipids are regulated, but it is unclear if these changes contribute to the *drs2*Δ phenotypes. We did, however, identify a significant drop in PS levels with concomitant increases in the amount of di-unsaturated PC and PI in response to cold shift across all strains, which suggest these alterations likely contribute to maintaining membrane fluidity at low temperatures. Unexpectedly, we also found a potential new substrate, lyso-PI, for one or more of the Dnf flippases. This is a novel finding as lyso-PI is a lipid that no flippase to date has been shown to translocate.

INTRODUCTION

In addition to being a useful model organism for studying protein trafficking, *S. cerevisiae* is also an excellent model organism for studying lipid homeostasis. The yeast lipidome is relatively simple with only a few hundred lipid species compared to the thousands of lipid species in higher eukaryotes (Yetukuri *et al.*, 2008; Ejsing *et al.*, 2009; Nielsen, 2009; Santos and Riezman, 2012; Klug and Daum, 2014; Santos *et al.*, 2014). Despite the lower complexity of the yeast lipidome, many features of lipid metabolism are well conserved with mammals (Nielsen, 2009; Breslow and Weissman, 2010; Santos and Riezman, 2012). The ease in which yeast can be genetically manipulated allows for efficient mutation or deletion of genes involved in lipid metabolic pathways. For example, many of the genes responsible for the early steps of sphingolipid synthesis were first identified using yeast genetics and then used to identify the homologous genes in humans (Guillas *et al.*, 2001, 2003; Schorling *et al.*, 2001; Riezman, 2006).

Early studies of lipids in a cellular context relied on techniques, such as thin layer chromatography (TLC), that have low sensitivity and poor resolution. At the time, lipid profiles could only be delineated to the level of lipid classes with much of the complexity of the lipidome below the level of detection. The level of detection of lipid species has since greatly improved with the advent of gas chromatography (GC), high performance liquid chromatography (HPLC), and later mass spectrometry (MS) (Bou Khalil *et al.*, 2010; Santos and Riezman, 2012; Santos *et al.*, 2014). These technological advances have made it possible for researchers to achieve a high coverage of the yeast lipidome down to the level of individual molecular lipid species (Gaspar *et al.*, 2007; Ejsing *et al.*, 2009; Bou Khalil *et al.*, 2010; Santos and Riezman, 2012; Santos *et al.*, 2014).

The three major eukaryotic lipid classes are sterols, glycerophospholipids, and sphingolipids (Daum *et al.*, 1998; Guan *et al.*, 2010). For glycerophospholipids and sphingolipids, a large amount of lipid diversity arises from all the possible combinations of different headgroups and fatty acid chains. The latter of which is largely controlled by the actions of the fatty acid synthase (Fas1 and Fas2), Δ-9 desaturase (Ole1), and elongases (Elo1, Elo2, and Elo3) (Stukey *et al.*, 1989; Oh *et al.*, 1997; Martin *et*

al., 2007; Tehlivets *et al.*, 2007; Ejsing *et al.*, 2009; Santos *et al.*, 2014). Glycerophospholipids generally have saturated or mono-saturated fatty acid chains that are predominantly 16 or 18 carbons in length. In contrast, yeast sphingolipids contain a ceramide backbone, consisting of sphingosine (18 carbons) and a very long chain fatty acid (26 carbons), both of which are fully saturated.

Although many of the proteins directly involved in lipid synthesis have been identified, there is still little known about what pathways regulate lipid homeostasis and how lipid composition responds to changes in environment. Summarized in this chapter is a lipidomic analysis we performed in collaboration with Howard Riezman's lab at the University of Geneva (lipidomic analysis workflow summarized in Figure 3-2) to determine if there are any detectable changes in lipid composition that may account for the cold tolerance defect of *drs2*Δ cells (Muthusamy *et al.*, 2009b) or the exocytic trafficking defects (Hankins *et al.*, 2015b). Flippases generate membrane asymmetry, which is a fundamental property of eukaryotic cellular membranes. Given the importance of membrane asymmetry, it is possible that there are regulatory mechanisms that can detect and elicit changes in lipid composition in response to loss of asymmetry or, rather, the regulatory mechanisms normally in place are disrupted when membrane asymmetry is lost.

In the case of the cold sensitivity phenotype of *drs2*Δ cells, the defect may be linked to defective lipidome remodeling at low temperature. If this is true, we would expect to see changes in lipid concentration(s) that mirror the pattern of the cold sensitivity defect and its suppression. The oxysterol binding protein homologue Kes1 is not cold sensitive, but loss of Kes1 suppresses cold sensitivity of *drs2*Δ cells (Muthusamy *et al.*, 2009b). Thus, if the cold sensitivity phenotype is connected to changes in the lipidome, we would expect to see changes in lipid concentration(s) in *drs2*Δ cells shifted to 20°C for 3 hours but not in *kes1*Δ or *drs2*Δ*kes1*Δ cells.

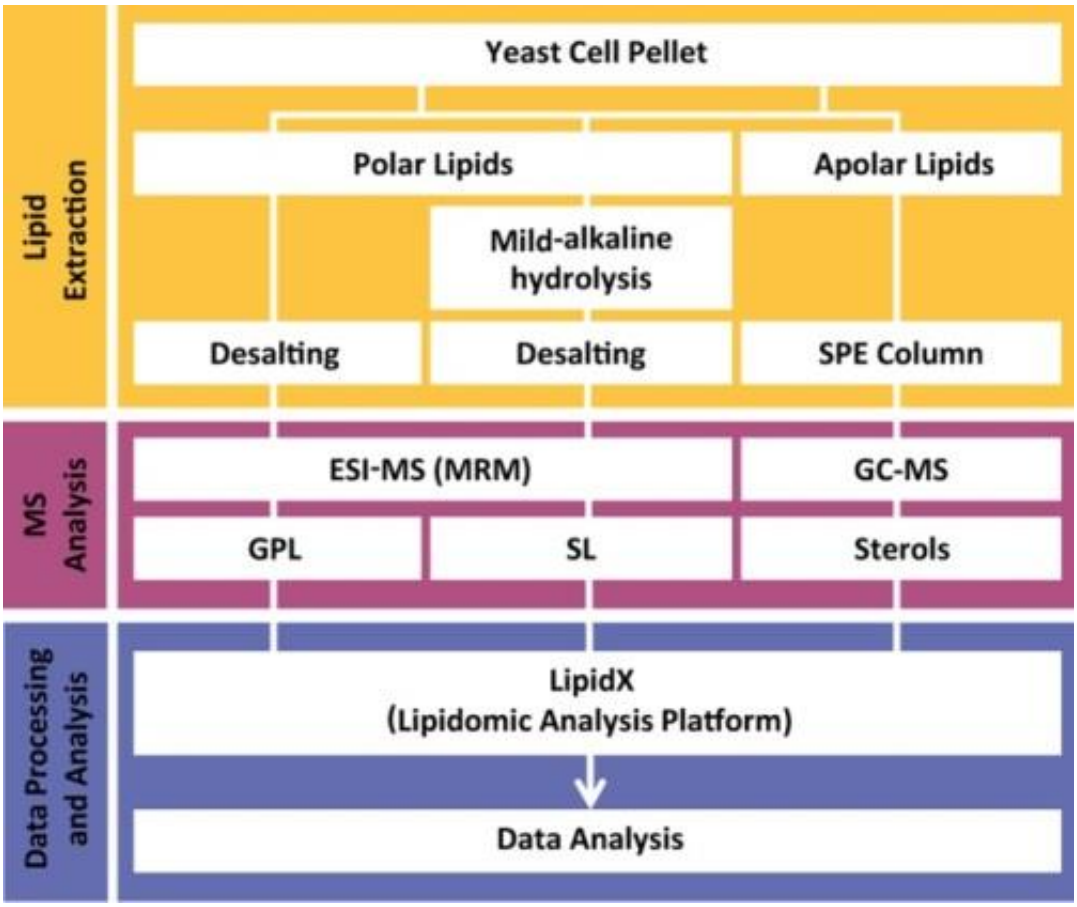

Figure 3-2. Flowchart of lipid extraction, mass spectrometric analysis, and data processing and analysis. Image is from Santos *et al*. 2014.

In the case of the exocytic trafficking defects of *drs2*Δ and *kes1*Δ mutants, we were particularly interested in changes in ergosterol or sphingolipid composition since mutations or treatments that perturb their synthesis have been linked to mislocalization of proteins that traffic to the plasma membrane via a domain-mediated mechanism (Surma *et al.*, 2012; Hankins *et al.*, 2015b). If changes in lipid concentration(s) are associated with the exocytic trafficking defects, we would expect to see changes in the lipidome that display the same pattern of co-suppression (altered in *drs2*Δ and *kes1*Δ mutants and WT-like in the *drs2*Δ*kes1*Δ double mutant). We hypothesized that there would be no major differences in lipid composition between WT and flippase or *kes1* mutants. If this hypothesis is correct, it would suggest

that the exocytic trafficking defects we observe are specific to loss of PS flippase activity at the TGN rather than an indirect consequence caused by an alteration in lipid composition.

RESULTS

Ergosterol levels are not significantly altered in flippase and kes1 mutants

Previous studies of the yeast lipidome have found that the concentration of the major yeast sterol, ergosterol, is relatively inflexible to changes in temperature, growth phase, or growth on different carbon sources (Klose *et al.,* 2012), suggesting that ergosterol levels are tightly regulated. Relative to WT cells, ergosterol levels are slightly elevated in *drs2*Δ and *kes1*Δ cells grown at 30°C, but appear WT-like in the *drs2*Δ*kes1*Δ double mutant (Figure 3-3A). However, these small differences are likely insignificant as other studies have failed to detect any difference in ergosterol concentration between WT and *drs2*Δ (or *cdc50*Δ) cells (Fei *et al.*, 2008; Muthusamy *et al.*, 2009b). We also observed no differences in ergosterol concentration when the strains were shifted to 20°C for 3 hours, which is consistent with a previous report that ergosterol concentration does not change in response to temperature (Klose *et al.,* 2012). We did not observed a significant change in ergosterol concentration when the *DNF* genes were deleted (*dnf1,2,3*Δ), suggesting the loss of other flippases also does not impact sterol homeostasis (Figure 3-3B).

Our findings suggest that even though ergosterol aberrantly accumulates intracellularly in *drs2*Δ and *kes1*Δ cells (Muthusamy *et al.,* 2009b; Hankins *et al.*, 2015b), the total amount of sterol in the cell is not substantially altered. This is also consistent with a previous report that deletion of *CDC50* (Drs2 chaperone) causes an increase in lipid droplet number and staining intensity despite unesterified ergosterol levels remaining unaffected in *drs2*Δ and *cdc50*Δ cells (Fei *et al.*, 2008). Our results suggest that the exocytic trafficking defects observed in *drs2*Δ and *kes1*Δ cells are unlikely to be an indirect effect of changes in total ergosterol concentration.

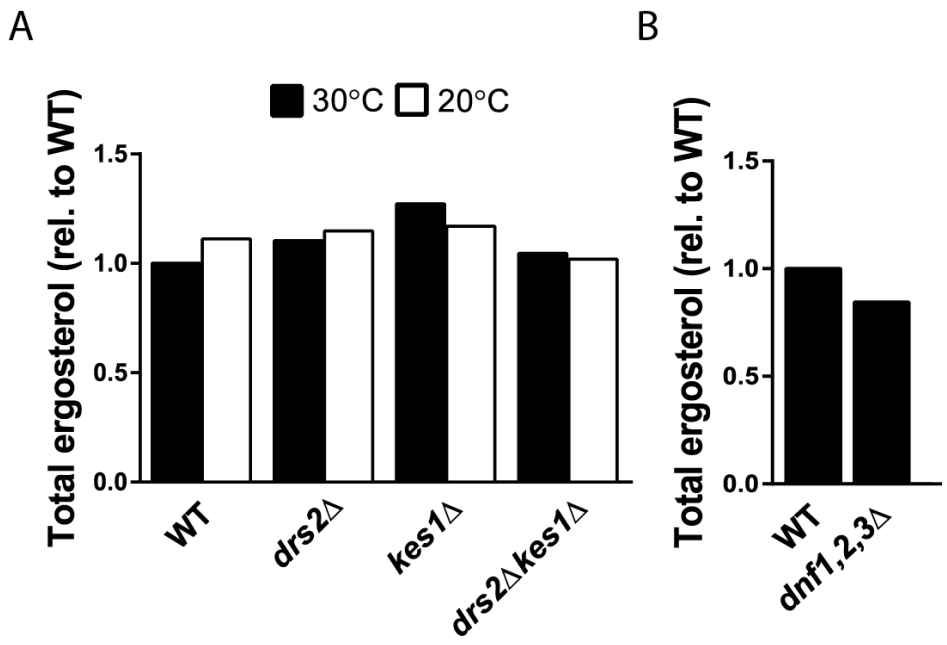

Figure 3-3. Total ergosterol level is relatively inflexible in response to (A) cold shift and (A, B) loss of flippases or Kes1. Data represented are the mean of three biological replicates. All values are relative to WT at 30ºC.

Sphingolipid biosynthesis is altered in flippase and kes1 mutants

Unlike mammalian sphingolipids, which have a considerable amount of diversity, there are only three major complex yeast sphingolipids and they all contain inositol and are synthesized from the less complex sphingolipid ceramide. The complex yeast sphingolipids in order of increasing complexity are inositol-phosphorylceramide (IPC), mannose-inositol-phosphorylceramide (MIPC), and mannose-(inositol-P)2-ceramide ($M(IP)_2C$) (Figure 3-4A). We first looked at the level of the less complex sphingolipid ceramide; ceramide levels modestly decreased in *drs2*Δ, *kes1*Δ, and *drs2*Δ*kes1*Δ cells similar to the drop that occurs in WT cells shifted from 30°C to 20°C (Figure 3-4B). The defects caused by *drs2*Δ, *kes1*Δ, and *drs2*Δ*kes1*Δ mutants are further exacerbated when the mutants are shifted to 20°C, although ceramide levels in *drs2*Δ cells decreased more than *kes1*Δ and *drs2*Δ*kes1*Δ cells. Interestingly, *dnf1,2,3*Δ cells had the most dramatic decrease in ceramide levels (Figure 3-4C), which suggests ceramide levels are more closely tied to the activity of one or more Dnf proteins rather than Drs2.

IPC levels were significantly decreased in *drs2*Δ cells at both 30°C and 20°C, but IPC levels in *kes1*Δ and *drs2*Δ*kes1*Δ were similar or slightly elevated relative to WT (Figure 3-4D). This is the pattern of suppression expected for changes that may correspond to cold sensitive growth. However, as in the case of ceramides, IPC levels were most significantly decreased in *dnf1,2,3*Δ cells, which are not cold sensitive (Figure 3-4E). The *dnf1,2,*3Δ triple mutant also does not appear to affect domain-mediated exocytic trafficking, so it is unlikely that the less severe alterations in ceramide and IPC levels in *drs2*Δ cells correlate with defective exocytosis at 30°C.

The concentration of MIPC was increased in the *drs2*Δ and *kes1*Δ single mutants, but was WT-like in the *drs2*Δ*kes1*Δ double mutant at 30°C (Figure 3-4F). This pattern of co-suppression at 30°C may suggest that elevated levels of MIPC may be negatively affect exocytic trafficking. Interestingly, MIPC levels increased 2.5-fold in WT cells after temperature shift to 20°C, whereas MIPC only slightly increased in *drs2*Δ, *kes1*Δ, and *drs2*Δ*kes1*Δ cells. This lack of responsiveness may suggest that the mutants are unable to appropriately detect and/or respond to changes in temperature. Unlike ceramides and the less complex IPC, the concentrations of MIPC was not altered in *dnf1,2,3*Δ cells (Figure 3-4G).

The concentration of the most complex sphingolipid, M(IP) $_2$C, was significantly increased in *drs2*Δ, *kes1*Δ, and *drs2*Δ*kes1*Δ cells at 30°C (Figure 3-4H), which does not fit the pattern of co-suppression expected if M(IP_2)C concentration is linked to the exocytosis defect. Similar to MIPC, WT M$(IP)_2$C concentration was very responsive to temperature shift to 20°C with a 3-fold increase. The flippase

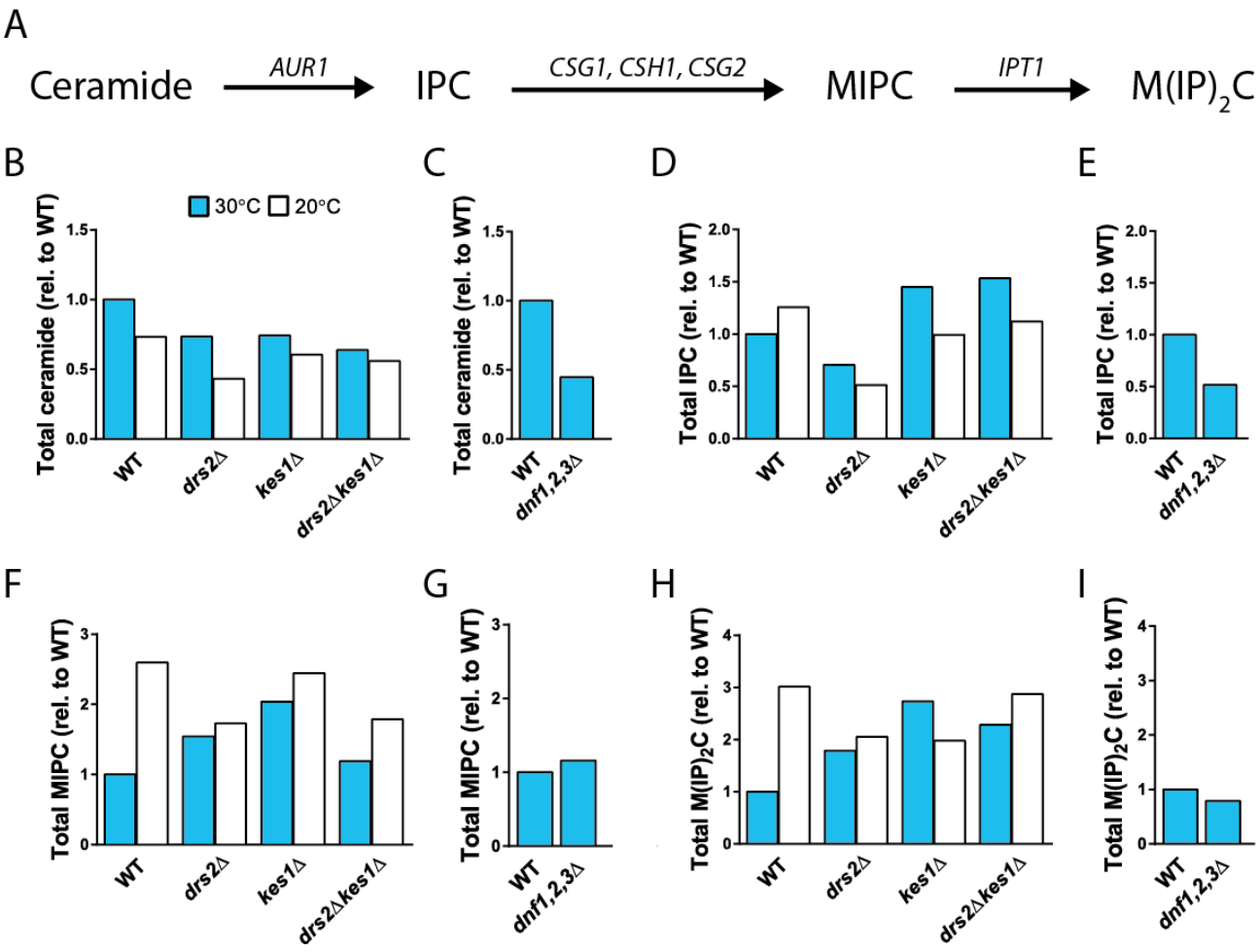

Figure 3-4. Changes in sphingolipid concentrations in response to cold shift or mutations. (A) Schematic of the final stages of complex yeast sphingolipid synthesis. Alterations in (B, C) ceramide, (D, E) IPC, (F, G) MIPC, and (H, I) $M(IP)_2C$ levels in response to cold shift or loss of flippases and Kes1. Data represented are the mean of three biological replicates. All values are relative to WT at 30ºC.

mutants had more modest changes in $M(IP_2)C$ levels with a slight increase in *drs2*Δ and *drs2*Δ*kes1*Δ upon temperature shift and a slight decrease in *kes1*Δ. Taken together with our MIPC results, our data suggest that cells respond to low temperatures with elevated levels of mannosylated sphingolipids, but this upregulation may be defective in *drs2* and *kes1* mutants. Like MIPC, $M(IP_2)C$ concentration was only slightly decreased in *dnf1,2,3*Δ cells (Figure 3-4I), indicating that the Dnf proteins are likely involved in ceramide and IPC homeostasis, but do not affect the levels of the more complex MIPC and $M(IP_2)C$. However, a caveat of these results is that it is difficult to reliably extract and quantify MIPC and $M(IP_2)C$

using our methods. This means we can detect trends in the data, but in the future we will need to use a second technique such as TLC to draw definitive conclusions.

Temperature, but not flippase or kes1 mutants, affects glycerophospholipid levels

We next examined the total concentrations of the glycerophospholipids phosphatidylcholine (PC), phosphatidylethanolamine (PE), phosphatidylinositol (PI), and phosphatidylserine (PS). We did not detect any significant changes in glycerophospholipid levels in *drs2*Δ, *kes1*Δ, and *drs2*Δ*kes1*Δ cells (Figure 3-5A). However, there was a general trend in reduced PS for all of the strains when shifted to 20°C, which suggests cells negatively regulate PS synthesis and/or increase PS conversion to PE in response to cold shift. The concentrations of the lipid species were also unaffected in *dnf1,2,3*Δ cells (Figure 3-5B), further indicating flippases do not regulate the total levels of any of the glycerophospholipid species.

Length of glycerophospholipid fatty acid chains is unchanged in flippase and kes1 mutants

Although we did not observe any changes to the total amounts of the different glycerophospholipid species, there could potentially be changes in the individual species produced in the mutants. One of the major determinants of glycerophospholipid diversity is fatty acid chain length. Most yeast glycerophospholipids have two fatty acid chains with a total of either 32 or 34 carbons, which we have designated short and long, respectively. We calculated the ratios of long/short fatty acid chains for PC, PE, PI, and PS but did not observe any significant changes in the flippase or *kes1* mutants, nor did we observe any changes upon shift to 20°C (Figure 3-6A, B).

Changes in degree of saturation in flippase and kes1 mutants and in response to temperature shift

Another way in which lipid species vary is the degree of saturation (0-2 double bonds) of their fatty acid chains. Membrane domains (lipid rafts) are proposed to contain primarily saturated lipids, so an increase in unsaturated lipids at 30°C could potentially impact their coalescence. On the other hand, unsaturated lipids have a fluidizing effect on membranes so a reduction in their levels at 20°C could negatively affect how the cell tolerates cold. At 30°C, we did not observe any changes in the lipid saturation of flippase and

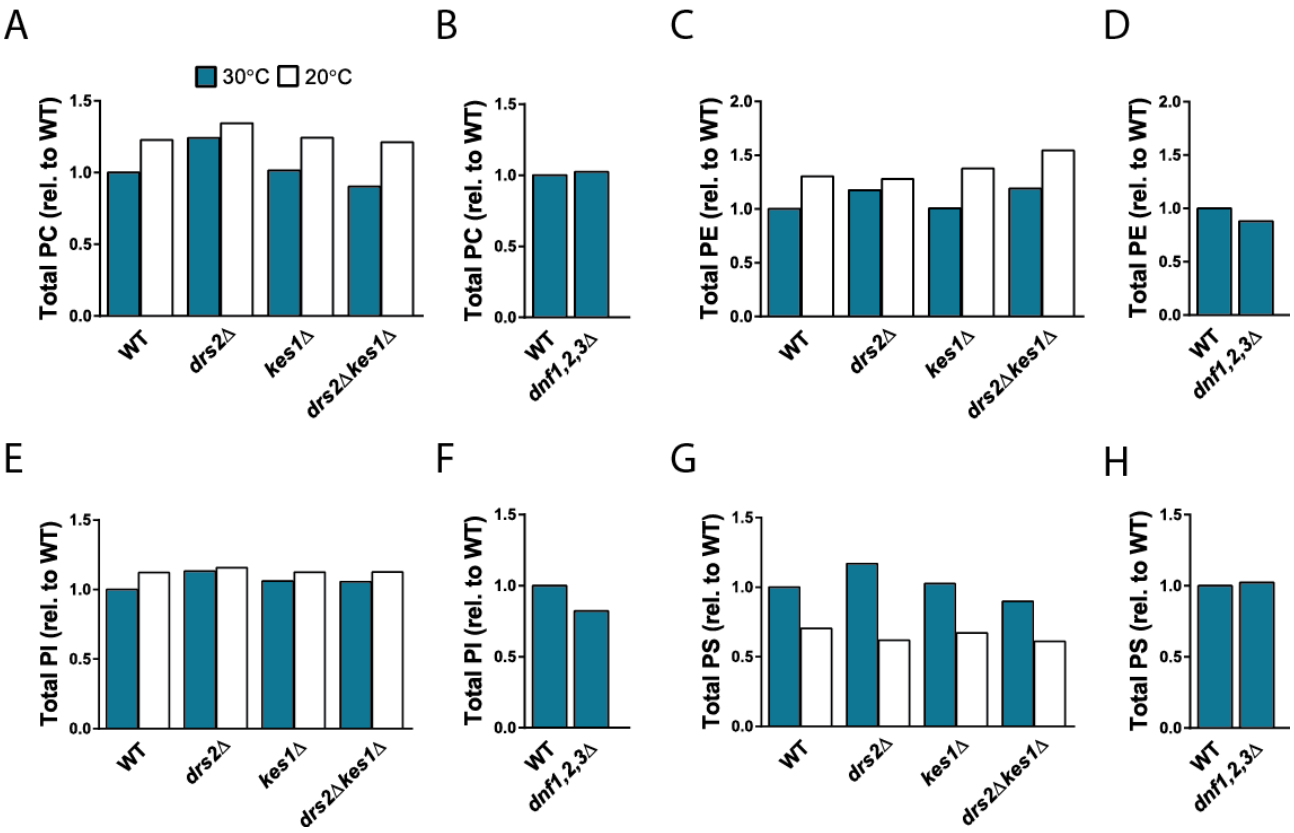

Figure 3-5. PS levels drop in response to cold shift. Alterations in (A, B) PC, (C, D) PE, (E, F) PI, and (G, H) PS levels in response to cold shift or loss of flippases and Kes1. Data represented are the mean of three biological replicates. All values are relative to WT at 30ºC.

kes1 mutants that fit the pattern of co-suppression expected if linked to the exocytic trafficking defect (data not shown). However, we did see temperature-dependent increases of both di-unsaturated PC and PE at 20°C (Figure 3-7). This increase in di-unsaturated PC and PE plus the decrease in total PS at 20°C are likely part of a homeostatic response to cold temperature to maintain membrane fluidity.

Lysophospholipids accumulate in dnf1,2,3Δ cells, but not drs2 and kes1 mutants

We next looked at the concentration of lysophospholipids, which are phospholipids with only one acyl chain. Accumulation of lysophospholipids can be disruptive to membrane stability as they resemble detergents. Cellular lysophospholipid levels are normally maintained at low concentration as lysophospholipids can be remodeled to diacylated phospholipids by cytosolic enzymes. However,

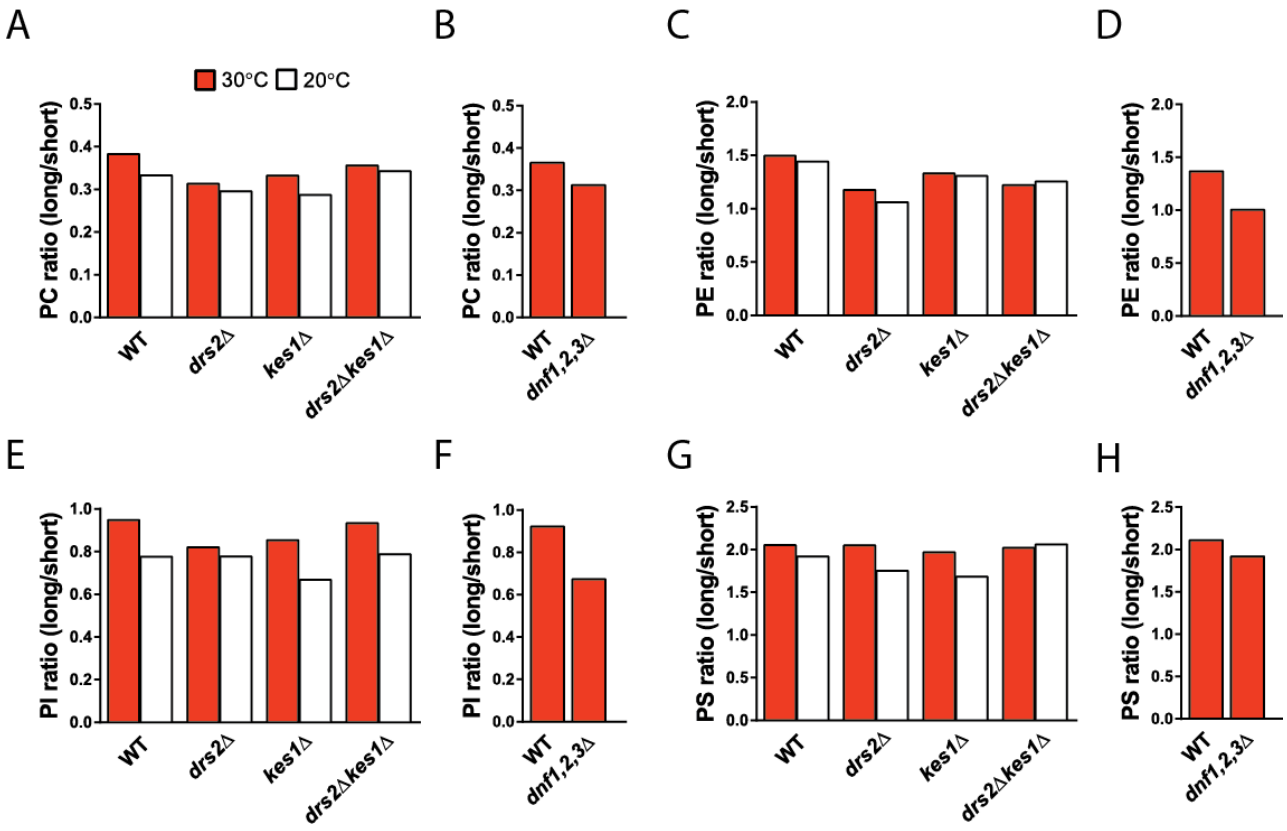

Figure 3-6. Fatty acid chain length is not significantly changed in response to cold shift or mutations. Alterations in (A, B) PC, (C, D) PE, (E, F) PI, and (G, H) PS levels in response to cold shift or loss of flippases and Kes1. Lipids that have fatty acid chains with 32 carbons or 34 carbons are designated short and long, respectively. Data represented are the mean of three biological replicates.

lysophospholipids in the extracellular/lumenal leaflet ("unflipped" lysophospholipids) would not be remodeled and thus may accumulate when a lysophospholipid-specific flippase is deleted.

For *drs2*Δ, *kes1*Δ, or *drs2*Δ*kes1*Δ cells, we found some decreases in the amount of individual lysophospholipids species, but no increases that would suggest lysophospholipids are accumulating at a disruptive level (Figure 3-8A, C, E, G). We also did not see any significant influence of temperature on lysophospholipid levels. Only one of the lysophospholipid species (lyso-PI) followed the pattern of defective *drs2*Δ and *kes1*Δ single mutants and WT-like *drs2*Δ*kes1*Δ double mutant, which would correspond with the sterol and exocytic trafficking phenotypes; however, it is unclear how a decrease in lyso-PI would alter sterol homeostasis or exocytosis.

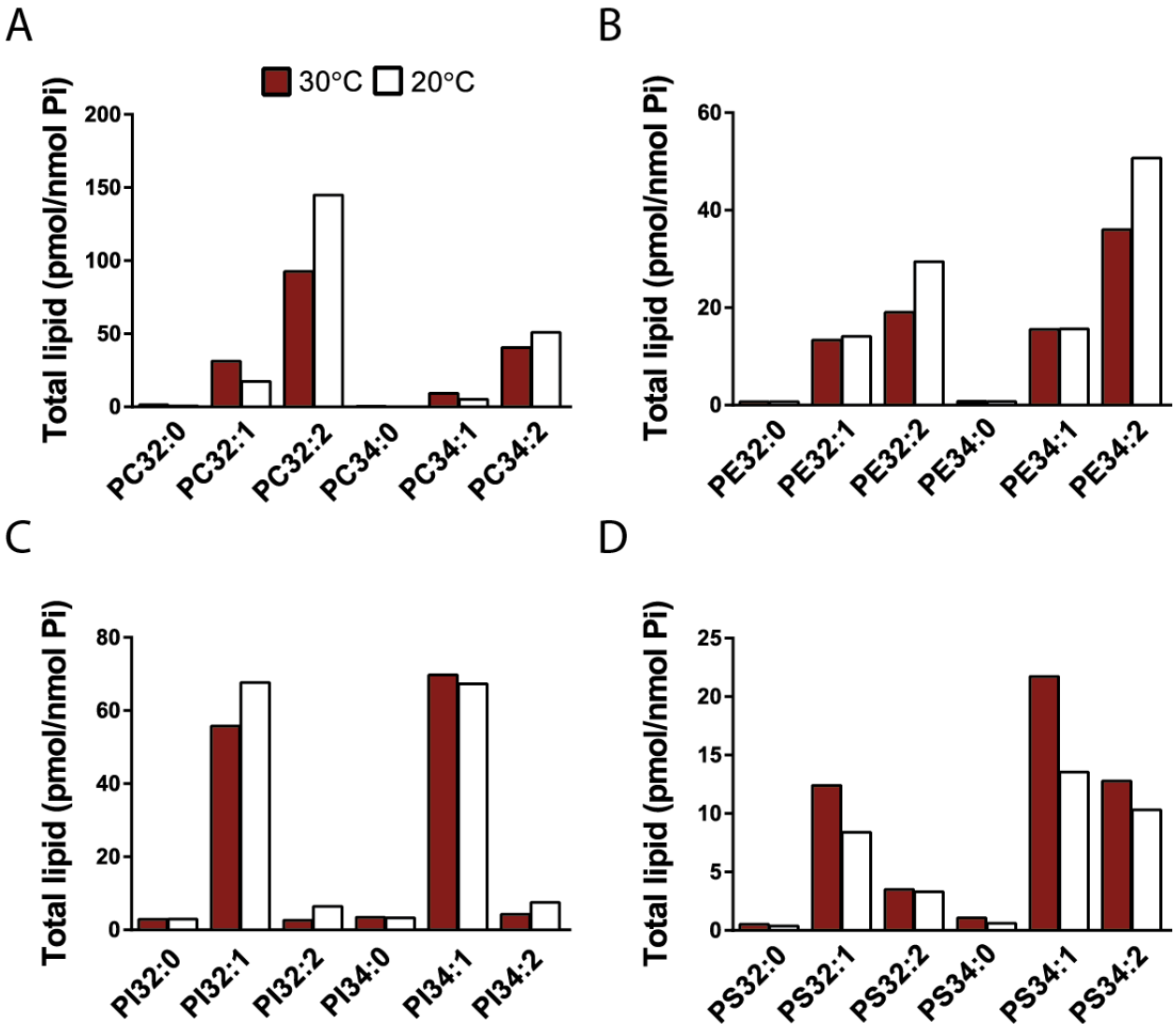

Figure 3-7. Levels of di-unsaturated PC and PE species increase in response to cold shift. Alterations in (A) PC species, (B) PE species, (C) PI species, and (D) PS species in response to cold shift in WT cells. Data represented are the mean of three biological replicates

In contrast to the relatively modest decreases in lysophospholipid levels in *drs2* and *kes1* mutants, *dnf1,2,3*Δ cells had large increases in lyso-PC, lyso-PE, lyso-PI, but not lyso-PS (Figure 3-8B, D, F, H). Dnf1 and Dnf2 have previously been shown to flip lyso-PC and lyso-PE (Baldridge *et al.*, 2013), so it was not surprising that lyso-PC and lyso-PE concentrations increased 2- and 4-fold, respectively, when the flippases were deleted. What was surprising was the 6.5-fold increase in lyso-PI in *dnf1,2,3*Δ cells, which

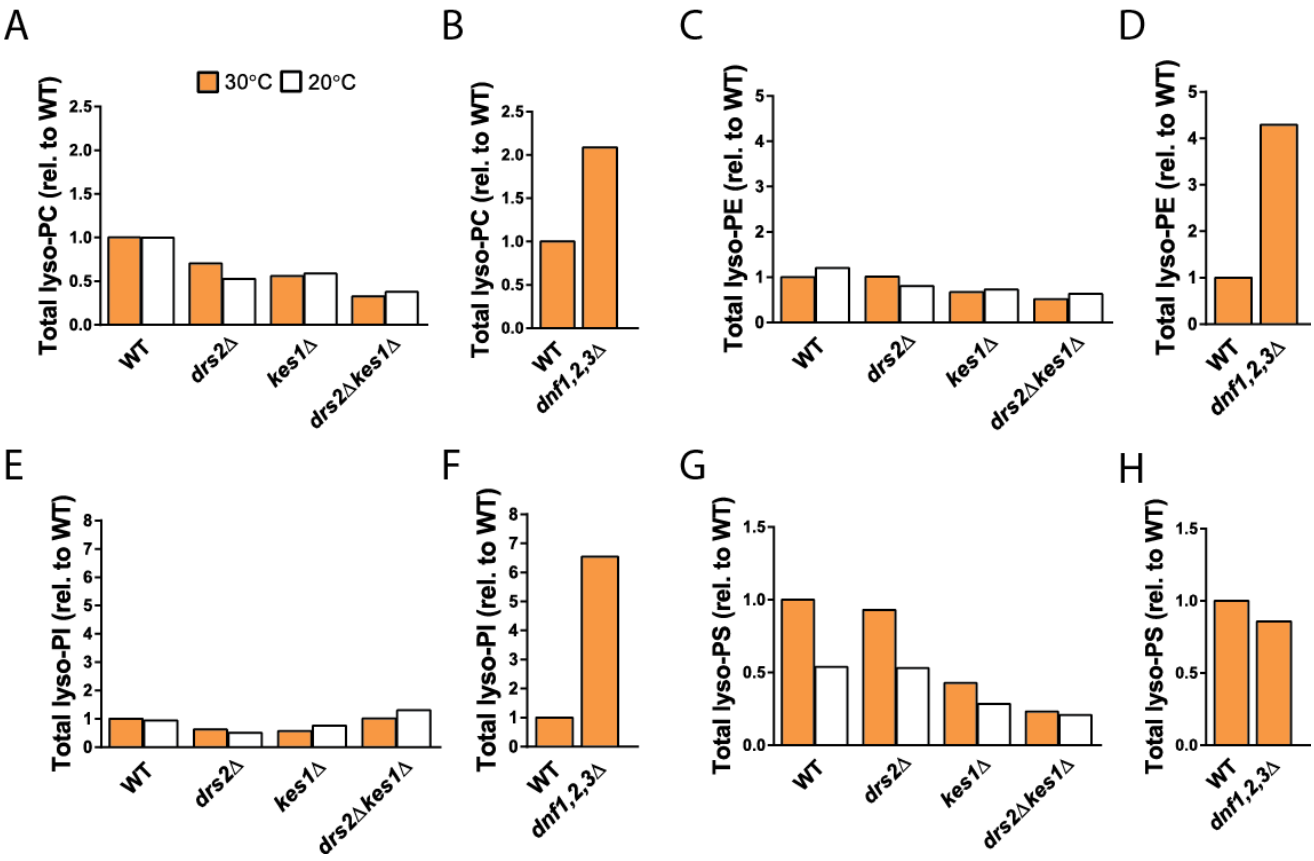

Figure 3-8. The concentrations of three lysophospholipid species are significantly increased in *dnf1,2,3*Δ cells. Alterations in (A, B) lyso-PC, (C, D) lyso-PE, (E, F) lyso-PI, and (G, H) lyso-PS levels in response to cold shift in WT cells. Data represented are the mean of three biological replicates. All values are relative to WT at 30ºC.

suggests one or more Dnf proteins flip lyso-PI. To date, no flippases have been shown to flip lyso-PI or di-acyl PI so this is a novel finding that requires further research to verify.

DISCUSSION

In this study, we looked for changes in the lipidomes of flippase mutants to determine if loss of membrane asymmetry alters cellular lipid composition and, if so, whether these alterations are linked to *drs2*Δ defects in cold tolerance or domain-mediated exocytosis. We found that the concentration of ergosterol was unresponsive to temperature change but was slightly elevated in the *drs2*Δ and *kes1*Δ single mutants. However, this difference is within the normal range of variability for this lipid species (Howard Riezman, personal communication) and not likely to be significant (Figure 3-3). This is

consistent with previous studies that reported ergosterol concentration is tightly regulated (Klose *et al.*, 2012) and is unaltered in *drs2*Δ and *cdc50*Δ cells (Fei *et al.*, 2008). These results suggest that although distribution of ergosterol appears to be altered in *drs2*Δ cells (Muthusamy *et al.*, 2009b; Hankins *et al.*, 2015b), the amount of ergosterol present is most likely unchanged.

Concentrations of ceramide and the complex yeast sphingolipids IPC, MIPC, $M(IP)_2C$ were considerably more responsive to mutations or changes in temperature. Ceramide levels decreased in *drs2*Δ, *kes1*Δ, and *drs2*Δ*kes1*Δ at both 30°C and 20°C but were most severely decreased in ***dnf1,2,3***Δ cells even at 30°C (Figure 3-4). IPC levels were also decreased in *drs2*Δ cells, but increased in *kes1*Δ and *drs2*Δ*kes1*Δ cells. However, both ceramide and IPC levels were most significantly decreased in *dnf1,2,3*Δ cells. Loss of Dnf proteins does not cause cold sensitivity and do not appear to impact domain-mediated exocytosis, so it seems unlikely that changes in ceramide and IPC levels perturb this process, especially since the decrease in ceramide and IPC is less drastic in *drs2*Δ cells.

Unlike ceramide and IPC, the concentrations of the more mature sphingolipids MIPC and $M(IP_2)C$ were largely unaffected in ***dnf1,2,3***Δ cells, but increased in *drs2*Δ and *kes1*Δ single mutants. However, the mutants were far less responsive to the cold shift-induced increases observed in WT cells. The elevated levels of mannosylated sphingolipids at 30°C and lack of responsiveness to cold shift may suggest that the *drs2* and *kes1* mutants are inappropriately sensing or responding to temperature. While a reduction in sphingolipid synthesis is known to negatively affect exocytic trafficking of certain proteins, such as Pma1 (Huang and Chang, 2011), it is not clear if or how increasing the level of MIPC and $M(IP_2)C$ would perturb exocytic trafficking. Due to some issues with reliably extracting and quantifying the mannosylated sphingolipids, further experiments will be needed to confirm if, and to what extent, MIPC and $M(IP_2)C$ levels are altered in the mutants and upon temperature shift.

We also looked at the total concentration of glycerophospholipids along with changes degree of saturation and fatty acid chain length and found some interesting changes in response to low temperature. Growth at lower temperatures increases the ordering of membrane lipids (i.e. membranes become more rigid), and

this can negatively affect the activity of membrane-associated proteins (Rodríguez-Vargas *et al.*, 2007). Many organisms, including budding yeast, have developed mechanisms to regulate membrane fluidity within considerable temperature ranges. For example, WT budding yeast strains can grow between 10-40°C. The most well-known change in lipid composition at low temperature is an increase in glycerophospholipids with unsaturated ("kinked") fatty acid chains, which decrease lipid packing and lower the melting point of the membrane (Nakagawa *et al.*, 2002; Rodríguez-Vargas *et al.*, 2007; van Meer *et al.*, 2008).

Consistent with previous reports on changes in lipid composition in response to cold shift, we found that the amount of di-unsaturated PC and PE species increased at 20°C, which may contribute to the maintenance of membrane fluidity at low temperatures. While there were no changes in the degree of saturation of PI and PS species, there was a substantial reduction in PS following cold shift to 20°C (Figure 3-5). Recent work from the Mayor lab suggests that PS in the inner leaflet is important for the formation of cholesterol rich GPI-anchor nanoclusters in the outer leaflet through transbilayer coupling (Raghupathy *et al.*, 2015). This finding could suggest that PS promotes localized membrane ordering in the opposite leaflet and that the reduction of PS levels at low temperatures is part of regulatory response to disrupt lipid coalescence and increase membrane fluidity. Although we observed changes upon temperature shift, we did not observe any significant changes in total glycerophospholipids, fatty acid chain lengths, or degree of saturation in the flippase or *kes1* mutants relative to WT at 30°C and 20°C (Figure 3-5, 3-6), indicating changes in these lipids are unlikely to contribute to the *drs2*Δ defects in cold sensitivity or exocytic trafficking.

We next looked at the concentration of lysophospholipids, which can be disruptive to membranes at high concentrations. Lysophospholipids are sparse within the cell and are thought to be primarily intermediates in the Lands cycle, where phospholipids are remodeled by cleavage of an acyl chain followed by re-acylation (Lands, 1958; Shindou *et al.*, 2009). However, if lysophospholipids are unable to be flipped and accumulate in the extracellular/lumenal leaflet because they are not accessible to acyltransferases, the

lysophospholipids may become detrimental to membrane stability. We found that the levels of lysophospholipids were subtly decreased in *drs2* and *kes1* cells (Figure 3-8), suggesting changes in lysophospholipid levels are unlikely to account for defective exocytosis. Remarkably, the most novel finding of our study was that levels of lyso-PC, lyso-PE, and lyso-PI were significantly increased in *dnf1,2,3Δ* cells. Dnf1 and Dnf2 are known to flip lyso-PC and lyso-PE (Baldridge *et al.*, 2013), but the implication that one or more Dnf proteins may flip lyso-PI is an exciting discovery as there are currently no known flippases that flip lyso-PI or di-acylated PI. Our future directions will focus on determining if lyso-PI is a substrate of the Dnf proteins and the residues involved in substrate recognition.

MATERIALS AND METHODS

Media, strains, and plasmids

Cell pellets were prepared as described as previously described (Santos *et al.*, 2014). Yeast cultures were grown in YPD with 2% glucose to saturation then diluted and grown to early exponential phase (1-2 OD_{600}/mL) with or without a 3 hour shift to 20°C as indicated. Cells were fixed by addition of trichloroacetic acid (TCA) to a final concentration of 5% (v/v) and cooled on ice. Cell pellets (25 OD_{600}) were washed with ice cold 5% TCA and rinsed with water. Pellets were flash frozen and stored at -80° in vials prior to lipid extraction. Strains used in this study are listed in Table 3-1.

Extraction and analysis of glycerophospholipids and sphingolipids

Extraction of lipids and analysis were performed as previously described (Guan *et al.*, 2010; Santos *et al.*, 2014). Briefly, cell pellets were resuspended in 1.5 mL of extraction solvent (15:15:5:1:0.018 ethanol, water, diethyl ether, pyridine, and 4.2 N ammonium hydroxide). A mixture of internal lipid standards (7.5 nmol of 17:0/14:1 PC, 7.5 nmol of 17:0/14:1 PE, 6.0 nmol of 17:0/14:1 PI, 4.0 nmol of 17:0/14:1 PS, 1.2 nmol of C17:0-ceramide, and 2.0 nmol of C8-glucosylceramide) were then spiked into the samples. Glass beads were added and the samples were vigorously vortexed to lyse the cells. The cell debris was pelleted and the supernatant was collected. Extraction was repeated and the two supernatants were pooled together

and dried under nitrogen. The sample was then resuspend and divided into two equal aliquots. One half was used for glycerophospholipids and the other for ceramides and sphingolipids, which was subjected to an extra step of mild-alkaline hydrolysis to reduce ion suppression due to glycerophospholipids. Both aliquots were then desalted, dried, and kept at -80°C prior to analysis.

For analysis by electrospray ionization-MS/MS using multiple reaction monitoring, lipid extracts were resuspended in 1:1 chloroform:methanol and diluted in 2:7:1 chloroform:methanol:water or 1:2 chloroform:methanol containing 5 mM ammonium acetate for positive and negative mode, respectively. Lipid species were identified and quantified using the internal lipid standards as previously described (Guan *et al.*, 2010; Santos *et al.*, 2014). Three biological replicates were used for each strain.

Extraction and analysis of sterols

Cell pellets were resuspended in 0.6 mL of water and 1.5 mL of methanol and vortexed with glass beads. 0.75 mL of chloroform was added and the samples were vortexed and centrifuged to pellet the beads and debris. The supernatant was collected and the beads were washed with 0.6 mL of chloroform:methanol and the supernatant was combined with the first one and 0.4 mL of water was added to induce phase separation. The samples were then centrifuged and the aqueous phase was discarded and the organic phase was transferred to a new tube and dried. Samples were resuspended in chloroform and fractionated on a solid-phase extraction column. The samples were then eluted by edition of chloroform and the sterol-containing eluent wad dried under a stream of nitrogen before storage. The extracted sterols were analyzed by GC-MS as previously described (Guan *et al.*, 2010; Santos and Riezman, 2012).

Phosphate measurement

The amount of lipids were normalized to the amount of inorganic phosphate present in the lipid extract as previously described (Santos *et al.*, 2014). For each sample, the total lipid extract was resuspended in 0.5 mL of 1:1 chloroform:methanol of which 50 µL was removed and placed in new tube. After solvent evaporation, 20 µL of water and 140 µL of 70% perchloric acid were added. The samples were then

heated for 1 hr at 100°C and cooled for 5 min at room temperature. Next, 800 µL of 5:2:1 water:1.25% NH_4 molybdate:1.67% ascorbic acid was added to the tubes. The samples were then heated for 5 min at 180°C. The samples were then cooled to room temperature and 100 µL of the sample was used for measurement of absorbance at 820 nm. The concentration of phosphate in the samples was then calculated using a standard curve generated with 0-20 µL of 3 mM KH_2PO_4 standard solution.

ACKNOWLEDGEMENTS

We thank Howard and Isaebelle Reizman at the University of Geneva for their work processing and analyzing the samples as well as their expertise interpreting the data. Research in the Graham lab is supported by a grant from the National Institutes of Health (1R01GM107978).

Table 3-1. Yeast strains used in this study.

Strain	Genotype	Source
BY4741	MATa *his3Δ1 leu2Δ0 ura3Δ0 met15Δ0*	Invitrogen
BY4742	MATα *his3Δ1 leu2Δ0 ura3Δ0 lys2Δ0*	Invitrogen
ZHY615M2D	MATα *his3Δ1 leu2Δ0 ura3Δ0 lys2Δ0 drs2Δ*	(Hua *et al.*, 2002)
BMY02	BY4742 *kes1Δ::HIS3*	(Muthusamy *et al.*, 2009)
BMY01	ZHY615M2D *kes1Δ::HIS3*	(Muthusamy *et al.*, 2009)
PFY3272C	MATa *his3Δ1 leu2Δ0 ura3Δ0 met15Δ0 dnf1Δ dnf2Δdnf3Δ*	(Hua *et al.*, 2002)

Chapter IV

COPI sorts ubiquitinated Snc1 into recycling pathway*

ABSTRACT

COPI is a coat protein that has a well-established role in vesicle-mediated protein transport between the Golgi and ER as well as intra-Golgi transport. However, a secondary pool of COPI that localizes to early endosomes has been observed in mammalian cells, but to date no direct function has been attributed to COPI in the endosomal system. Our data suggest that early endosome-localized COPI is involved in the retrieval of the v-SNARE Snc1 from early endosomes to the TGN in budding yeast. By fusing a potent deubiquitinase to Snc1, we found that Snc1 ubiquitination is essential for its retrieval from early endosomes. Deletion of COPI β-propeller domains, which bind ubiquitin, also blocks Snc1 retrieval and causes Snc1 to accumulate in early endosomes. This defect appears to be specific to loss of a COPI-ubiquitin interaction as Snc1 traffics normally when the β-propeller domain is replaced with an unrelated ubiquitin-binding domain. While the ability of COPI to bind ubiquitin is essential for Snc1 trafficking from early endosomes to the TGN, ubiquitin-binding is dispensable for COPI function at the Golgi. Our results suggest that Snc1 ubiquitination functions as a retrieval signal that allows Snc1 incorporation into COPI vesicles for delivery to the TGN.

*This chapter contains data I contributed to that is part of a larger manuscript currently in preparation as Xu, P., **Hankins, H. M.**, Diab, N. S., Erlinger, S. J., MacGurn, J. A., Jackson, L. P., and Graham, T. R. COPI sorts ubiquitinated cargo at early endosomes. *In preparation*.

INTRODUCTION

COPI is an essential protein coat that is evolutionarily conserved from yeast to humans (Jackson, 2014). The heptameric COPI coat complex is composed of an adaptor-like F-subcomplex (β, γ, δ, ζ) and a clathrin-like B-subcomplex (α, β', ε) (Figure 4-1A). COPI is recruited to Golgi membranes, where it mediates retrograde trafficking of specific cargo proteins. The most extensively studied COPI cargo proteins are those that bear KKxx or KxKxx sorting motifs with which COPI interacts via the β-propeller domains of the COPI α and β' subunits (Figure 4-1B; Jackson *et al.*, 2012; Ma and Goldberg, 2013). Importantly for this work, these COPI β-propeller domains have also been shown to interact with ubiquitin (Pashkova *et al.*, 2010). In addition to its Golgi localization, COPI has also been shown to localize to early endosomes in mammalian cells. However, to date there has not been a clear function attributed to COPI at early endosomes (Whitney *et al.*, 1995; Aniento *et al.*, 1996; Daro *et al.*, 1997; Gu *et al.*, 1997).

In support of COPI functioning at early endosomes, mutations that disrupt COPI function (e.g. *sec21-1* or *ret1-1*) disrupt the trafficking of the v-SNARE Snc1 (Lewis *et al.*, 2000), which is the yeast homolog of synaptobrevin/VAMP proteins in animal cells (Protopopov *et al.*, 1993; Grote *et al.*, 1995; Lewis *et al.*, 2000). Snc1 cycles between the TGN, plasma membrane, early endosomes, and back to the TGN but primarily localizes to the plasma membrane because endocytosis is the rate limiting step of the cycle. When COPI function is lost, Snc1 accumulates in intracellular punctae, suggesting the cycle is blocked (Lewis *et al.*, 2000). However, from this study it was unclear if the defect in Snc1 trafficking is a direct effect caused by loss of COPI function at early endosomes or an indirect effect caused by the Golgi being grossly perturbed when COPI function is lost.

Snc1 is ubiquitinated (Peng *et al.*, 2003; Chen *et al.*, 2011; Silva *et al.*, 2015) and it has been previously shown that mutating the lysine at position 63 (Snc1-K63R) severely decreases the amount of ubiquitinated Snc1 in the cell and disrupts Snc1 retrieval from the early endosomes to the TGN (Chen *et al.*, 2011). This finding suggests that ubiquitination of Snc1 is important for its transport back to the

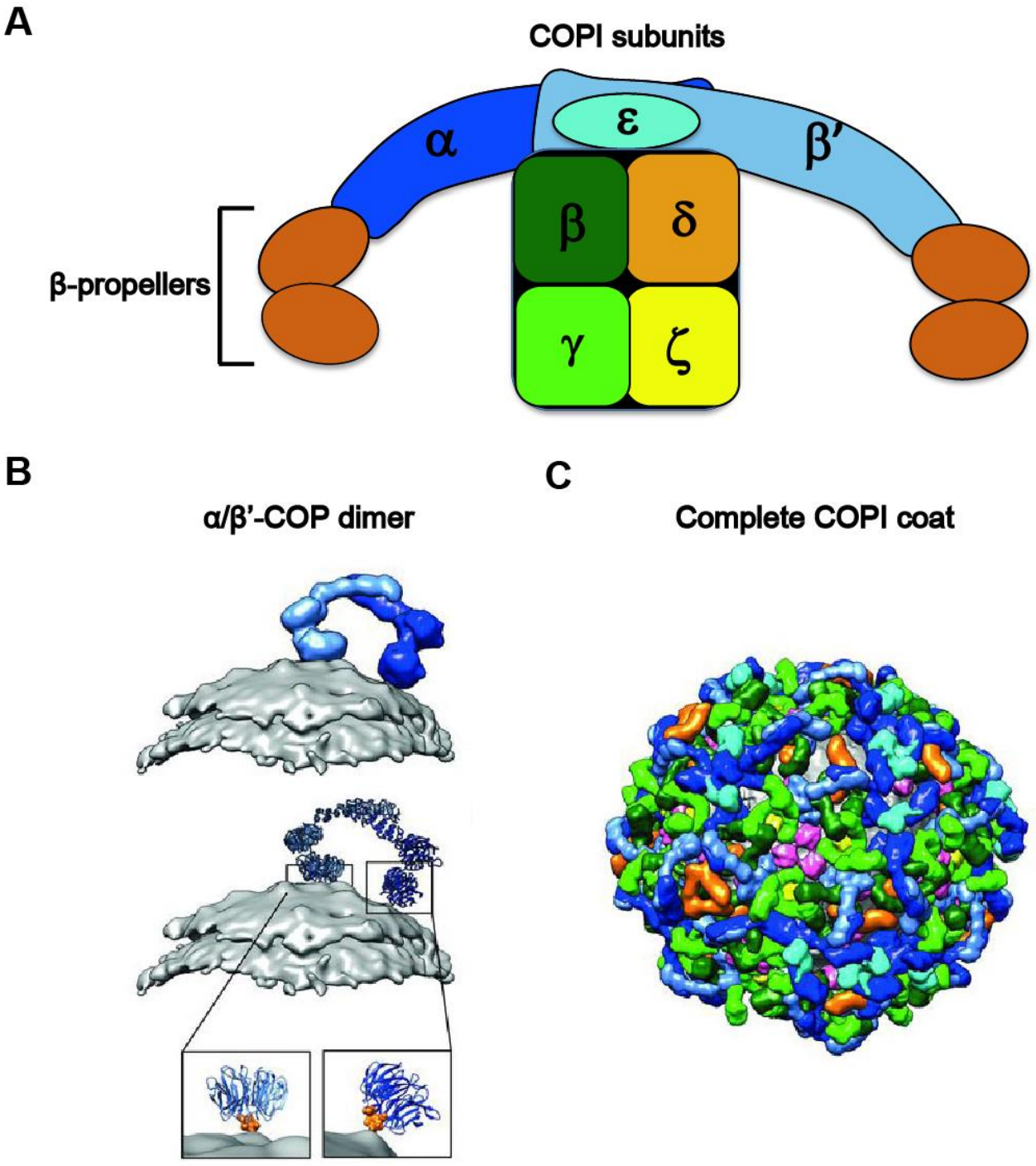

Figure 4-1. Structure of the COPI coat complex. (A) Cartoon model of the COPI subunits. Subunit colors cheme is used throughout the figure. (B) α/β'-COP dimer with β-propeller depicted in orange interacting with a membrane. (C) Model of a COPI-coated vesicle. Images from (B) and (C) are adapted from (Dodonova *et al.*, 2015).

TGN; however, lysines are also common among sorting signals (e.g. KxKxx and KKxx), so it is possible that the Snc1 trafficking defect is due to disrupting a sorting signal rather than blocking ubiquitination.

Ubiquitination is typically thought of as a degradation signal; however, how the polyubiquitin linkages are formed dictates the fate of the ubiquitinated protein. Therefore, ubiquitination is not necessarily a one way ticket for protein degradation. Polyubiquitin chains form as individual ubiquitin monomers bond to different lysine residues on the ubiquitin chain itself. Linkages formed on the K48 residue of ubiquitin are associated with protein degradation, whereas K63-linked ubiquitin chains have been implicated in processes such as DNA damage tolerance, ribosomal protein synthesis, oxidative stress response, and protein trafficking (Spence *et al.*, 1995; Hicke and Dunn, 2003; Peng *et al.*, 2003; Pickart and Fushman, 2004; Varadan *et al.*, 2004; Chen and Sun, 2009; Xu *et al.*, 2009; Silva *et al.*, 2015)

In this study, we sought to address if Snc1 ubiquitination is essential for its recycling and also if early endosome-localized COPI has a specific function in Snc1 recycling. To test if ubiquitination is important for Snc1 trafficking, we fused a potent deubiquitinase to the N-terminus of GFP-Snc1 to efficiently and specifically remove ubiquitin modifications. A major advantage of this approach over previous approaches to study Snc1 ubiquitination is that it requires no mutation of the primary sequence of Snc1 that could disrupt a potential sorting signal.

To determine if COPI is directly involved in Snc1 trafficking, we mutated or deleted the β-propeller domains of the COPI α and β' subunits. These β-propeller domains have been shown to bind ubiquitin and thus may potentially recognize ubiquitinated Snc1 to allow for Snc1 incorporation into COPI vesicles originating from early endosomes.

RESULTS

Snc1 ubiquitination is required for retrieval from early endosomes

To determine if Snc1 ubiquitination is required for its recycling, we fused the herpes simplex virus 1 UL36 deubiquitinase (DUB) catalytic domain (Kattenhorn *et al.*, 2005; Stringer and Piper, 2011; Sette *et*

al., 2013) onto GFP-Snc1 to generate ubiquitination-resistant GFP-Snc1 (DUB-GFP-Snc1). As a control, we also fused a catalytically inactive DUB mutant (DUB*) onto GFP-Snc1 (DUB*-GFP-Snc1), which should not prevent Snc1 ubiquitination. GFP-Snc1 primarily localized to the plasma membrane in WT cells (Figure 4-2A, B) because endocytosis is the rate limiting step of Snc1 trafficking. In contrast, DUB-GFP-Snc1 primarily accumulated in intracellular punctae and colocalized with the early endosome/TGN marker Tlg1 (Figure 4-2C, D). Mislocalization appears to be specific to DUB activity as DUB*-GFP-Snc1 localized to the plasma membrane similar to GFP-Snc1 (Figure 4-2A). To determine which step of Snc1 trafficking was disrupted (i.e. early endosome -> TGN vs TGN -> plasma membrane) for DUB-GFP-Snc1, we fused the DUB domain to an endocytosis-resistant Snc1 mutant (Lewis *et al.*, 2000) (DUB-GFP-Snc1-PM). DUB-GFP-Snc1-PM localized to the plasma membrane and was indistinguishable from the localization of GFP-Snc1-PM, suggesting that the defect observed for DUB-GFP-Snc1 is downstream of the endocytic step. Taken together, these results indicate that Snc1 ubiquitination is required for Snc1 retrieval from early endosomes to the TGN but is not required for Snc1 endocytosis or its trafficking from the TGN to the plasma membrane.

Work from the Segev lab implicated the F-box protein Rcy1 in Snc1 ubiquitination (Chen *et al.*, 2005). However, Rcy1 is also known to bind to the C-terminal regulatory domain of the flippase Drs2 (Furuta *et al.*, 2007), which is both a regulator and cargo of the trafficking pathway between the early endosomes and TGN that Snc1 uses. Thus, it is possible that Rcy1 exerts its effect in Snc1 recycling by ubiquitinating Drs2 rather than Snc1 itself. To test these possibilities, we fused DUB and DUB* to the C-terminus of Drs2 (Figure 4-3C). Loss of Drs2 completely disrupts this pathway and causes Snc1 to accumulate in early endosomes (Figure 4-3A, B; Hua *et al.*, 2002; Furuta *et al.*, 2007). However, GFP-Snc1 recycling is restored in *drs2*Δ cells expressing Drs2-DUB or Drs2-DUB* with GFP-Snc1 primarily localized to the plasma membrane. Because fusing DUB to an essential component of this trafficking pathway had no effect on GFP-Snc1 trafficking, it suggests that the DUB must be fused to GFP-Snc1 to block its retrieval from the early endosomes to the TGN. Furthermore, fusion of DUB to the C-terminus

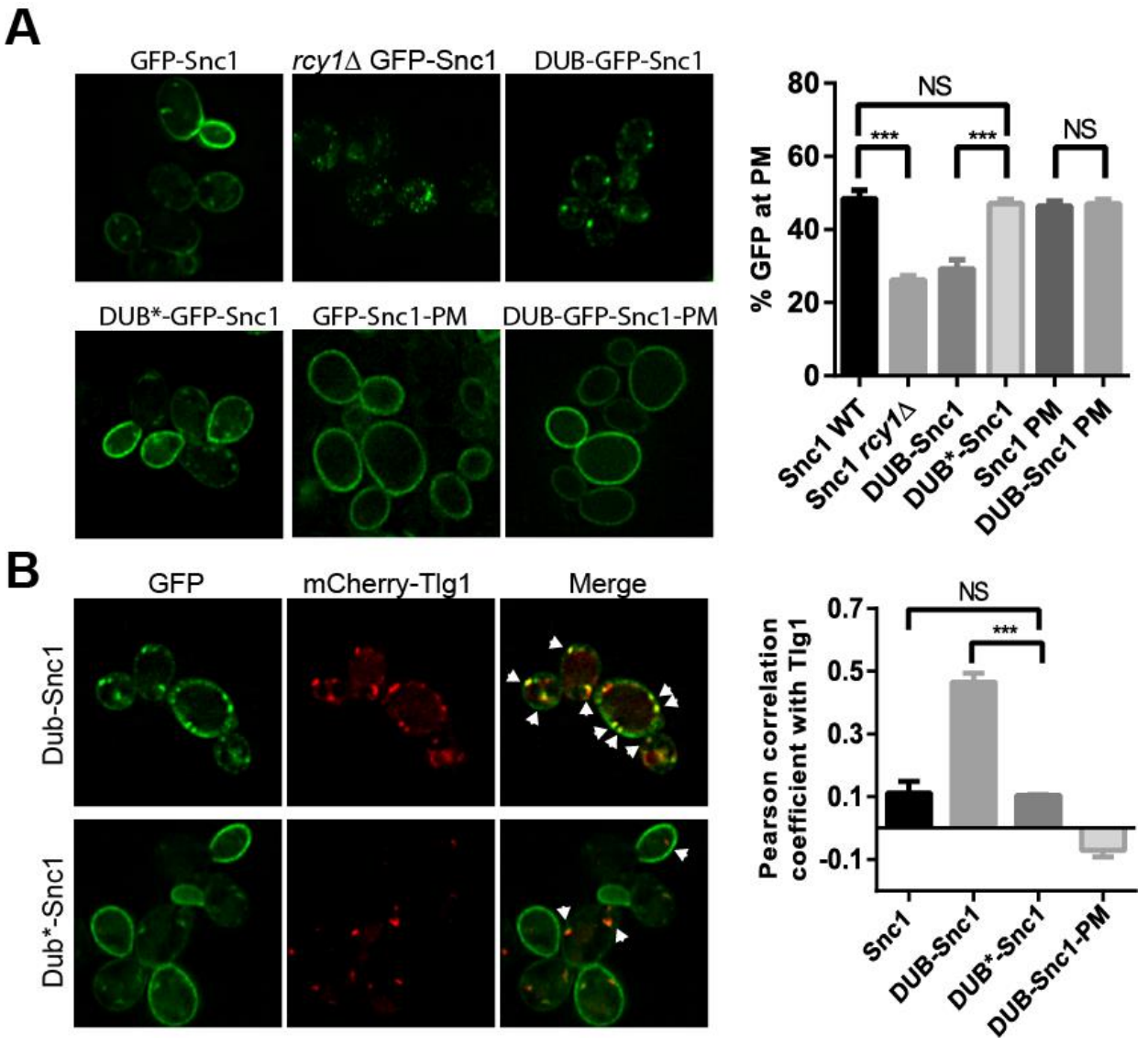

Figure 4-2. Snc1 ubiquitination is required for retrieval from early endosomes. (A) Cells expressing different GFP-Snc1 constructs were grown to mid-log phase prior to imaging. (B) The % GFP at PM was calculated from images taken of the strains from panel A (n = 3, total of 150 cells/strain, one-way ANOVA, ***p < 0.001). (C) Colocalization of different GFP-Snc1 constructs with mCherry-Tlg1 (D) as measured by PCC (n = 3, total of 60 cells/strain, one-way ANOVA, ***p < 0.001). Most of the imaging was performed by Peng Xu.

of α-COP (distal to β-propeller) did not affect GFP-Snc1 recycling, indicating the placement of the DUB fusion on the cargo protein itself (Snc1) is important for removal of ubiquitin (Peng Xu, unpublished). These findings further support the idea that ubiquitination on GFP-Snc1 functions as a sorting signal for this recycling pathway.

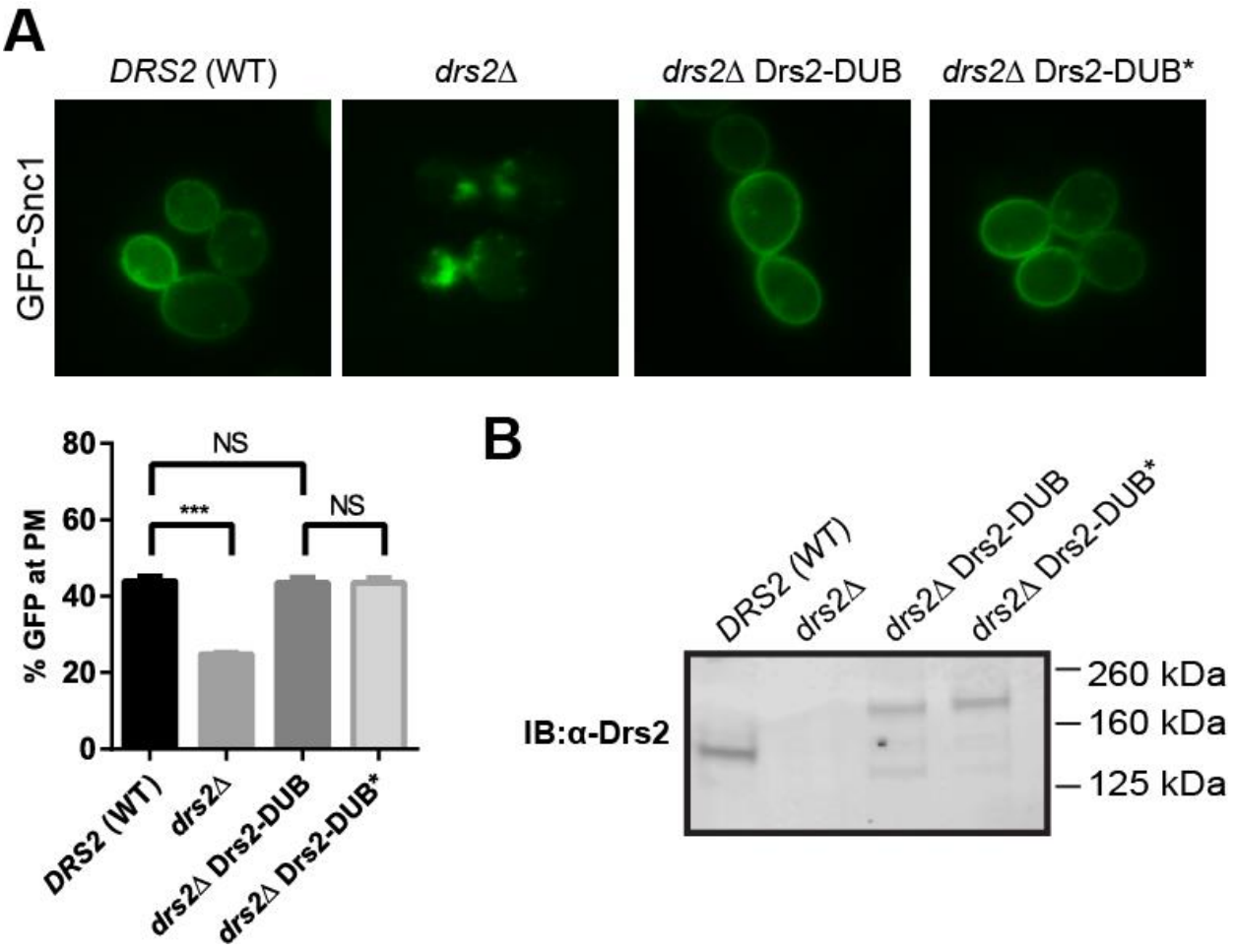

Figure 4-3. Fusing DUB to Drs2 has no effect on GFP-Snc1 trafficking. (A) Localization of GFP-Snc1 in *drs2*Δ cells expressing the indicated constructs. (B) The % GFP at PM was calculated from images taken of the strains from panel A (n = 3, total of 150 cells/strain, one-way ANOVA, ***p < 0.001). (C) Strains from panel A were probed with anti-Drs2 antibody to confirm DUB/DUB* integration, which is indicated by an upward shift in the Drs2 band.

First β-propellers of COPI mediate ubiquitin-dependent Snc1 recycling

Since ubiquitin appeared to be acting as a sorting signal for Snc1, we next sought to determine the coat complex responsible for recognizing the signal. It has been previously reported that clathrin adaptor and retromer mutants do not affect GFP-Snc1 recycling (Lewis *et al.*, 2000; Peng Xu, unpublished). GFP-Snc1 recycling is perturbed in cells expressing COPI temperature-sensitive alleles when shifted to the nonpermissive temperature for 1 hour (Lewis *et al.*, 2000); however, GFP-Snc1 mislocalization could be

an indirect consequence of losing COPI function in intra-Golgi and Golgi → ER transport, which greatly perturbs the Golgi.

To distinguish if GFP-Snc1 mislocalization is a direct or indirect consequence of loss of a COPI function, we focused our research on COPI domains likely to interact with ubiquitin: the β-propeller domains. The Piper lab has previously reported that many β-propeller domains, including those found in COPI α and β'subunits, have the ability to bind ubiquitin (Pashkova *et al.*, 2010). The clathrin-like β' and α subunits of COPI each have two β-propellers at their N-termini. We have found that the first β-propeller of β'-COP (1-304) and to a lesser extent α-COP (1-327) bind to K63-linked tetra-ubiquitin, but do not bind to free ubiquitin or tetra-ubiquitin with different linkages (Peng Xu, unpublished). Furthermore, β'-COP (1-304) also failed to bind K63-linked di-ubiquitin and bound weakly to K63-linked tri-ubiquitin, indicating the interaction is also specific to the length of the ubiquitin chain (Peng Xu, unpublished). This finding suggests that the first β-propellers of the β'and α subunits bind ubiquitin and they do so in a highly specific manner.

Yeast strains with the first β-propeller of either β'-COP (Δ2-304) or α -COP (Δ1-327) deleted were viable, but mislocalized GFP-Snc1 from the plasma membrane to punctae marked with Tlg1 (Figure 4-4A, B). The defect caused by α -COP (Δ1-327) was less severe than that of β'-COP (Δ2-304), which is consistent with α-COP (1-327) binding K63-linked tetra-ubiquitin more weakly than β'-COP (1-304) (Peng Xu, unpublished). Because GFP-Snc1 localization appeared to be more dependent on the first β-propeller of β'-COP, we next mutated the RKR motif in this domain (β'-COP RKR) that recognizes dilysine (KxKxx) sorting signals, such as the one found in the COPI vesicle cargo protein Emp47 that primarily localizes to the Golgi (Schröder *et al.*, 1995; Jackson *et al.*, 2012). β'-COP RKR mislocalized and degraded myc-Emp47 (Peng Xu, unpublished) but did not alter the localization of GFP-Snc1 (Figure 4-4A-D), suggesting the trafficking of GFP-Snc1 is not dependent on the ability of β'-COP to recognize dilysine motifs.

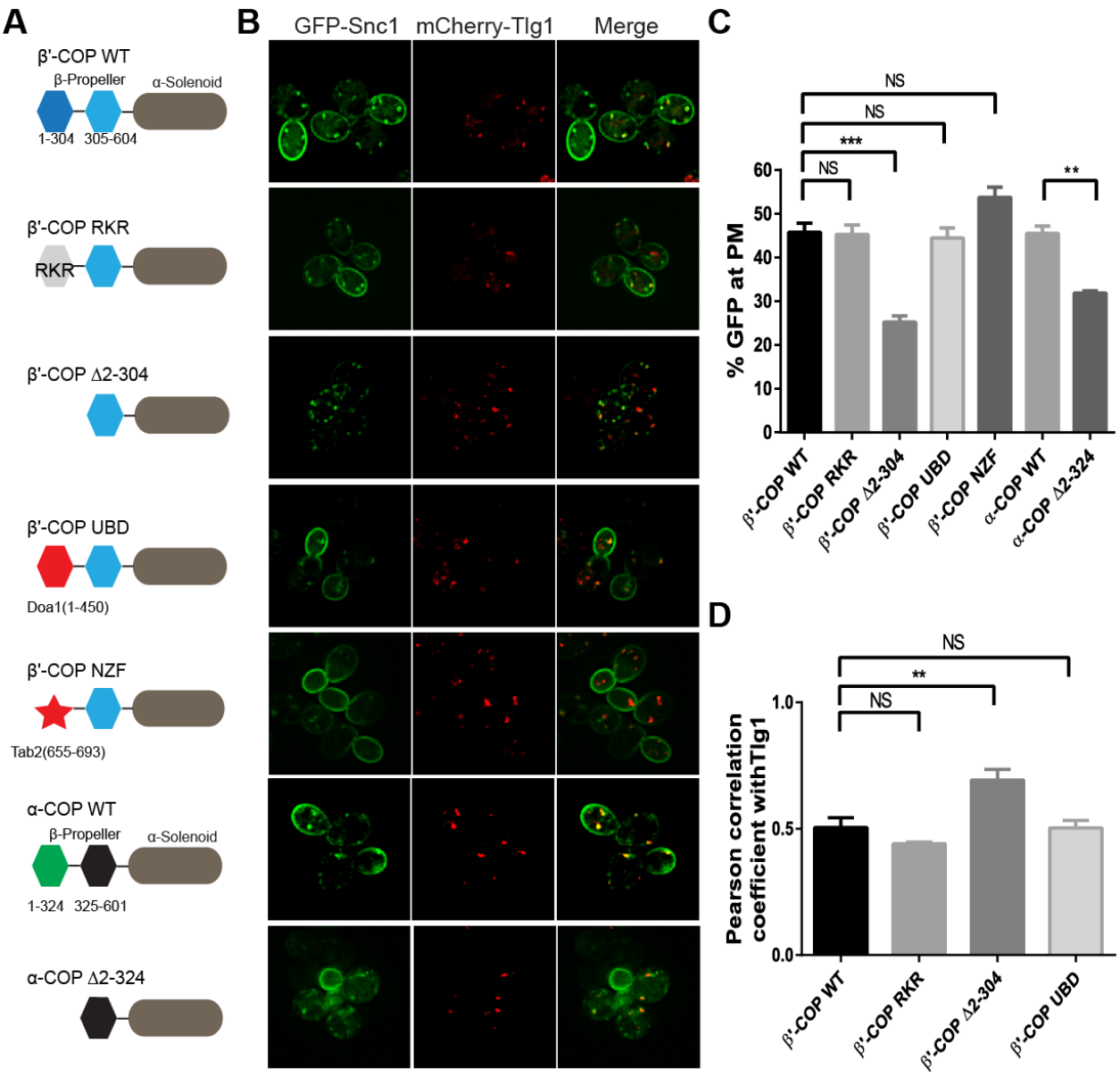

Figure 4-4. First β-propellers of COPI mediate ubiquitin-dependent Snc1 recycling. (A) Schematics of β'-COP and α-COP mutants and fusion used. (B) Colocalization of GFP-Snc1 with mCherry-Tlg1 expressed in the indicated strains from panel A. (C) The % GFP at PM was calculated from images taken of the strains from panel B (n = 3, total of 150 cells/strain, one-way ANOVA, ***p < 0.001). (D) Colocalization between Snc1 and Tlg1 as measured by PCC (n = 3, total of 60 cells/strain, one-way ANOVA, ***p < 0.001). Diagrams and imaging were done by Peng Xu.

We next tested if the function of the first β-propeller of β'-COP in GFP-Snc1 sorting is specific to its ability to recognize and bind ubiquitin. To do this, we replaced the first β-propeller of β'-COP with domains known to bind ubiquitin: the ubiquitin-binding domain (UBD) from Doa1 (β'-COP UBD) and

the Npl4 zinc finger (NZF) domain from the TAB2 subunit of TAK1 (β'-COP NZF). Doa1 binds to mono-ubiquitin and polyubiquitin without linkage specificity and is involved in ubiquitin-mediated protein degradation (Mullally *et al.*, 2006; Ren *et al.*, 2008; Pashkova *et al.*, 2010), whereas TAK1 binds specifically to K63-linked ubiquitin and is involved in NF-κB signaling (Kulathu *et al.*, 2009; Sato *et al.*, 2009). Remarkably, both β'-COP UBD and β'-COP NZF restored GFP-Snc1 localization to the plasma membrane similar to β'-COP WT (Figure 4-4A-D). These results suggest that COPI β-propeller-ubiquitin interaction is essential for its role in Snc1 trafficking from the early endosomes to the TGN.

COPI binding to ubiquitin is not required for COPI function at the early Golgi

Although β'-COP UBD and β'-COP NZF restored normal GFP-Snc1 trafficking, the chimeras failed to restore Golgi localization and stability of the COPI cargo Emp47 (Peng Xu, unpublished). Furthermore, the β'-COP mutants β'-COP (Δ2-304), β'-COP RKR, and β'-COP UBD retained function in the early Golgi as indicated by the normal trafficking of the *cis*-Golgi COPI cargo GFP-Rer1 (Figure 4-5A, B). In contrast, complete inactivation of COPI with the temperature-sensitive *ret1-1* (α-COP) allele increased GFP-Rer1 mislocalization to the vacuole. Taken together with the Snc1 trafficking data (Figure 4-4A-D), these results indicate that COPI function at the *cis*-Golgi is not ubiquitin-dependent and does not require the first β-propeller of β'-COP.

DISCUSSION

The data presented here suggest that Snc1 ubiquitination is essential for its recycling from early endosomes to the TGN. Fusing a deubiquitinase (DUB) to Snc1 caused Snc1 to accumulate in early endosomes, whereas the inactive DUB (DUB*) fusion had no effect on Snc1 trafficking (Figure 4-2A, B). This effect appears to be specific to ubiquitination of Snc1 as fusing DUB/DUB* to Drs2, which is an essential component of the recycling pathway that Snc1 transits, had no effect on Snc1 trafficking (Figure 4-3A, B). These results suggest that ubiquitin functions as a sorting signal for Snc1, which is consistent with work by the Segev lab that showed that the Snc1-K63R mutant is less ubiquitinated than WT and has defective Snc1 recycling (Chen *et al.*, 2011). Although our results and the work of others suggest that

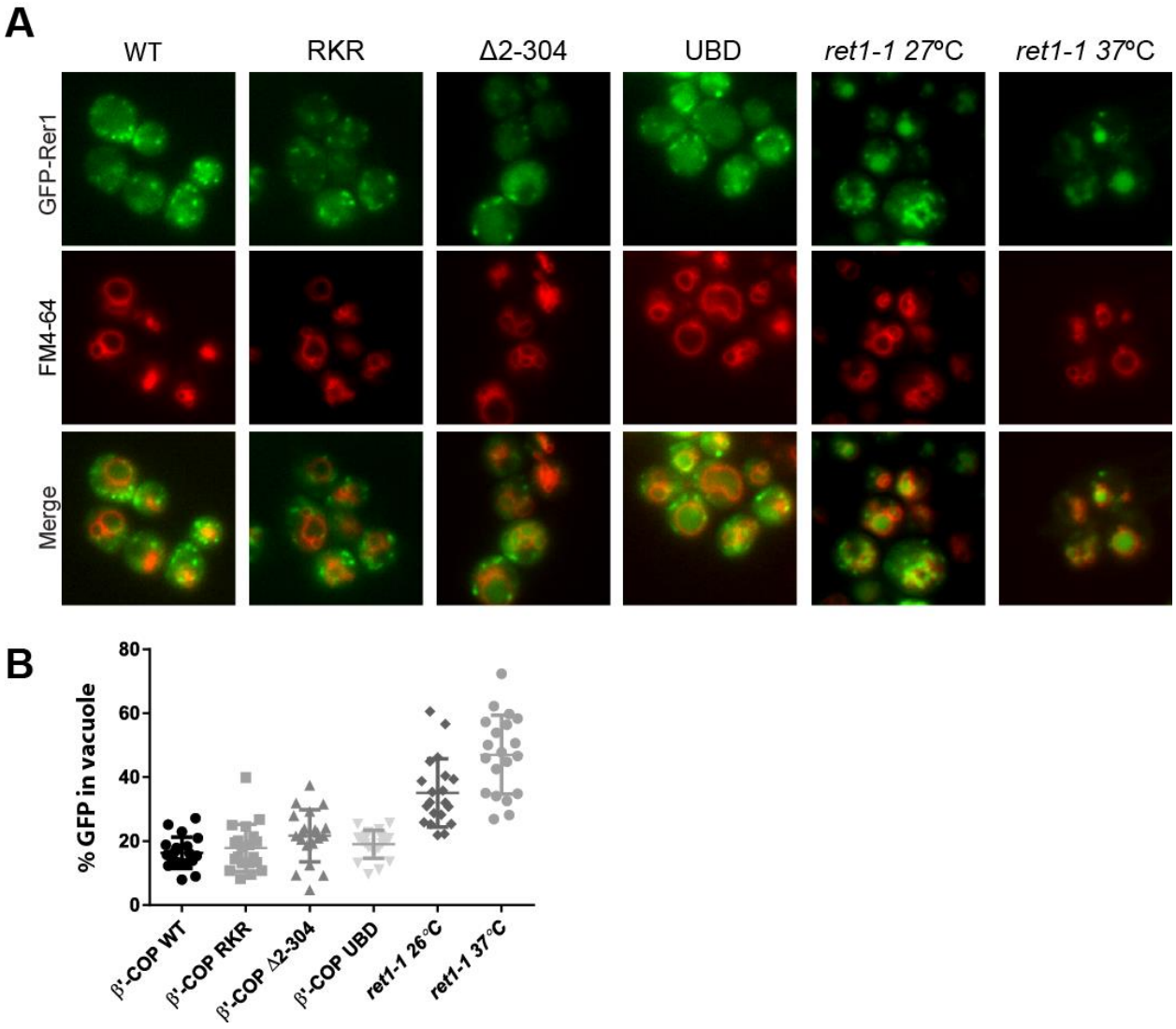

Figure 4-5. COPI binding to ubiquitin is not required for COPI function at the early Golgi. (A) β'-COP mutants do not affect Rer1-GFP localization, whereas complete inactivation of COPI (*ret1-1*) causes Rer1causes Rer1-GFP to mislocalize to the vacuole, as confirmed by FM4-64 labeling. (B) The % GFP in vacuole was calculated from images taken of the strains from panel A (n = 3, total of 60 cells/strain). Imaging was performed by Peng Xu.

ubiquitination of Snc1 itself is important for its trafficking, it is also possible that other components of the COPI machinery (e.g. COPI, Arf-GEF, or Arf-GAP) must be ubiquitinated to function at early endosomal membranes.

Addition of a polyubiquitin chain has been traditionally thought of as a death sentence for the target protein. However, this is not always the case as addition of a polyubiquitin chain can trigger a variety of

different functions depending on which ubiquitin lysine residue is used to grow the chain. The three most abundant linkages in unstressed *S. cerevisiae* cells are K48 (~29%), K11 (~28%), and K63 (~16%) (Xu *et al.*, 2009). K48 linkage is the most studied type of linkage and is associated with protein degradation along with K11 linkage. Less is known about K63 ubiquitination, but there have been reports that have implicated this linkage type with DNA damage tolerance, ribosomal protein synthesis, oxidative stress response, and protein trafficking (Spence *et al.*, 1995; Hicke and Dunn, 2003; Peng *et al.*, 2003; Pickart and Fushman, 2004; Varadan *et al.*, 2004; Chen and Sun, 2009; Xu *et al.*, 2009; Silva *et al.*, 2015). In a recent report, the polyubiquitin chain attached to Snc1 was shown to be K63-linked (Silva *et al.*, 2015), which is consistent with our findings that Snc1 ubiquitination supports protein trafficking rather than protein degradation (Figure 4-2A, B).

Interestingly, the COPI β–propellers are able to bind to K63-linked tetra-ubiquitin, but not mono-ubiquitin or tetra-ubiquitin with different linkage types (Peng Xu, unpublished). This finding suggests that COPI could be able to recognize K63-linked Snc1, which could allow for Snc1 incorporation into COPI vesicles. Deletion of the COPI β–propellers caused Snc1 to accumulate at early endosomes. This observation could indicate that even though Snc1 is ubiquitinated, ubiquitinated Snc1 must be recognized by COPI to be incorporated into vesicles and trafficked to the TGN.

To ensure that the essential function of the COPI β–propellers in Snc1 trafficking is specific to their ability to bind to ubiquitin, we replaced the first β–propeller of the β'subunit with different UBDs (Figure 4-4A-D). The UBD of Doa1 has previously been shown to bind to mono-ubiquitin and polyubiquitin regardless of linkage types (Mullally *et al.*, 2006). The chimeric protein (β'-COP UBD) restored Snc1 recycling, indicating ubiquitin binding is the essential function of the β–propeller. We also replaced the β–propeller with the NZF domain of the TAB2 subunit of TAK1 (β'-COP NZF). Unlike the UBD of Doa1, the NZF domain of TAB2 specifically binds to K63-linked polyubiquitin chains (Kulathu *et al.*, 2009). β'-COP NZF also restored Snc1 recycling, suggesting the essential function of the COPI β-propeller in Snc1 trafficking is specific to its ability to bind to K63 ubiquitin linkages.

The ability of COPI to recognize ubiquitin is not essential for COPI function at the Golgi. When COPI function is lost, the COPI cargo protein GFP-Rer1 mislocalizes from the Golgi to the vacuole (Figure 4-5A, B). Deletion of the β'-COP subunit does not affect GFP-Rer1 trafficking, but it does cause the Golgi protein Emp47 to mislocalize (Peng Xu, unpublished). However, Emp47 also mislocalizes in the β'-COP RKR mutant that is unable to recognize KKxx proteins, suggesting mislocalization is due to losing the ability to recognize the dilysine sorting signal of Emp47 rather than losing the ability to bind ubiquitin. In contrast, β'-COP RKR did not affect Snc1 recycling. These result suggests that i) the Golgi is not grossly perturbed in the β'-COP (Δ2-304) mutant, ii) COPI has a direct role in Snc1 trafficking, and iii) the COPI β-propeller-ubiquitin interaction is specific to its role in protein trafficking in the endosomal system.

Taken together, our results suggest novel and direct roles for COPI and ubiquitin for protein trafficking within the endosomal system.

MATERIALS AND METHODS

Media, strains, and plasmids

Yeast strains were grown in yeast extract peptone dextrose (YPD) or synthetic minimal medium (SD) containing required nutrients and 2% glucose. All yeast transformations were performed by the lithium acetate method (Gietz and Schiestl, 2007). PCR-based genomic integration of fluorescent tags was carried out according to the method described by Janke *et al.* (Janke *et al.*, 2004). COPI mutant strains were constructed by plasmids shuffling on 5'-flouro-orotic acid (5-FOA) plates. Plasmids were constructed using standard molecular manipulation. Mutations were introduced using a Q5 Site-Directed Mutagenesis Kit or Gibson Assembly Master Mix (New England Biolabs, Ipswich, MA). Lists of strains and plasmids used in this study are listed in Tables 4-1 and 4-2, respectively.

Western blot

Samples were prepared using a protocol modified from Chang and Slayman (Chang and Slayman, 1991). Cell pellets were resuspended in lysis buffer (10 mM Tris, pH 7.4, 0.3 M sorbitol, 0.1 M NaCl, and 5 mM

MgCl2) containing 1 mM phenylmethylsulfonyl fluoride and 1× protease inhibitor cocktail (ThermoFisher Scientific, San Jose, CA). The cells were then lysed by vortexing for 6 min with 1 min pulses at 4°C. The beads were allowed to settle without centrifugation for 10 min at 4°C before removing the lysate supernatant. The lysates were then added 1:1 to Laemmli buffer and incubated at 37°C for 5 min. The samples were then subjected to SDS–PAGE and transferred to a polyvinylidene fluoride membrane. Rabbit anti-Drs2 primary antibody (Chen *et al.*, 1999) and an IR800CW secondary antibody (LI-COR Biosciences, Lincoln, NE) were used at 1:2,000 and 1:5,000 dilution, respectively. The bands were imaged and quantified using an Odyssey CLx infrared imager and its software (LI-COR Biosciences, Lincoln, NE).

Vacuolar labeling with FM4-64

Mid log-phase cells were labeled with the lipophilic dye FM4-64 (Life Technologies, Grand Island, NY) as described previously (Babu *et al.*, 2012). Cells were labeled with 32 μM FM4-64 for 20 min in the dark at 30°C. The cells were then washed with 1× phosphate-buffered saline (PBS) and resuspended in SD medium for 30 min at 30°C. The cells were washed twice in 1× PBS before imaging.

Fluorescence microscopy

The majority of images were taken with a DeltaVision Elite Imaging system (Applied Precision, Issaquah, WA). A *Z*-stack was acquired with 200-nm intervals, and the images were deconvolved in SoftWoRx (Applied Precision, Issaquah, WA). All other images were taken with an Axioplan microscope (Carl Zeiss, Thornwood, NY) equipped with a Zyla sCMOS 5.5-megapixel camera (Andor, Belfast, United Kingdom) and micromanager software (University of California, San Francisco, San Francisco, CA). GFP-tagged proteins were imaged using a GFP filter set; RFP-tagged proteins and FM4-64 were imaged using an RFP filter set. Images were merged and pseudocolored in ImageJ (National Institutes of Health, Bethesda, MD).

Data analysis

The percentage of Snc1 localized to the plasma membrane (%PM-localized) was calculated by first outlining the outside of each cell using the freehand selection tool in ImageJ and measuring the total fluorescence of the cell ($Fluor_{Total}$). Next, the area just within the plasma membrane was outlined using the freehand selection tool to give the total internal fluorescence excluding the plasma membrane ($Fluor_{int}$). Internal fluorescence was then subtracted from the total to determine the fluorescence at the plasma membrane ($Fluor_{Total} - Fluor_{int} = Fluor_{PM}$). Finally, the fluorescence at the plasma membrane was divided by the total fluorescence of the cell to give %PM-localized fluorescence ($Fluor_{PM}/Fluor_{Total}$ = %PM-localized Snc1). The percentage of Rer1-GFP localized in the vacuole (%GFP in vacuole) was calculated by outlining the vacuole limiting membrane in the red (FM4-64) channel and then measuring the fluorescent intensity of that area in the green (Rer1) channel to give $Fluor_{Vac}$. $Fluor_{Vac}$ was then divided by $Fluor_{Total}$ to give the % of GFP signal in the vacuole ($Fluor_{Vac}/Fluor_{Total}$ = %GFP in vacuole).

To determine the degree of colocalization between different markers, individual cells taken from one slice of a deconvolved Z-stack were outlined using the freehand selection tool in ImageJ and copied into new images to produce two images, one in the GFP channel and one in the RFP channel. To quantify colocalization between two fluorescent markers, the Pearson's Correlation Coefficient was calculated for each cell using the ImageJ plugin Just Another Colocalization Plugin with Costes Automatic Thresholding (Bolte and Cordelières, 2006).

ACKNOWLEDGEMENTS

We thank Scott Emr (Cornell University), Natasha Pashkova and Robert Piper (University of Iowa), Richard Chi and Chris Burd (Yale University), Thomas Mund and Hugh Pelham (MRC Laboratory of Molecular Biology), and Daniel Finley (Harvard Medical School) for plasmids and yeast strains. We thank Ryan Baldridge (Harvard Medical School) and Ming Li (Cornell University) for helpful discussions. These studies were supported by NIH Grant R01 GM62637 to TRG.

Table 4-1. Yeast strains used in this study.

Strain	Genotype	Source
BY4742	MATα *his3Δ1 leu2Δ0 ura3Δ0 lys2Δ0*	Invitrogen
ZHY615M2D	MATα *his3Δ1 leu2Δ0 ura3Δ0 lys2Δ0 drs2Δ*	(Hua, et al. 2002)
PXY2174	*MATα his3 leu2 ura3 lys2 sec27Δ::Hygro p315-SEC27* (β'-COP WT)	(Peng Xu, unpublished)
PXY2175	*MATα his3 leu2 ura3 lys2 sec27Δ::Hygro p315-sec27Δ2-304* (β'-COP Δ2-304)	(Peng Xu, unpublished)
PXY2186	*MATα his3 leu2 ura3 lys2 sec27Δ::Hygro p315-sec27 RKR* (β'-COP RKR)	(Peng Xu, unpublished)
PXY2184	*MATα his3 leu2 ura3 lys2 sec27Δ::Hygro p315-Doa1(1-450)-sec27(305-889)* (β'-COP UBD)	(Peng Xu, unpublished)
PXY2192	*MATα his3 leu2 ura3 lys2 sec27Δ::Hygro p315-NZF-sec27(305-899)* (β'-COP NZF)	(Peng Xu, unpublished)
PXY2198	*MATα his3 leu2 ura3 lys2 cop1Δ::Hygro p313-COP1* (α-COP WT)	(Peng Xu, unpublished)
PXY2199	*MATα his3 leu2 ura3 lys2 cop1Δ::Hygro p313-cop1(325-1201)* (α-COP Δ2-304)	(Peng Xu, unpublished)
PXY46	MATα *his3Δ1 leu2Δ0 ura3Δ0 lys2Δ0 drs2Δ DRS2::UL36-3xHA::ClonNAT* (Drs2-DUB)	(Peng Xu, unpublished)
PXY47	*MATα his3 leu2 ura3 lys2 DRS2::UL36*-3xHA::ClonNAT* (DRS2-DUB*)	(Peng Xu, unpublished)
EGY101-16D	MATa *leu2-3,112 ura3-52 his3-Δ200 trp1-Δ901 suc2-Δ9 ret1-1*	(Letourneur *et al.*, 1994b)

Table 4-2. Plasmids used in this study.

Plasmid	Description	Source
pRS416-GFP-Snc1	GFP-tagged Snc1	(Lewis *et al.*, 2000)
pRS416-DUB-GFP-Snc1	Deubiqutinase(UL36) catalytic domain tagged GFP-Snc1	(Peng Xu, unpublished)
pRS416-DUB*-GFP-Snc1	Catalytic dead form of deubiqutinase fused to GFP-Snc1	(Peng Xu, unpublished)
pRS416-GFP-Snc1-PM	GFP tagged Snc1 plasma membrane form	(Peng Xu, unpublished)
pRS416-DUB-GFP-Snc1-PM	Deubiqutinase tagged GFP-Snc1 plasma membrane form	(Peng Xu, unpublished)
pRS315-mCherry-Tlg1	mCherry-tagged Tlg1	(Xu *et al.*, 2013)
pSKY5	GFP-tagged Rer1 (cen-based URA3 plasmid)	(Sato *et al.*, 2001)

Chapter V

Discussion

Opposing roles of Drs2 and Kes1 in exocytic protein trafficking

Phospholipids are amphiphilic molecules that can move laterally within a membrane leaflet, but face a steep energy barrier when moving between the two membrane leaflets (McConnell and Kornberg, 1971; Devaux, 1992; Pomorski *et al.*, 2001; Daleke, 2003). Without assistance, the half-time for spontaneous phospholipid flip-flop ranges from hours to days. However, there exist classes of protein transporters (flippases, floppases, and scramblases) that facilitate and accelerate phospholipid transport between the two leaflets. In particular, my research focuses on phospholipid transport by flippases, which are also known as P4-ATPases.

In budding yeast, there are five flippases: Drs2, Dnf1, Dnf2, Dnf3, and Neo1. Drs2 and the three Dnf proteins constitute an essential group (*drs2*Δ*dnf1,2,3*Δ cells are inviable), whereas Neo1 by itself is essential (Hua *et al.*, 2002). Drs2 and Dnf3 primarily localize to the *trans*-Golgi network (TGN), Dnf1 and Dnf2 primarily localize to the bud plasma membrane, and Neo1 localizes to the Golgi. Drs2 primarily flips PS and, to a lesser extent, PE (Natarajan *et al.*, 2004; Zhou and Graham, 2009), while Dnf1 and Dnf2 flip lysophospholipids (Riekhof *et al.*, 2007; Baldridge *et al.*, 2013). The substrate specificites of Neo1 and Dnf3 have yet to be determined.

Flippases recognize and translocate their specific phospholipid substrates from the extracellular/lumenal leaflet to the cytosolic leaflet (Daleke, 2007; Tanaka *et al.*, 2011). In doing so, flippases create a membrane bilayer that has an asymmetric distribution of lipids between the two leaflets. The lipids

primarily enriched in the extracellular leaflet of the plasma membrane include phosphatidylcholine (PC) and sphingolipids, whereas phosphatidylserine (PS), phosphatidylethanolamine (PE), and phosphatidylinositol (PI) are enriched in the cytosolic leaflet (Seigneuret and Devaux, 1984; Devaux, 1992; Zachowski, 1993).

The asymmetric structure of the membrane means that the two sides of the membrane have distinct chemical properties, which is important for the function of integral membrane proteins. The enrichment of negatively charged lipids in the cytosolic leaflet also provides an anionic surface on which polycationic cytosolic proteins are recruited (van Meer *et al.*, 2008; Xu *et al.*, 2013; Stahelin *et al.*, 2014). In addition, loss of asymmetry in the form of PS exposure in the extracellular leaflet has important roles in processes such as apoptosis, cytokinesis, blood clotting, and in some instances of host-pathogen interactions (Bevers *et al.*, 1983; Fadok *et al.*, 1992; Emoto *et al.*, 1996; Bratton *et al.*, 1997; Zwaal and Schroit, 1997; Williamson and Schlegel, 2002; Lentz, 2003; Mercer and Helenius, 2008).

Phospholipid translocation by flippases also has an important role in vesicle-mediated protein trafficking pathways (Muthusamy *et al.*, 2009a). The precise function carried out by flippases to support protein trafficking remains to be elucidated but likely involves a combination of the following two proposed mechanisms. The first mechanism is that flippases generate membrane curvature, which is needed to bud vesicles from the membrane. By flipping lipids in a unidirectional direction to the cytosolic leaflet, flippases cause one leaflet of the membrane to expand while the other leaflet contracts. In order for the two leaflets to remain in contact, the membrane must bend. This phenomenon of membrane bending when the two leaflets are unbalanced was first described by Sheetz and Singer over 50 years ago and is known as the bilayer couple hypothesis (Sheetz and Singer, 1974).

A second mechanism by which flippases may support protein trafficking is through the enrichment of specific lipids, such as the anionic lipid PS, to the cytosolic leaflet. The anionic surface created by PS enrichment may act as a platform for the recruitment of components of the trafficking machinery. A combination of the two mechanisms appears to be involved in the Drs2-dependent membrane recruitment

of the Arf GTPase-activating protein (ArfGAP) Gcs1 to endosomes (Xu *et al.*, 2013). In this case, both the membrane curvature and negative charge of the cytosolic leaflet imparted by Drs2 PS flip are sensed and required for the recruitment of Gcs1 by its ArfGAP lipid packing sensor (ALPS) motif.

As described in more detail in Chapter I, the different yeast flippases are involved in multiple trafficking pathways with some degree of functional overlap between flippases (Graham, 2004). For this chapter, I will focus only on Drs2-dependent trafficking pathways as it is the flippase of interest in Chapter II. The link between flippases and protein trafficking was first established as a result from a screen for proteins that have genetic interactions with the ADP-ribosylation factor Arf1 (Chen and Graham, 1998). Among the seven hits, Drs2 and its beta-subunit Cdc50 were both identified from this screen by their synthetic lethal relationship with *arf1*Δ (Chen and Graham, 1998; Chen *et al.*, 1999, 2006). Drs2 and Cdc50 also have a synthetic lethal relationship with clathrin mutants, and clathrin-dependent protein trafficking pathways are disrupted in *drs2*Δ cells (Chen *et al.*, 1999; Hua *et al.*, 2002; Liu *et al.*, 2008).

In addition to the TGN, Drs2 also localizes to early endosomes and is a shared and essential component of the AP-1/clathrin-dependent and Rcy1-dependent transport pathways between the TGN and early endosomes (Furuta *et al.*, 2007; Liu *et al.*, 2008). Drs2 is itself a cargo of the early endosome to TGN recycling pathway along with the v-SNARE Snc1 (Furuta *et al.*, 2007). Snc1 normally cycles between the TGN, plasma membrane, early endosomes, and back to the TGN (Lewis *et al.*, 2000). However, GFP-Snc1 accumulates in early endosomes in *drs2*Δ and *rcy1*Δ cells, indicating trafficking between early endosomes and the TGN is blocked in these cells (Hua *et al.*, 2002; Furuta *et al.*, 2007).

While the trafficking between the TGN and early endosomes appears to be Drs2-specific, there are pathways in which flippases are functionally redundant (Hua *et al.*, 2002; Muthusamy *et al.*, 2009a). Transport and processing of the GGA pathway (Golgi → endosome → vacuole) cargo protein CPY is normal in *drs2*Δ and *dnf1*Δ single mutants, but defective in the *drs2*Δ*dnf1*Δ double mutant. Likewise, transport of the AP-3 pathway (Golgi → vacuole) cargo protein ALP is unaffected in *drs2*Δ and *dnf1*Δ single mutants, but is disrupted in the *drs2*Δ*dnf1*Δ double mutant. These results suggest that Drs2

functionally overlaps with Dnf1 in trafficking pathways between the Golgi and late endosomal and vacuolar systems.

Drs2 appears to be the only flippase that functions in protein trafficking from the TGN to the plasma membrane in a process known as exocytosis. There are two distinct vesicle populations (dense and light) in which exocytic cargo proteins may be incorporated. The Graham lab has previously found that the formation of the clathrin-dependent dense class of vesicles is disrupted in *drs2*Δ cells (Gall *et al.*, 2002). However, dense vesicle cargo proteins, such as invertase and acid phosphatase, still reach the plasma membrane as they can be incorporated into light vesicles (Chen *et al.*, 1999; Hua *et al.*, 2002). Prior to the work presented in Chapter II, Drs2 was not known to also be involved in the light vesicle branch of exocytosis, which is involved in the transport of putative raft-associated proteins.

My research was based on observations made by a previous graduate student in the Graham lab, Baby-Periyanayaki Muthusamy, whose dissertation project focused on determining why Drs2 is essential for growth at cold (≤20°C) temperatures (Muthusamy *et al.*, 2009b). To do this, Muthusamy screened for spontaneous bypass suppressors that would allow for growth of *drs2*Δ cells at nonpermissive growth temperatures. From this screen, she found that the cold sensitivity phenotype of *drs2*Δ cells could be suppressed by loss of function *kes1* alleles. Kes1 (also known as Osh4) is a member of the oxysterol-binding homologue family in yeast and is involved in non-vesicular lipid transport.

Kes1 and its mammalian homologue oxysterol-binding protein (OSBP) have distinct but overlapping binding pockets for sterol and phosphatidylinositol-4-phosphate (PI4P) such that the proteins can bind to either lipid but not at the same time (Saint-Jean *et al.*, 2011). The Antonny and Drin labs have demonstrated that Kes1 and OSBP can differentiate between donor and acceptor membranes to give directional transport of sterol and PI4P between the TGN and ER (Mesmin *et al.*, 2013; Moser von Filseck *et al.*, 2015). This Kes1/OSBP-dependent exchange of lipids results in sterol enriching at the TGN and PI4P being delivered to the ER, where it is dephosphorylated to PI by Sac1. The conversion of PI4P

to PI at the ER is particularly important as it prevents PI4P from accumulating at the ER, thereby allowing the directional exchange of sterol and PI4P to continue.

While characterizing Kes1 suppression of the *drs2*Δ cold tolerance defect, Muthusamy discovered that Drs2 and Kes1 have an antagonistic relationship in sterol homeostasis (Muthusamy *et al.*, 2009b). Deletion of either *DRS2* or *KES1* causes ergosterol, the main sterol in yeast, to partially accumulate in intracellular structures instead of enriching at the plasma membrane. Drs2 and Kes1 appear to regulate each other's activity as loss of one protein results in hyperactivity of the other protein. Interestingly, ergosterol enrichment at the plasma membrane is restored in *drs2*Δ*kes1*Δ cells, suggesting that the mutual suppression of Drs2 and Kes1 is part of a homeostatic process that is involved in ergosterol enrichment at the plasma membrane.

For my dissertation project, I was interested in whether the change in ergosterol distribution observed in *drs2*Δ and *kes1*Δ cells affects the trafficking of proteins that associate with sterol- and sphingolipid-rich membrane domains, which are often referred to as "lipid rafts" in mammalian cells. As mentioned earlier, the TGN acts as the major sorting station of the cell (Papanikou and Glick, 2014). Drs2 has already been implicated in a number of trafficking pathways originating from the TGN (Muthusamy *et al.*, 2009a). However, Drs2 was previously not known to function in the light vesicle branch of exocytosis that delivers raft-associated proteins to the plasma membrane.

Unlike the dense class of exocytic vesicles, light vesicles do not associate with clathrin or any known coat proteins (Surma *et al.*, 2012). A lipid raft-based model has been proposed to explain how cargoes are selectively incorporated into the vesicles, but the mechanism and proteins involved in the process of protein sorting and vesicle budding remain unclear (Simons and van Meer, 1988; Simons and Ikonen, 1997; Ikonen and Simons, 1998; Bagnat and Simons, 2002; Klemm *et al.*, 2009; Surma *et al.*, 2012). Interestingly, Kes1 was identified in a screen for proteins involved in the exocytosis of a raft-associated protein (Proszynski *et al.*, 2005); however, the precise function of Kes1 in exocytosis remains to be determined.

To determine if Drs2 and Kes1 are involved in the exocytosis of raft-associated proteins, I looked at the distribution of two plasma membrane proteins: the plasma membrane ATPase Pma1 and the arginine permease Can1. Unlike mammals, yeast form much larger and more stable raft-like domains (also referred to as membrane compartments) that can be easily resolved by conventional microscopy (Spira *et al.*, 2012; Malinsky *et al.*, 2013). These markers were selected because although the two proteins traffic to the plasma membrane via light vesicles, they occupy distinct regions of the plasma membrane termed the membrane compartment of Pma1 (MCP) and membrane compartment of Can1 (MCC) (Bagnat and Simons, 2002; Malínská *et al.*, 2003; Malinska *et al.*, 2004; Grossmann *et al.*, 2007; Spira *et al.*, 2012; Surma *et al.*, 2012; Ziółkowska *et al.*, 2012). This combination of protein markers allowed me to determine if there are defects in exocytosis and/or defects in the lateral compartmentalization of the plasma membrane in *drs2*Δ cells.

We found that there was not a significant increase in Pma1-RFP and Can1-GFP colocalization at the plasma membrane of *drs2*Δ cells, suggesting compartmentalization of the plasma membrane is not perturbed when Drs2 is lost (Hankins *et al.*, 2015b). However, partial mislocalization of both Pma1-GFP and Can1-GFP to the vacuole was evident in the *drs2*Δ and *kes1*Δ single mutants. Like the ergosterol distribution defect, the exocytosis defect was reversed in the *drs2*Δ*kes1*Δ double mutant. Moreover, we found that both the ergosterol and exocytosis defects of *drs2*Δ cells were specific to the loss of PS flippase activity as determined using flippase mutants that either specifically gain (Dnf1-N550S) or lose (Drs2-[QQ→GA] the ability to flip PS without altering their other substrate specificities (Baldridge and Graham, 2013; Baldridge *et al.*, 2013; Hankins *et al.*, 2015b).

Using the endocytosis inhibitor latrunculin-A and an endocytosis-resistant Can1 mutant, I determined that mislocalization of Pma1-GFP and Can1-GFP to the vacuole was due to a defect in protein sorting at the TGN rather than an increased rate of endocytosis (Hankins *et al.*, 2015b). This is consistent with the proposed model that raft structures are formed at the TGN, which is also the location that both Drs2 and Kes1 are known to function (Chen *et al.*, 1999; Hua *et al.*, 2002; Natarajan *et al.*, 2004; Liu *et al.*, 2008;

Surma *et al.*, 2012; Moser von Filseck *et al.*, 2015). Disrupting other TGN-associated pathways (AP-1, Rcy1, GGA, and AP-3) that Drs2 is involved in did not affect the trafficking of Pma1-GFP or Can1-GFP, suggesting that the exocytosis defect of *drs2*Δ cells is not an indirect consequence of perturbing another pathway.

Based on our results, we hypothesize that PS flip by Drs2 at the TGN regulates the sterol loading activity of Kes1 either by imparting a negative charge to the membrane or by inducing membrane curvature. The similar phenotypes of *kes1*Δ and *drs2*Δ mutants suggest that ergosterol overloading or underloading at the TGN caused by Kes1 hyperactivity or inactivity, respectively, disrupts the balance required for concentrating Pma1 and Can1 into exocytic vesicles. Another explanation is that failure to remove PS from the lumenal leaflet prevents efficient sorting of Pma1 and Can1 into exocytic vesicles. However, cells lacking the PS synthase (*cho1*Δ) mislocalize Pma1 and Can1 similar to *drs2*Δ cells, but it is unclear how ergosterol distribution is affected in *cho1*Δ cells due to the high amount of variability we observed within and across different assays conditions (discussed in detail in Chapter II).

These observations suggest that the presence of PS likely has a positive role in exocytosis, but may or may not be involved in sterol homeostasis. Recent work from the Mayor lab suggests that PS is important for the formation of cholesterol-enriched glycosylphosphatidylinositol (GPI)-anchor nanoclusters in mammalian cells (Raghupathy *et al.*, 2015). The researchers found that transbilayer interactions between PS in the inner leaflet and long saturated acyl chains in the outer leaflet promote nanoclustering of the GPI-anchor in an actin-dependent manner. In the context of my work, this finding may suggest that PS flip is important because it enriches PS in the cytosolic leaflet, where it can promote coalescence of raft domains via interactions with the long saturated acyl chains of sphingolipids or GPI-anchored proteins in the lumenal leaflet. However, it remains to be determined if a similar transbilayer coupling phenomenon occurs in budding yeast as it does in mammalian cells.

Changes in the yeast lipidome in flippases mutants and in response to temperature shift

A second part of my dissertation research was to determine what, if any, impact loss of flippase activity has on the yeast lipidome. Many of the proteins involved in yeast lipid synthesis have been elucidated, but there remain many open questions about how cellular lipid concentrations are regulated and how lipid composition changes in response to different conditions. Membrane asymmetry is a fundamental property of eukaryotic membranes that is important for a variety of different cellular processes, so it seems plausible that cells have a mechanism for sensing loss of membrane asymmetry and eliciting changes to the lipidome. Or, on the other hand, loss of membrane asymmetry could perturb regulatory pathways involved in lipid homeostasis such that the concentrations or ratios of different lipid species are no longer maintained at normal levels.

As a follow up to the research presented in Chapter II, I was interested in seeing if there are changes in the yeast lipidome that may account for the exocytic trafficking defects or the cold sensitivity phenotype of *drs2*Δ cells. If a change in a lipid concentration is linked to the exocytic trafficking defect, we would expect that changes in the lipid concentration would follow the same pattern of co-suppression: altered in *drs2*Δ and *kes1*Δ cells but normal in *drs2*Δ*kes1*Δ cells (Muthusamy *et al.*, 2009b). In the case of cold sensitivity, changes in lipid composition at 20°C would follow a separate pattern with the lipid concentration altered in *drs2*Δ cells, but not *kes1*Δ and *drs2*Δ*kes1*Δ cells. For this project, I was particularly interested in changes in ergosterol and sphingolipid concentrations as perturbation of their synthesis is known to affect the trafficking of some raft-associated proteins (Surma *et al.*, 2012).

For our lipidomic analysis, we collaborated with Howard Riezman's lab at the University of Geneva. The Reizman lab, particularly Howard Riezman and Isabelle Riezman, have experience performing large-scale lipidomic studies in budding yeast (Santos *et al.*, 2014) and handled all of lipid extraction and data analysis of the samples I prepared. Among the major findings from our analysis is that ergosterol levels are not significantly altered in flippase mutants or in response to a cold shift, which is consistent with

previous reports that ergosterol concentration is not altered in *drs2*Δ cells (Fei *et al.*, 2008) and is relatively inflexible in response to changes in temperature (Klose *et al.*, 2012).

However, we did observe some interesting changes in the composition of the sphingolipids ceramide, inositol-phosphorylceramide (IPC), mannose-inositol-phosphorylceramide (MIPC), and mannose-(inositol-P)2-ceramide (M(IP)2C). The most striking phenotypes for ceramide and IPC were that at 20°C *drs2*Δ cells have significant reduction of both lipids, but their levels are similar to WT in *kes1*Δ and *drs2*Δ*kes1*Δ cells: the pattern we expected for lipids involved in cold tolerance phenotype. However, *dnf1,2,3*Δ cells, which are not cold sensitive, have a similar reduction in both ceramide and IPC even at 30°C, which would suggest that reduction of the two lipids by themselves is not sufficient for the cold tolerance defect of *drs2*Δ cells.

There is a trend toward increased MIPC concentration in the *drs2*Δ and *kes1*Δ single mutants and a WT-like MIPC *drs2*Δ*kes1*Δ double mutant, which fits the exocytosis defect pattern of co-suppression. However, the concentration of M(IP)2C was elevated in *drs2*Δ, *kes1*Δ, and *drs2*Δ*kes1*Δ at 30°C relative to WT, which does not correlate with the co-suppression phenotype. Unlike ceramide and IPC, neither MIPC nor M(IP)2C levels were altered in *dnf1,2,3*Δ cells. The elevated MIPC levels in *drs2*Δ and *kes1*Δ cells may be related to the exocytic trafficking defect, but a caveat of these results is that there are issues with reliably extracting and quantifying MIPC and especially M(IP)2C using this method, which makes it difficult to draw definitive conclusions. In the future, we will need to use a technique, such as thin layer chromatography (TLC), to determine if the changes observed in *drs2*Δ cells are real or an artifact of the system.

We also looked at the total level of glycerophospholipids as well as their acyl chain lengths and degree of saturation as alterations in any of these could potentially account for the *drs2*Δ defects. Although we did not observe any significant changes in total glycerophospholipid levels, acyl chain lengths, or degree of saturation in the flippase or *kes1* mutants, there was a significant drop in PS in response to cold shift. If the findings by the Mayor lab regarding PS-dependent transbilayer coupling hold true in yeast, this

downregulation of PS may reduce the coalescence of raft-like domains (Raghupathy *et al.*, 2015). Thus, disruption of transbilayer coupling and raft coalescence may be a homeostatic response to keep membranes fluid at low temperatures. While there was no decrease in total levels of the other glycerophospholipids, the amount of di-unsaturated PC and PE species increased at 20°C, which may also contribute to membrane fluidity at low temperatures.

The final group of lipids that we examined was the lysophospholipids, which are glycerophospholipids with only one acyl chain. Lysophospholipids are thought to be primarily intermediates produced during glycerophospholipid remodeling via the Lands cycle. Cellular lysophospholipids are generally maintained at very low concentrations, but if allowed to accumulate, lysophospholipids can become disruptive to membranes as they act as detergents. However, a scenario in which lysophospholipids would accumulate is if they were unable to be flipped and remained in the extracellular/lumenal leaflet where they would be inaccessible to acyltransferases that could re-acylate them.

We actually found the opposite effect for *drs2* and *kes1* mutants: lysophospholipid levels modestly decreased in some instances, but never increased about WT levels. Temperature shift also did not significantly alter lysophospholipid levels with the exception of lyso-PS, which had a similar drop as PS upon cold shift. However, one lysophospholipid (lyso-PI) followed the co-suppression model with decreased lyso-PI in the single mutants, but normal levels in the double mutant. Therefore, the decrease in lyso-PI may be associated with defective exocytosis, but further research will be required to determine if a reduction in lyso-PI directly correlates with the defect and, if so, how lyso-PI contributes to exocytic trafficking.

In contrast to *drs2*Δ cells, the concentrations of three of the four lysophospholipid species (lyso-PC, lyso-PE, and lyso-PI) were greatly increased in *dnf1,2,3*Δ cells. The fact that lyso-PC and lyso-PE levels increased was expected as Dnf1 and Dnf2 are known to flip these substrates (Baldridge *et al.*, 2013), so it makes sense that in the absence of these flippases lyso-PC and lyso-PE accumulate in the extracellular/lumenal leaflet where they cannot be remodeled. However, to date there are no flippases

known to recognize and flip lyso-PI. Our data strongly indicate that lyso-PI is accumulating in high quantity (6.5-fold increased relative to WT) in *dnf1,2,3*Δ cells, which suggests that one or more Dnf proteins have the ability to flip lyso-PI to the cytosolic leaflet. However, it will require further work to determine with certainty that lyso-PI is substrate of the Dnf proteins.

Taken together, the lyso-PI data may suggest that the concentration of lyso-PI is differentially regulated in *drs2*Δ and *kes1*Δ single mutants, but regulated normally in the *drs2*Δ*kes1*Δ double mutants. This reduction could be due to changes in the regulation of PI-specific remodeling proteins of the Lands cycle (Lands, 1958; Shindou *et al.*, 2009), such as an upregulation of phospholipase activity (acyl chain removal) or a downregulation of acyltransferase activity (acyl chain addition). Lyso-PI, like PS, is a negatively charged lipid. PS in the cytosolic leaflet has previously been shown to be important for the membrane recruitment of cytosolic proteins with cationic patches (van Meer *et al.*, 2008; Xu *et al.*, 2013; Stahelin *et al.*, 2014). Thus, it is possible that the *drs2*Δ defects are a result of a failure to recruit unknown protein factors involved in exocytic trafficking. If this is true, lyso-PI flip at the TGN by the Dnf proteins could potentially substitute for PS flip in recruiting these cytosolic proteins in the *drs2*Δ*kes1*Δ double mutant but not when the flux of lyso-PI is reduced as in the case of the *drs2*Δ single mutant. Another explanation for the lyso-PI reduction could be that Dnf proteins are hyperactive in the *drs2*Δ and *kes1*Δ single mutants and that this is somehow deleterious to exocytic trafficking; however, previous experiments performed by the Graham lab have not detected increased Dnf flippase activity at the TGN when Drs2 is knocked out.

Roles of COPI and ubiquitin in protein trafficking

In addition to my main project, I also worked on a project led by Peng Xu, a postdoctoral fellow in the Graham lab. Like my project that found a novel function for Drs2 in exocytosis, this side project focuses on discovering a novel function for another protein with an already well-established role in protein trafficking: COPI. COPI is an evolutionarily conserved protein coat that functions in *intra*-Golgi trafficking and retrograde trafficking from the Golgi to the ER (Jackson, 2014). In addition to Golgi-

associated COPI, a subset of COPI has long been known to colocalize with early endosomes in mammalian cells (Whitney *et al.*, 1995; Aniento *et al.*, 1996; Daro *et al.*, 1997; Gu *et al.*, 1997). To date, no definitive function has been attributed to COPI in the endosomal system, so it has been unclear what, if any, significance the pool of endosome-localized COPI has in protein trafficking.

In support for a role of COPI in the endosomal system, the Pelham lab has demonstrated that temperature sensitive mutations that disrupt COPI function (e.g. *sec21-1* or *ret1-1*) block retrieval of GFP-Snc1 from early endosomes to the TGN (Lewis *et al.*, 2000). A caveat of this study, however, is that loss of COPI function grossly perturbs the organization of the Golgi. This complicating factor makes it unclear whether the defect in GFP-Snc1 trafficking is due to losing COPI on endosomal membranes or if it is simply an indirect consequence of disrupting the Golgi, which can have numerous downstream effects.

The COPI coat is a heptameric complex composed of an adaptor-like F-subcomplex (β, γ, δ, ζ) and a clathrin-like B-subcomplex (α, β', ε). The most extensively studied COPI cargo proteins are those that bear KKxx or KxKxx sorting motifs. COPI interacts with these motifs via the β-propeller domains of the COPI α and β' subunits (Jackson *et al.*, 2012; Ma and Goldberg, 2013). Importantly for this work, these β-propeller domains have also been shown to bind ubiquitin (Pashkova *et al.*, 2010). Ubiquitination is best known for its role in protein degradation but can actually be involved in a variety of processes depending on how the polyubiquitin chains are formed (Spence *et al.*, 1995; Hicke and Dunn, 2003; Peng *et al.*, 2003; Pickart and Fushman, 2004; Varadan *et al.*, 2004; Chen and Sun, 2009; Xu *et al.*, 2009; Silva *et al.*, 2015).

For instance, Snc1 is ubiquitinated and it appears that ubiquitination is important for its retrieval from early endosomes (Peng *et al.*, 2003; Chen *et al.*, 2011; Silva *et al.*, 2015). The Segev lab has shown that mutation of the lysine at position 63 (Snc1-K63R) decreases the amount of Snc1 ubiquitination and disrupts Snc1 retrieval from early endosomes to the TGN (Chen *et al.*, 2011). However, dilysine motifs are common sorting signals, so it is possible that the trafficking defect is due to disrupting a sorting signal rather than specifically blocking Snc1 ubiquitination.

In our study, we sought to address whether COPI is directly involved in Snc1 trafficking from early endosomes. To do so, we mutated or deleted the ubiquitin-interacting β-propeller domains of the COPI α and β' subunits. To specifically test if ubiquitination is important for Snc1 trafficking, we fused a potent deubiquitinase to the N-terminus of GFP-Snc1. The primary advantage of this approach is that no mutation of the Snc1 primary sequence is required that could disrupt a sorting signal. We hypothesized that the COPI β-propellers recognize ubiquitinated Snc1 to allow for Snc1 incorporation into COPI vesicles originating from early endosomes.

Our results suggest that Snc1 ubiquitination is indeed essential for its recycling from early endosomes to the TGN. Fusing the deubiquitinase (DUB) to GFP-Snc1 (DUB-GFP-Snc1) caused Snc1 to accumulate in early endosomes. In contrast, fusing a catalytically inactive form of the DUB to GFP-Snc1 (DUB*-GFP-Snc1) had no effect on Snc1 trafficking. This appears to be specific to Snc1 ubiquitination as fusing the DUB to Drs2, an essential component of the Snc1 recycling pathway, has no effect on Snc1 trafficking. These results strongly argue that ubiquitin functions as a sorting signal for Snc1, rather than a degradation signal. Consistent with our findings, the polyubiquitin chain attached to Snc1 has been reported to be K63-linked, which is one of the ubiquitin linkages not associated with protein degradation (Xu *et al.*, 2009; Silva *et al.*, 2015).

Interestingly, the COPI β–propellers are able to bind to K63-linked tetra-ubiquitin, but not mono-ubiquitin or tetra-ubiquitin with different linkage types (Peng Xu, unpublished). This finding indicates that COPI may recognize K63-linked Snc1 for its incorporation into COPI vesicles. Furthermore, deletion of the COPI β–propellers caused GFP-Snc1 to accumulate at early endosomes, suggesting a block in the recycling pathway. Our results suggest that even when Snc1 is ubiquitinated, it must also be recognized by COPI in order to be incorporated into vesicles and recycled back to the TGN.

To ensure that the essential function of the COPI β–propellers in Snc1 trafficking is specific to their ability to bind to ubiquitin, we substituted the first β–propeller of the β'subunit with the ubiquitin-binding domain (UBD) of Doa1 or the NZF domain of TAB2. The UBD of Doa1 is known to associate with both

mono-ubiquitin and polyubiquitin regardless of linkage type (Mullally *et al.*, 2006), whereas the NZF domain of TAB2 is specific to K63-linked polyubiquitin chains (Kulathu *et al.*, 2009). We found that replacement of the β–propeller of β'-COP with either the UBD or NZF domain was sufficient to restore Snc1 recycling. This restoration of Snc1 trafficking in the β'-COP NZF chimera strongly argues that the ability to bind K63-linked ubiquitin chains is the essential function for the COPI β-propeller in Snc1 trafficking.

An issue that plagued earlier studies is dissecting whether or not defects caused by COPI mutants are specific, suggesting COPI has an active role in the process, or simply a downstream effect of perturbed Golgi organization. Our work has the advantage of using COPI mutants that do not affect Golgi organization. Deletion of the β-propeller of β'-COP does not affect the normal trafficking of the Golgi-localized COPI cargo protein GFP-Rer1, which mislocalizes to the vacuole when COPI function is lost. Taken together, our results strongly suggests that the β-propeller of β'-COP has an essential function in the ubiquitin-dependent retrieval of Snc1 from early endosomes, but is dispensable for COPI function at the Golgi.

Concluding statement

The work described in this dissertation has uncovered novel functions for already well-established components of the budding yeast trafficking machinery (Figure 5-1). We have shown that Drs2 has a role in the raft-associated light vesicle branch of exocytosis in addition to its roles in other TGN-associated trafficking pathways. We have also found that COPI, in addition to its role at the Golgi, functions in the recycling pathway between the early endosomes and TGN. Of interest, Drs2 is both a cargo and regulator of this recycling pathway and COPI β-propeller mutants and *drs2*Δ cells have a similar trafficking defect (i.e. GFP-Snc1 accumulates at early endosomes). These observations suggests that COPI and Drs2 may function together in this trafficking pathway. For instance, Drs2 flippase activity may be required to

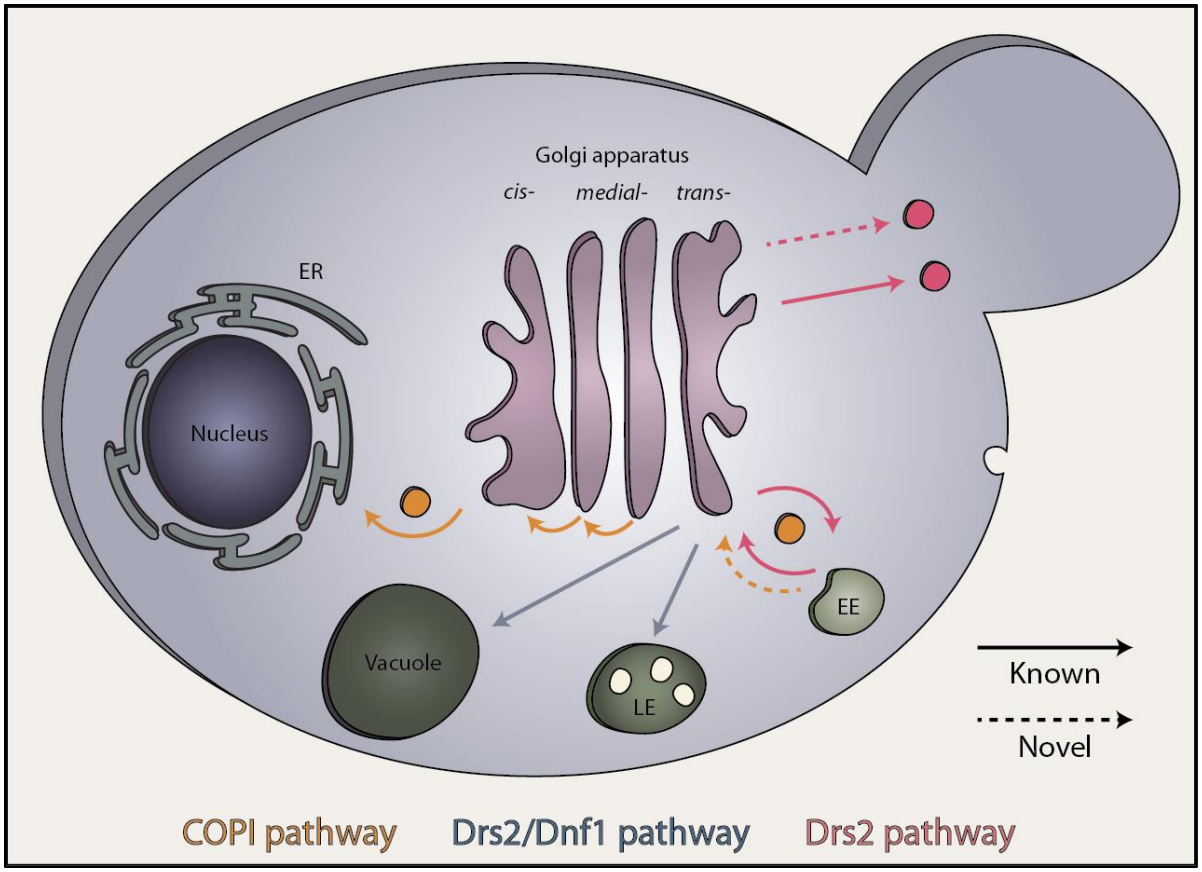

Figure 5-1. Known and novel Drs2- and COPI-dependent protein trafficking pathways in *S. cerevisiae*.

recruit COPI to endosomal membranes. Taken together, this work highlights the interconnectedness of the different yeast trafficking pathways and demonstrates the multifunctionality of the trafficking machinery.

REFERENCES

Alder-Baerens, N., Lisman, Q., Luong, L., Pomorski, T., and Holthuis, J. C. M. (2006). Loss of P4 ATPases Drs2p and Dnf3p Disrupts Aminophospholipid Transport and Asymmetry in Yeast Post-Golgi Secretory Vesicles. Mol. Biol. Cell *17*, 1632–1642.

Alfaro, G., Johansen, J., Dighe, S. A., Duamel, G., Kozminski, K. G., and Beh, C. T. (2011). The Sterol-Binding Protein Kes1/Osh4p Is a Regulator of Polarized Exocytosis. Traffic *12*, 1521–1536.

Alvarez, F. J., Douglas, L. M., and Konopka, J. B. (2007). Sterol-Rich Plasma Membrane Domains in Fungi. Eukaryot. Cell *6*, 755–763.

Anand, V. C., Daboussi, L., Lorenz, T. C., and Payne, G. S. (2009). Genome-wide Analysis of AP-3–dependent Protein Transport in Yeast. Mol. Biol. Cell *20*, 1592–1604.

Aniento, F., Gu, F., Parton, R. G., and Gruenberg, J. (1996). An endosomal beta COP is involved in the pH-dependent formation of transport vesicles destined for late endosomes. J. Cell Biol. *133*, 29–41.

Atkinson, K. D., Jensen, B., Kolat, A. I., Storm, E. M., Henry, S. A., and Fogel, S. (1980). Yeast mutants auxotrophic for choline or ethanolamine. J. Bacteriol. *141*, 558–564.

Axelsen, K. B., and Palmgren, M. G. (1998). Evolution of substrate specificities in the P-type ATPase superfamily. J. Mol. Evol. *46*, 84–101.

Babu, M. *et al.* (2012). Interaction landscape of membrane-protein complexes in Saccharomyces cerevisiae. Nature *489*, 585–589.

Bagnat, M., Chang, A., and Simons, K. (2001). Plasma Membrane Proton ATPase Pma1p Requires Raft Association for Surface Delivery in Yeast. Mol. Biol. Cell *12*, 4129–4138.

Bagnat, M., Keränen, S., Shevchenko, A., Shevchenko, A., and Simons, K. (2000). Lipid rafts function in biosynthetic delivery of proteins to the cell surface in yeast. Proc. Natl. Acad. Sci. *97*, 3254–3259.

Bagnat, M., and Simons, K. (2002). Lipid Rafts in Protein Sorting and Cell Polarity in Budding Yeast Saccharomyces cerevisiae. Biol. Chem. *383*.

Balderhaar, H. J. kleine, Arlt, H., Ostrowicz, C., Bröcker, C., Sündermann, F., Brandt, R., Babst, M., and Ungermann, C. (2010). The Rab GTPase Ypt7 is linked to retromer-mediated receptor recycling and fusion at the yeast late endosome. J Cell Sci *123*, 4085–4094.

Baldridge, R. D., and Graham, T. R. (2012). Identification of residues defining phospholipid flippase substrate specificity of type IV P-type ATPases. Proc. Natl. Acad. Sci. U. S. A. *109*, E290–298.

Baldridge, R. D., and Graham, T. R. (2013). Two-gate mechanism for phospholipid selection and transport by type IV P-type ATPases. Proc. Natl. Acad. Sci. U. S. A. *110*, E358–367.

Baldridge, R. D., Xu, P., and Graham, T. R. (2013). Type IV P-type ATPases distinguish mono- versus diacyl phosphatidylserine using a cytofacial exit gate in the membrane domain. J. Biol. Chem. *288*, 19516–19527.

Barlowe, C. K., and Miller, E. A. (2013). Secretory protein biogenesis and traffic in the early secretory pathway. Genetics *193*, 383–410.

Baumann, N. A., Sullivan, D. P., Ohvo-Rekilä, H., Simonot, C., Pottekat, A., Klaassen, Z., Beh, C. T., and Menon, A. K. (2005). Transport of newly synthesized sterol to the sterol-enriched plasma membrane occurs via nonvesicular equilibration. Biochemistry (Mosc.) *44*, 5816–5826.

Beh, C. T., and Rine, J. (2004). A role for yeast oxysterol-binding protein homologs in endocytosis and in the maintenance of intracellular sterol-lipid distribution. J. Cell Sci. *117*, 2983–2996.

Bell, R. M., Ballas, L. M., and Coleman, R. A. (1981). Lipid topogenesis. J. Lipid Res. *22*, 391–403.

Berchtold, D., Piccolis, M., Chiaruttini, N., Riezman, I., Riezman, H., Roux, A., Walther, T. C., and Loewith, R. (2012). Plasma membrane stress induces relocalization of Slm proteins and activation of TORC2 to promote sphingolipid synthesis. Nat. Cell Biol. *14*, 542–547.

Berchtold, D., and Walther, T. C. (2009). TORC2 Plasma Membrane Localization Is Essential for Cell Viability and Restricted to a Distinct Domain. Mol. Biol. Cell *20*, 1565–1575.

Bevers, E. M., Comfurius, P., and Zwaal, R. F. A. (1983). Changes in membrane phospholipid distribution during platelet activation. Biochim. Biophys. Acta BBA - Biomembr. *736*, 57–66.

Bishop, W. R., and Bell, R. M. (1985). Assembly of the endoplasmic reticulum phospholipid bilayer: the phosphatidylcholine transporter. Cell *42*, 51–60.

Boehm, M., and Bonifacino, J. S. (2002). Genetic analyses of adaptin function from yeast to mammals. Gene *286*, 175–186.

Bolte, S., and Cordelières, F. P. (2006). A guided tour into subcellular colocalization analysis in light microscopy. J. Microsc. *224*, 213–232.

Bonifacino, J. S. (2004). The GGA proteins: adaptors on the move. Nat. Rev. Mol. Cell Biol. *5*, 23–32.

Brach, T., Specht, T., and Kaksonen, M. (2011). Reassessment of the role of plasma membrane domains in the regulation of vesicular traffic in yeast. J. Cell Sci. *124*, 328–337.

Bratton, D. L., Fadok, V. A., Richter, D. A., Kailey, J. M., Guthrie, L. A., and Henson, P. M. (1997). Appearance of Phosphatidylserine on Apoptotic Cells Requires Calcium-mediated Nonspecific Flip-Flop and Is Enhanced by Loss of the Aminophospholipid Translocase. J. Biol. Chem. *272*, 26159–26165.

Breslow, D. K., and Weissman, J. S. (2010). Membranes in Balance: Mechanisms of Sphingolipid Homeostasis. Mol. Cell *40*, 267–279.

Bryde, S., Hennrich, H., Verhulst, P. M., Devaux, P. F., Lenoir, G., and Holthuis, J. C. M. (2010). CDC50 proteins are critical components of the human class-1 P4-ATPase transport machinery. J. Biol. Chem. *285*, 40562–40572.

Buton, X., Morrot, G., Fellmann, P., and Seigneuret, M. (1996). Ultrafast Glycerophospholipid-selective Transbilayer Motion Mediated by a Protein in the Endoplasmic Reticulum Membrane. J. Biol. Chem. *271*, 6651–6657.

Cai, S.-Y., Gautam, S., Nguyen, T., Soroka, C. J., Rahner, C., and Boyer, J. L. (2009). ATP8B1 deficiency disrupts the bile canalicular membrane bilayer structure in hepatocytes, but FXR expression and activity are maintained. Gastroenterology *136*, 1060–1069.

Carroll, S. Y., Stirling, P. C., Stimpson, H. E. M., Gießelmann, E., Schmitt, M. J., and Drubin, D. G. (2009). A yeast killer toxin screen provides insights into A/B toxin entry, trafficking and killing mechanisms. Dev. Cell *17*, 552–560.

Chang, A., and Fink, G. R. (1995). Targeting of the yeast plasma membrane [H+]ATPase: a novel gene AST1 prevents mislocalization of mutant ATPase to the vacuole. J. Cell Biol. *128*, 39–49.

Chang, A., and Slayman, C. W. (1991). Maturation of the yeast plasma membrane [H+]ATPase involves phosphorylation during intracellular transport. J. Cell Biol. *115*, 289–295.

Chen, B., Jiang, Y., Zeng, S., Yan, J., Li, X., Zhang, Y., Zou, W., and Wang, X. (2010). Endocytic sorting and recycling require membrane phosphatidylserine asymmetry maintained by TAT-1/CHAT-1. PLoS Genet. *6*, e1001235.

Chen, C.-Y., and Graham, T. R. (1998). An arf1Δ Synthetic Lethal Screen Identifies a New Clathrin Heavy Chain Conditional Allele That Perturbs Vacuolar Protein Transport in Saccharomyces cerevisiae. Genetics *150*, 577–589.

Chen, C.-Y., Ingram, M. F., Rosal, P. H., and Graham, T. R. (1999). Role for Drs2p, a P-Type Atpase and Potential Aminophospholipid Translocase, in Yeast Late Golgi Function. J. Cell Biol. *147*, 1223–1236.

Chen, S. H., Chen, S., Tokarev, A. A., Liu, F., Jedd, G., and Segev, N. (2005). Ypt31/32 GTPases and Their Novel F-Box Effector Protein Rcy1 Regulate Protein Recycling. Mol. Biol. Cell *16*, 178–192.

Chen, S. H., Shah, A. H., and Segev, N. (2011). Ypt31/32 GTPases and their F-Box effector Rcy1 regulate ubiquitination of recycling proteins. Cell. Logist. *1*, 21–31.

Chen, S., Wang, J., Muthusamy, B.-P., Liu, K., Zare, S., Andersen, R. J., and Graham, T. R. (2006). Roles for the Drs2p–Cdc50p Complex in Protein Transport and Phosphatidylserine Asymmetry of the Yeast Plasma Membrane. Traffic *7*, 1503–1517.

Chen, Z. J., and Sun, L. J. (2009). Nonproteolytic functions of ubiquitin in cell signaling. Mol. Cell *33*, 275–286.

Coleman, J. A., Kwok, M. C. M., and Molday, R. S. (2009). Localization, Purification, and Functional Reconstitution of the P4-ATPase Atp8a2, a Phosphatidylserine Flippase in Photoreceptor Disc Membranes. J. Biol. Chem. *284*, 32670–32679.

Costaguta, G., Stefan, C. J., Bensen, E. S., Emr, S. D., and Payne, G. S. (2001). Yeast Gga Coat Proteins Function with Clathrin in Golgi to Endosome Transport. Mol. Biol. Cell *12*, 1885–1896.

Cowles, C. R., Odorizzi, G., Payne, G. S., and Emr, S. D. (1997). The AP-3 Adaptor Complex Is Essential for Cargo-Selective Transport to the Yeast Vacuole. Cell *91*, 109–118.

D'Angelo, G., Rega, L. R., and De Matteis, M. A. (2012). Connecting vesicular transport with lipid synthesis: FAPP2. Biochim. Biophys. Acta BBA - Mol. Cell Biol. Lipids *1821*, 1089–1095.

Daicho, K., Makino, N., Hiraki, T., Ueno, M., Uritani, M., Abe, F., and Ushimaru, T. (2009). Sorting defects of the tryptophan permease Tat2 in an erg2 yeast mutant. FEMS Microbiol. Lett. *298*, 218–227.

Daleke, D. L. (2003). Regulation of transbilayer plasma membrane phospholipid asymmetry. J. Lipid Res. *44*, 233–242.

Daleke, D. L. (2007). Phospholipid Flippases. J. Biol. Chem. *282*, 821–825.

Daro, E., Sheff, D., Gomez, M., Kreis, T., and Mellman, I. (1997). Inhibition of endosome function in CHO cells bearing a temperature-sensitive defect in the coatomer (COPI) component epsilon-COP. J. Cell Biol. *139*, 1747–1759.

Darsow, T., Burd, C. G., and Emr, S. D. (1998). Acidic Di-leucine Motif Essential for AP-3–dependent Sorting and Restriction of the Functional Specificity of the Vam3p Vacuolar t-SNARE. J. Cell Biol. *142*, 913–922.

Daum, G., Lees, N. D., Bard, M., and Dickson, R. (1998). Biochemistry, cell biology and molecular biology of lipids of Saccharomyces cerevisiae. Yeast Chichester Engl. *14*, 1471–1510.

Van der Velden, L. M., van de Graaf, S. F. J., and Klomp, L. W. J. (2010). Biochemical and cellular functions of P 4 ATPases. Biochem. J. *431*, 1–11.

Devaux, P. F. (1992). Protein Involvement in Transmembrane Lipid Asymmetry. Annu. Rev. Biophys. Biomol. Struct. *21*, 417–439.

Dhar, M. S., Sommardahl, C. S., Kirkland, T., Nelson, S., Donnell, R., Johnson, D. K., and Castellani, L. W. (2004). Mice heterozygous for Atp10c, a putative amphipath, represent a novel model of obesity and type 2 diabetes. J. Nutr. *134*, 799–805.

Dhar, M. S., Yuan, J. S., Elliott, S. B., and Sommardahl, C. (2006). A type IV P-type ATPase affects insulin-mediated glucose uptake in adipose tissue and skeletal muscle in mice. J. Nutr. Biochem. *17*, 811–820.

Ding, J., Wu, Z., Crider, B. P., Ma, Y., Li, X., Slaughter, C., Gong, L., and Xie, X. S. (2000). Identification and functional expression of four isoforms of ATPase II, the putative aminophospholipid translocase. Effect of isoform variation on the ATPase activity and phospholipid specificity. J. Biol. Chem. *275*, 23378–23386.

Dodonova, S. O., Diestelkoetter-Bachert, P., Appen, A. von, Hagen, W. J. H., Beck, R., Beck, M., Wieland, F., and Briggs, J. a. G. (2015). A structure of the COPI coat and the role of coat proteins in membrane vesicle assembly. Science *349*, 195–198.

Drabikowski, W., Łagwińska, E., and Sarzała, M. G. (1973). Filipin as a fluorescent probe for the location of cholesterol in the membranes of fragmented sarcoplasmic reticulum. Biochim. Biophys. Acta BBA - Biomembr. *291*, 61–70.

Dupuis, J. *et al.* (2010). New genetic loci implicated in fasting glucose homeostasis and their impact on type 2 diabetes risk. Nat. Genet. *42*, 105–116.

Ejsing, C. S., Sampaio, J. L., Surendranath, V., Duchoslav, E., Ekroos, K., Klemm, R. W., Simons, K., and Shevchenko, A. (2009). Global analysis of the yeast lipidome by quantitative shotgun mass spectrometry. Proc. Natl. Acad. Sci. U. S. A. *106*, 2136–2141.

Emoto, K., Kobayashi, T., Yamaji, A., Aizawa, H., Yahara, I., Inoue, K., and Umeda, M. (1996). Redistribution of phosphatidylethanolamine at the cleavage furrow of dividing cells during cytokinesis. Proc. Natl. Acad. Sci. *93*, 12867–12872.

Emre Onat, O., Gulsuner, S., Bilguvar, K., Nazli Basak, A., Topaloglu, H., Tan, M., Tan, U., Gunel, M., and Ozcelik, T. (2013). Missense mutation in the ATPase, aminophospholipid transporter protein ATP8A2 is associated with cerebellar atrophy and quadrupedal locomotion. Eur. J. Hum. Genet. *21*, 281–285.

Eugster, A., Frigerio, G., Dale, M., and Duden, R. (2004). The α- and β′-COP WD40 Domains Mediate Cargo-selective Interactions with Distinct Di-lysine Motifs. Mol. Biol. Cell *15*, 1011–1023.

Fadok, V. A., Voelker, D. R., Campbell, P. A., Cohen, J. J., Bratton, D. L., and Henson, P. M. (1992). Exposure of phosphatidylserine on the surface of apoptotic lymphocytes triggers specific recognition and removal by macrophages. J. Immunol. *148*, 2207–2216.

Fairn, G. D., Curwin, A. J., Stefan, C. J., and McMaster, C. R. (2007). The oxysterol binding protein Kes1p regulates Golgi apparatus phosphatidylinositol-4-phosphate function. Proc. Natl. Acad. Sci. *104*, 15352–15357.

Fairn, G. D., Schieber, N. L., Ariotti, N., Murphy, S., Kuerschner, L., Webb, R. I., Grinstein, S., and Parton, R. G. (2011). High-resolution mapping reveals topologically distinct cellular pools of phosphatidylserine. J. Cell Biol. *194*, 257–275.

Fang, M., Kearns, B. G., Gedvilaite, A., Kagiwada, S., Kearns, M., Fung, M. K., and Bankaitis, V. A. (1996). Kes1p shares homology with human oxysterol binding protein and participates in a novel regulatory pathway for yeast Golgi-derived transport vesicle biogenesis. EMBO J. *15*, 6447–6459.

Fei, W., Alfaro, G., Muthusamy, B.-P., Klaassen, Z., Graham, T. R., Yang, H., and Beh, C. T. (2008). Genome-Wide Analysis of Sterol-Lipid Storage and Trafficking in Saccharomyces cerevisiae. Eukaryot. Cell *7*, 401–414.

Feyder, S., De Craene, J.-O., Bär, S., Bertazzi, D. L., and Friant, S. (2015). Membrane Trafficking in the Yeast Saccharomyces cerevisiae Model. Int. J. Mol. Sci. *16*, 1509–1525.

Flamant, S., Pescher, P., Lemercier, B., Clément-Ziza, M., Képès, F., Fellous, M., Milon, G., Marchal, G., and Besmond, C. (2003). Characterization of a putative type IV aminophospholipid transporter P-type ATPase. Mamm. Genome Off. J. Int. Mamm. Genome Soc. *14*, 21–30.

Foti, M., Audhya, A., and Emr, S. D. (2001). Sac1 Lipid Phosphatase and Stt4 Phosphatidylinositol 4-Kinase Regulate a Pool of Phosphatidylinositol 4-Phosphate That Functions in the Control of the Actin Cytoskeleton and Vacuole Morphology. Mol. Biol. Cell *12*, 2396–2411.

Fuller, N., Benatti, C. R., and Rand, R. P. (2003). Curvature and Bending Constants for Phosphatidylserine-Containing Membranes. Biophys. J. *85*, 1667–1674.

Funato, K., and Riezman, H. (2001). Vesicular and nonvesicular transport of ceramide from ER to the Golgi apparatus in yeast. J. Cell Biol. *155*, 949–960.

Furuita, K., Jee, J., Fukada, H., Mishima, M., and Kojima, C. (2010). Electrostatic interaction between oxysterol-binding protein and VAMP-associated protein A revealed by NMR and mutagenesis studies. J. Biol. Chem. *285*, 12961–12970.

Furuta, N., Fujimura-Kamada, K., Saito, K., Yamamoto, T., and Tanaka, K. (2007). Endocytic Recycling in Yeast Is Regulated by Putative Phospholipid Translocases and the Ypt31p/32p–Rcy1p Pathway. Mol. Biol. Cell *18*, 295–312.

Gaigg, B., Toulmay, A., and Schneiter, R. (2006). Very Long-chain Fatty Acid-containing Lipids rather than Sphingolipids per se Are Required for Raft Association and Stable Surface Transport of Newly Synthesized Plasma Membrane ATPase in Yeast. J. Biol. Chem. *281*, 34135–34145.

Galan, J. M., and Haguenauer-Tsapis, R. (1997). Ubiquitin lys63 is involved in ubiquitination of a yeast plasma membrane protein. EMBO J. *16*, 5847–5854.

Galan, J.-M., Wiederkehr, A., Seol, J. H., Haguenauer-Tsapis, R., Deshaies, R. J., Riezman, H., and Peter, M. (2001). Skp1p and the F-Box Protein Rcy1p Form a Non-SCF Complex Involved in Recycling of the SNARE Snc1p in Yeast. Mol. Cell. Biol. *21*, 3105–3117.

Gall, W. E., Geething, N. C., Hua, Z., Ingram, M. F., Liu, K., Chen, S. I., and Graham, T. R. (2002). Drs2p-Dependent Formation of Exocytic Clathrin-Coated Vesicles In Vivo. Curr. Biol. *12*, 1623–1627.

Gall, W. E., Higginbotham, M. A., Chen, C.-Y., Ingram, M. F., Cyr, D. M., and Graham, T. R. (2000). The auxilin-like phosphoprotein Swa2p is required for clathrin function in yeast. Curr. Biol. *10*, 1349–1358.

Gaspar, M. L., Aregullin, M. A., Jesch, S. A., Nunez, L. R., Villa-García, M., and Henry, S. A. (2007). The emergence of yeast lipidomics. Biochim. Biophys. Acta BBA - Mol. Cell Biol. Lipids *1771*, 241–254.

Gatta, A. T., Wong, L. H., Sere, Y. Y., Calderón-Noreña, D. M., Cockcroft, S., Menon, A. K., and Levine, T. P. (2015). A new family of StART domain proteins at membrane contact sites has a role in ER-PM sterol transport. eLife *4*.

Georgiev, A. G., Sullivan, D. P., Kersting, M. C., Dittman, J. S., Beh, C. T., and Menon, A. K. (2011). Osh Proteins Regulate Membrane Sterol Organization but Are Not Required for Sterol Movement Between the ER and PM. Traffic *12*, 1341–1355.

Gietz, R. D., and Schiestl, R. H. (2007). High-efficiency yeast transformation using the LiAc/SS carrier DNA/PEG method. Nat. Protoc. *2*, 31–34.

Godi, A., Di Campli, A., Konstantakopoulos, A., Di Tullio, G., Alessi, D. R., Kular, G. S., Daniele, T., Marra, P., Lucocq, J. M., and De Matteis, M. A. (2004). FAPPs control Golgi-to-cell-surface membrane traffic by binding to ARF and PtdIns(4)P. Nat. Cell Biol. *6*, 393–404.

Gong, E.-Y., Park, E., Lee, H. J., and Lee, K. (2009). Expression of Atp8b3 in murine testis and its characterization as a testis specific P-type ATPase. Reprod. Camb. Engl. *137*, 345–351.

Goode, B. L., Eskin, J. A., and Wendland, B. (2015). Actin and Endocytosis in Budding Yeast. Genetics *199*, 315–358.

Graham, T. R. (2004). Flippases and vesicle-mediated protein transport. Trends Cell Biol. *14*, 670–677.

Graham, T. R., and Burd, C. G. (2011). Coordination of Golgi functions by phosphatidylinositol 4-kinases. Trends Cell Biol. *21*, 113–121.

Grossmann, G., Malinsky, J., Stahlschmidt, W., Loibl, M., Weig-Meckl, I., Frommer, W. B., Opekarová, M., and Tanner, W. (2008). Plasma membrane microdomains regulate turnover of transport proteins in yeast. J. Cell Biol. *183*, 1075–1088.

Grossmann, G., Opekarova, M., Malinsky, J., Weig-Meckl, I., and Tanner, W. (2007). Membrane potential governs lateral segregation of plasma membrane proteins and lipids in yeast. EMBO J. *26*, 1–8.

Grossmann, G., Opekarova, M., Novakova, L., Stolz, J., and Tanner, W. (2006). Lipid Raft-Based Membrane Compartmentation of a Plant Transport Protein Expressed in Saccharomyces cerevisiae. Eukaryot. Cell *5*, 945–953.

Grote, E., Hao, J. C., Bennett, M. K., and Kelly, R. B. (1995). A targeting signal in VAMP regulating transport to synaptic vesicles. Cell *81*, 581–589.

Gu, F., Aniento, F., Parton, R. G., and Gruenberg, J. (1997). Functional dissection of COP-I subunits in the biogenesis of multivesicular endosomes. J. Cell Biol. *139*, 1183–1195.

Gu, F., Crump, C. M., and Thomas, G. (2001). Trans-Golgi network sorting. Cell. Mol. Life Sci. CMLS *58*, 1067–1084.

Guan, X. L., Riezman, I., Wenk, M. R., and Riezman, H. (2010). Chapter 15 - Yeast Lipid Analysis and Quantification by Mass Spectrometry. ed. B.-M. in Enzymology, Academic Press, 369–391.

Guillas, I., Jiang, J. C., Vionnet, C., Roubaty, C., Uldry, D., Chuard, R., Wang, J., Jazwinski, S. M., and Conzelmann, A. (2003). Human Homologues of LAG1 Reconstitute Acyl-CoA-dependent Ceramide Synthesis in Yeast. J. Biol. Chem. *278*, 37083–37091.

Guillas, I., Kirchman, P. A., Chuard, R., Pfefferli, M., Jiang, J. C., Jazwinski, S. M., and Conzelmann, A. (2001). C26-CoA-dependent ceramide synthesis of Saccharomyces cerevisiae is operated by Lag1p and Lac1p. EMBO J. *20*, 2655–2665.

Gurunathan, S., David, D., and Gerst, J. E. (2002). Dynamin and clathrin are required for the biogenesis of a distinct class of secretory vesicles in yeast. EMBO J. *21*, 602–614.

Haglund, K., Sigismund, S., Polo, S., Szymkiewicz, I., Di Fiore, P. P., and Dikic, I. (2003). Multiple monoubiquitination of RTKs is sufficient for their endocytosis and degradation. Nat. Cell Biol. *5*, 461–466.

Hanada, K., Kumagai, K., Yasuda, S., Miura, Y., Kawano, M., Fukasawa, M., and Nishijima, M. (2003). Molecular machinery for non-vesicular trafficking of ceramide. Nature *426*, 803–809.

Hankins, H. M., Baldridge, R. D., Xu, P., and Graham, T. R. (2015a). Role of flippases, scramblases and transfer proteins in phosphatidylserine subcellular distribution. Traffic Cph. Den. *16*, 35–47.

Hankins, H. M., Sere, Y. Y., Diab, N. S., Menon, A. K., and Graham, T. R. (2015b). Phosphatidylserine translocation at the yeast trans-Golgi network regulates protein sorting into exocytic vesicles. Mol. Biol. Cell *26*, 4674–4685.

Harsay, E., and Bretscher, A. (1995). Parallel secretory pathways to the cell surface in yeast. J. Cell Biol. *131*, 297–310.

Harsay, E., and Schekman, R. (2002). A subset of yeast vacuolar protein sorting mutants is blocked in one branch of the exocytic pathway. J. Cell Biol. *156*, 271–286.

Helmkamp, G. M., Jr (1986). Phospholipid transfer proteins: mechanism of action. J. Bioenerg. Biomembr. *18*, 71–91.

Herrmann, A., Zachowski, A., and Devaux, P. F. (1990). Protein-mediated phospholipid translocation in the endoplasmic reticulum with a low lipid specificity. Biochemistry (Mosc.) *29*, 2023–2027.

Hettema, E. H., Lewis, M. J., Black, M. W., and Pelham, H. R. B. (2003). Retromer and the sorting nexins Snx4/41/42 mediate distinct retrieval pathways from yeast endosomes. EMBO J. *22*, 548–557.

Hicke, L., and Dunn, and R. (2003). Regulation of Membrane Protein Transport by Ubiquitin and Ubiquitin-Binding Proteins. Annu. Rev. Cell Dev. Biol. *19*, 141–172.

Higgins, J. A., and Dawson, R. M. C. (1977). Asymmetry of the phospholipid bilayer of rat liver endoplasmic reticulum. Biochim. Biophys. Acta BBA - Biomembr. *470*, 342–356.

Hirst, J., Lui, W. W. Y., Bright, N. A., Totty, N., Seaman, M. N. J., and Robinson, M. S. (2000). A Family of Proteins with γ-Adaptin and Vhs Domains That Facilitate Trafficking between the Trans-Golgi Network and the Vacuole/Lysosome. J. Cell Biol. *149*, 67–80.

Holthuis, J. C. M., and Levine, T. P. (2005). Lipid traffic: floppy drives and a superhighway. Nat. Rev. Mol. Cell Biol. *6*, 209–220.

Hsu, V. W., Lee, S. Y., and Yang, J.-S. (2009). The evolving understanding of COPI vesicle formation. Nat. Rev. Mol. Cell Biol. *10*, 360–364.

Hua, Z., Fatheddin, P., and Graham, T. R. (2002). An Essential Subfamily of Drs2p-related P-Type ATPases Is Required for Protein Trafficking between Golgi Complex and Endosomal/Vacuolar System. Mol. Biol. Cell *13*, 3162–3177.

Hua, Z., and Graham, T. R. (2003). Requirement for neo1p in retrograde transport from the Golgi complex to the endoplasmic reticulum. Mol. Biol. Cell *14*, 4971–4983.

Huang, C., and Chang, A. (2011). pH-dependent Cargo Sorting from the Golgi. J. Biol. Chem. *286*, 10058–10065.

Ikonen, E., and Simons, K. (1998). Protein and lipid sorting from thetrans–Golgi network to the plasma membrane in polarized cells. Semin. Cell Dev. Biol. *9*, 503–509.

Im, Y. J., Raychaudhuri, S., Prinz, W. A., and Hurley, J. H. (2005). Structural mechanism for sterol sensing and transport by OSBP-related proteins. Nature *437*, 154–158.

Irvin, M. R. *et al.* (2011). Genome-wide detection of allele specific copy number variation associated with insulin resistance in African Americans from the HyperGEN study. PloS One *6*, e24052.

Jackson, L. P. (2014). Structure and mechanism of COPI vesicle biogenesis. Curr. Opin. Cell Biol. *29*, 67–73.

Jackson, L. P., Lewis, M., Kent, H. M., Edeling, M. A., Evans, P. R., Duden, R., and Owen, D. J. (2012). Molecular Basis for Recognition of Dilysine Trafficking Motifs by COPI. Dev. Cell *23*, 1255–1262.

Jackson, M. R., Nilsson, T., and Peterson, P. A. (1990). Identification of a consensus motif for retention of transmembrane proteins in the endoplasmic reticulum. EMBO J. *9*, 3153–3162.

Jackson, M. R., Nilsson, T., and Peterson, P. A. (1993). Retrieval of transmembrane proteins to the endoplasmic reticulum. J. Cell Biol. *121*, 317–333.

Jacquot, A., Montigny, C., Hennrich, H., Barry, R., Maire, M. le, Jaxel, C., Holthuis, J., Champeil, P., and Lenoir, G. (2012). Phosphatidylserine Stimulation of Drs2p·Cdc50p Lipid Translocase Dephosphorylation Is Controlled by Phosphatidylinositol-4-phosphate. J. Biol. Chem. *287*, 13249–13261.

Janke, C. *et al.* (2004). A versatile toolbox for PCR-based tagging of yeast genes: new fluorescent proteins, more markers and promoter substitution cassettes. Yeast *21*, 947–962.

Jiang, B., Brown, J. L., Sheraton, J., Fortin, N., and Bussey, H. (1994). A new family of yeast genes implicated in ergosterol synthesis is related to the human oxysterol binding protein. Yeast Chichester Engl. *10*, 341–353.

Kaiser, S. E., Brickner, J. H., Reilein, A. R., Fenn, T. D., Walter, P., and Brunger, A. T. (2005). Structural basis of FFAT motif-mediated ER targeting. Struct. Lond. Engl. 1993 *13*, 1035–1045.

Kaksonen, M., Toret, C. P., and Drubin, D. G. (2005). A Modular Design for the Clathrin- and Actin-Mediated Endocytosis Machinery. Cell *123*, 305–320.

Kaksonen, M., Toret, C. P., and Drubin, D. G. (2006). Harnessing actin dynamics for clathrin-mediated endocytosis. Nat. Rev. Mol. Cell Biol. *7*, 404–414.

Kato, U., Emoto, K., Fredriksson, C., Nakamura, H., Ohta, A., Kobayashi, T., Murakami-Murofushi, K., Kobayashi, T., and Umeda, M. (2002). A Novel Membrane Protein, Ros3p, Is Required for Phospholipid

Translocation across the Plasma Membrane in Saccharomyces cerevisiae. J. Biol. Chem. *277*, 37855–37862.

Kattenhorn, L. M., Korbel, G. A., Kessler, B. M., Spooner, E., and Ploegh, H. L. (2005). A Deubiquitinating Enzyme Encoded by HSV-1 Belongs to a Family of Cysteine Proteases that Is Conserved across the Family Herpesviridae. Mol. Cell *19*, 547–557.

Kelley, M. J., Bailis, A. M., Henry, S. A., and Carman, G. M. (1988). Regulation of phospholipid biosynthesis in Saccharomyces cerevisiae by inositol. Inositol is an inhibitor of phosphatidylserine synthase activity. J. Biol. Chem. *263*, 18078–18085.

Bou Khalil, M., Hou, W., Zhou, H., Elisma, F., Swayne, L. A., Blanchard, A. P., Yao, Z., Bennett, S. A. L., and Figeys, D. (2010). Lipidomics era: Accomplishments and challenges. Mass Spectrom. Rev. *29*, 877–929.

Kim, Y. J., Hernandez, M.-L. G., and Balla, T. (2013). Inositol lipid regulation of lipid transfer in specialized membrane domains. Trends Cell Biol. *23*, 270–278.

Kirchhausen, T. (1999). Adaptors for Clathrin-Mediated Traffic. Annu. Rev. Cell Dev. Biol. *15*, 705–732.

Kishimoto, T., Yamamoto, T., and Tanaka, K. (2005). Defects in Structural Integrity of Ergosterol and the Cdc50p-Drs2p Putative Phospholipid Translocase Cause Accumulation of Endocytic Membranes, onto Which Actin Patches Are Assembled in Yeast. Mol. Biol. Cell *16*, 5592–5609.

Klemm, R. W. *et al.* (2009). Segregation of sphingolipids and sterols during formation of secretory vesicles at the trans-Golgi network. J. Cell Biol. *185*, 601–612.

Klose, C., Surma, M. A., Gerl, M. J., Meyenhofer, F., Shevchenko, A., and Simons, K. (2012). Flexibility of a Eukaryotic Lipidome – Insights from Yeast Lipidomics. PLoS ONE *7*, e35063.

Klug, L., and Daum, G. (2014). Yeast lipid metabolism at a glance. FEMS Yeast Res. *14*, 369–388.

Kuismanen, E., and Saraste, J. (1989). Low temperature-induced transport blocks as tools to manipulate membrane traffic. Methods Cell Biol. *32*, 257–274.

Kulathu, Y., Akutsu, M., Bremm, A., Hofmann, K., and Komander, D. (2009). Two-sided ubiquitin binding explains specificity of the TAB2 NZF domain. Nat. Struct. Mol. Biol. *16*, 1328–1330.

Lands, W. E. M. (1958). Metabolism of Glycerolipides: A Comparison of Lecithin and Triglyceride Synthesis. J. Biol. Chem. *231*, 883–888.

Lemmon, M. A. (2008). Membrane recognition by phospholipid-binding domains. Nat. Rev. Mol. Cell Biol. *9*, 99–111.

Lentz, B. R. (2003). Exposure of platelet membrane phosphatidylserine regulates blood coagulation. Prog. Lipid Res. *42*, 423–438.

Letourneur, F., Gaynor, E. C., Hennecke, S., Démollière, C., Duden, R., Emr, S. D., Riezman, H., and Cosson, P. (1994a). Coatomer is essential for retrieval of dilysine-tagged proteins to the endoplasmic reticulum. Cell *79*, 1199–1207.

Letourneur, F., Gaynor, E. C., Hennecke, S., Démollière, C., Duden, R., Emr, S. D., Riezman, H., and Cosson, P. (1994b). Coatomer is essential for retrieval of dilysine-tagged proteins to the endoplasmic reticulum. Cell *79*, 1199–1207.

Lev, S. (2010). Non-vesicular lipid transport by lipid-transfer proteins and beyond. Nat. Rev. Mol. Cell Biol. *11*, 739–750.

Levano, K., Punia, V., Raghunath, M., Debata, P. R., Curcio, G. M., Mogha, A., Purkayastha, S., McCloskey, D., Fata, J., and Banerjee, P. (2012). Atp8a1 deficiency is associated with phosphatidylserine externalization in hippocampus and delayed hippocampus-dependent learning. J. Neurochem. *120*, 302–313.

Levine, T. (2004). Short-range intracellular trafficking of small molecules across endoplasmic reticulum junctions. Trends Cell Biol. *14*, 483–490.

Levine, T. P., and Munro, S. (2002). Targeting of Golgi-specific pleckstrin homology domains involves both PtdIns 4-kinase-dependent and -independent components. Curr. Biol. CB *12*, 695–704.

Lewis, M. J., Nichols, B. J., Prescianotto-Baschong, C., Riezman, H., and Pelham, H. R. B. (2000). Specific Retrieval of the Exocytic SNARE Snc1p from Early Yeast Endosomes. Mol. Biol. Cell *11*, 23–38.

Li, H. *et al.* (2008). Candidate single-nucleotide polymorphisms from a genomewide association study of Alzheimer disease. Arch. Neurol. *65*, 45–53.

Li, X., Rivas, M. P., Fang, M., Marchena, J., Mehrotra, B., Chaudhary, A., Feng, L., Prestwich, G. D., and Bankaitis, V. A. (2002). Analysis of oxysterol binding protein homologue Kes1p function in regulation of Sec14p-dependent protein transport from the yeast Golgi complex. J. Cell Biol. *157*, 63–78.

Lin, C. H., MacGurn, J. A., Chu, T., Stefan, C. J., and Emr, S. D. (2008). Arrestin-related ubiquitin-ligase adaptors regulate endocytosis and protein turnover at the cell surface. Cell *135*, 714–725.

Liu, K., Hua, Z., Nepute, J. A., and Graham, T. R. (2007). Yeast P4-ATPases Drs2p and Dnf1p Are Essential Cargos of the NPFXD/Sla1p Endocytic Pathway. Mol. Biol. Cell *18*, 487–500.

Liu, K., Surendhran, K., Nothwehr, S. F., and Graham, T. R. (2008). P4-ATPase Requirement for AP-1/Clathrin Function in Protein Transport from the trans-Golgi Network and Early Endosomes. Mol. Biol. Cell *19*, 3526–3535.

Liu, Y., Kahn, R. A., and Prestegard, J. H. (2009). Structure and Membrane Interaction of Myristoylated ARF1. Struct. Lond. Engl. 1993 *17*, 79–87.

Loewen, C. J. R., Roy, A., and Levine, T. P. (2003). A conserved ER targeting motif in three families of lipid binding proteins and in Opi1p binds VAP. EMBO J. *22*, 2025–2035.

López-Marqués, R. L., Poulsen, L. R., Hanisch, S., Meffert, K., Buch-Pedersen, M. J., Jakobsen, M. K., Pomorski, T. G., and Palmgren, M. G. (2010). Intracellular targeting signals and lipid specificity determinants of the ALA/ALIS P4-ATPase complex reside in the catalytic ALA alpha-subunit. Mol. Biol. Cell *21*, 791–801.

Luo, W., and Chang, A. (2000). An Endosome-to-Plasma Membrane Pathway Involved in Trafficking of a Mutant Plasma Membrane ATPase in Yeast. Mol. Biol. Cell *11*, 579–592.

Lyssenko, N. N., Miteva, Y., Gilroy, S., Hanna-Rose, W., and Schlegel, R. A. (2008). An unexpectedly high degree of specialization and a widespread involvement in sterol metabolism among the C. elegans putative aminophospholipid translocases. BMC Dev. Biol. *8*, 96.

Ma, W., and Goldberg, J. (2013). Rules for the recognition of dilysine retrieval motifs by coatomer. EMBO J. *32*, 926–937.

Maeda, K., Anand, K., Chiapparino, A., Kumar, A., Poletto, M., Kaksonen, M., and Gavin, A.-C. (2013). Interactome map uncovers phosphatidylserine transport by oxysterol-binding proteins. Nature *501*, 257–261.

Malinska, K., Malinsky, J., Opekarova, M., and Tanner, W. (2004). Distribution of Can1p into stable domains reflects lateral protein segregation within the plasma membrane of living S. cerevisiae cells. J. Cell Sci. *117*, 6031–6041.

Malínská, K., Malínský, J., Opekarová, M., and Tanner, W. (2003). Visualization of protein compartmentation within the plasma membrane of living yeast cells. Mol. Biol. Cell *14*, 4427–4436.

Malinsky, J., Opekarová, M., Grossmann, G., and Tanner, W. (2013). Membrane Microdomains, Rafts, and Detergent-Resistant Membranes in Plants and Fungi. Annu. Rev. Plant Biol. *64*, 501–529.

Van der Mark, V., Elferink, R., and Paulusma, C. (2013). P4 ATPases: Flippases in Health and Disease. Int. J. Mol. Sci. *14*, 7897–7922.

Martin, C. E., Oh, C.-S., and Jiang, Y. (2007). Regulation of long chain unsaturated fatty acid synthesis in yeast. Biochim. Biophys. Acta BBA - Mol. Cell Biol. Lipids *1771*, 271–285.

Maxfield, F. R., and Wüstner, D. (2012). Analysis of cholesterol trafficking with fluorescent probes. Methods Cell Biol. *108*, 367–393.

McConnell, H. M., and Kornberg, R. D. (1971). Inside-outside transitions of phospholipids in vesicle membranes. Biochemistry (Mosc.) *10*, 1111–1120.

McIntosh, A. L., Atshaves, B. P., Huang, H., Gallegos, A. M., Kier, A. B., and Schroeder, F. (2008). Fluorescence Techniques Using Dehydroergosterol to Study Cholesterol Trafficking. Lipids *43*, 1185–1208.

Van Meer, G., Voelker, D. R., and Feigenson, G. W. (2008). Membrane lipids: where they are and how they behave. Nat. Rev. Mol. Cell Biol. *9*, 112–124.

Mercer, J., and Helenius, A. (2008). Vaccinia Virus Uses Macropinocytosis and Apoptotic Mimicry to Enter Host Cells. Science *320*, 531–535.

Mesmin, B., Bigay, J., Moser von Filseck, J., Lacas-Gervais, S., Drin, G., and Antonny, B. (2013). A Four-Step Cycle Driven by PI(4)P Hydrolysis Directs Sterol/PI(4)P Exchange by the ER-Golgi Tether OSBP. Cell *155*, 830–843.

Mikitova, V., and Levine, T. P. (2012). Analysis of the Key Elements of FFAT-Like Motifs Identifies New Proteins That Potentially Bind VAP on the ER, Including Two AKAPs and FAPP2. PLoS ONE *7*.

Milagro, F. I., Campión, J., Cordero, P., Goyenechea, E., Gómez-Uriz, A. M., Abete, I., Zulet, M. A., and Martínez, J. A. (2011). A dual epigenomic approach for the search of obesity biomarkers: DNA methylation in relation to diet-induced weight loss. FASEB J. Off. Publ. Fed. Am. Soc. Exp. Biol. *25*, 1378–1389.

Miyoshi, N., Ishii, H., Mimori, K., Tanaka, F., Nagai, K., Uemura, M., Sekimoto, M., Doki, Y., and Mori, M. (2010). ATP11A is a novel predictive marker for metachronous metastasis of colorectal cancer. Oncol. Rep. *23*, 505–510.

Moreira, K. E., Walther, T. C., Aguilar, P. S., and Walter, P. (2009). Pil1 Controls Eisosome Biogenesis. Mol. Biol. Cell *20*, 809–818.

Moser von Filseck, J., Vanni, S., Mesmin, B., Antonny, B., and Drin, G. (2015). A phosphatidylinositol-4-phosphate powered exchange mechanism to create a lipid gradient between membranes. Nat. Commun. *6*, 6671.

Mullally, J. E., Chernova, T., and Wilkinson, K. D. (2006). Doa1 Is a Cdc48 Adapter That Possesses a Novel Ubiquitin Binding Domain. Mol. Cell. Biol. *26*, 822–830.

Muthusamy, B.-P., Natarajan, P., Zhou, X., and Graham, T. R. (2009a). Linking phospholipid flippases to vesicle-mediated protein transport. Biochim. Biophys. Acta BBA - Mol. Cell Biol. Lipids *1791*, 612–619.

Muthusamy, B.-P., Raychaudhuri, S., Natarajan, P., Abe, F., Liu, K., Prinz, W. A., and Graham, T. R. (2009b). Control of Protein and Sterol Trafficking by Antagonistic Activities of a Type IV P-type ATPase and Oxysterol Binding Protein Homologue. Mol. Biol. Cell *20*, 2920–2931.

Nakagawa, Y., Sakumoto, N., Kaneko, Y., and Harashima, S. (2002). Mga2p is a putative sensor for low temperature and oxygen to induce OLE1 transcription in Saccharomyces cerevisiae. Biochem. Biophys. Res. Commun. *291*, 707–713.

Natarajan, P., and Graham, T. R. (2006). Measuring translocation of fluorescent lipid derivatives across yeast Golgi membranes. Methods San Diego Calif *39*, 163–168.

Natarajan, P., Liu, K., Patil, D. V., Sciorra, V. A., Jackson, C. L., and Graham, T. R. (2009). Regulation of a Golgi flippase by phosphoinositides and an ArfGEF. Nat. Cell Biol. *11*, 1421–1426.

Natarajan, P., Wang, J., Hua, Z., and Graham, T. R. (2004). Drs2p-coupled aminophospholipid translocase activity in yeast Golgi membranes and relationship to in vivo function. Proc. Natl. Acad. Sci. U. S. A. *101*, 10614–10619.

Newpher, T. M., Smith, R. P., Lemmon, V., and Lemmon, S. K. (2005). In Vivo Dynamics of Clathrin and Its Adaptor-Dependent Recruitment to the Actin-Based Endocytic Machinery in Yeast. Dev. Cell *9*, 87–98.

Nielsen, J. (2009). Systems biology of lipid metabolism: From yeast to human. FEBS Lett. *583*, 3905–3913.

Norman, A. W., Demel, R. A., Kruyff, B. de, and Deenen, L. L. M. van (1972). Studies on the Biological Properties of Polyene Antibiotics EVIDENCE FOR THE DIRECT INTERACTION OF FILIPIN WITH CHOLESTEROL. J. Biol. Chem. *247*, 1918–1929.

Novick, P., Ferro, S., and Schekman, R. (1981). Order of events in the yeast secretory pathway. Cell *25*, 461–469.

Obara, K., Miyashita, N., Xu, C., Toyoshima, I., Sugita, Y., Inesi, G., and Toyoshima, C. (2005). Structural role of countertransport revealed in Ca2+ pump crystal structure in the absence of Ca2+. Proc. Natl. Acad. Sci. U. S. A. *102*, 14489–14496.

Odorizzi, G., Babst, M., and Emr, S. D. (1998a). Fab1p PtdIns(3)P 5-Kinase Function Essential for Protein Sorting in the Multivesicular Body. Cell *95*, 847–858.

Odorizzi, G., Cowles, C. R., and Emr, S. D. (1998b). The AP-3 complex: a coat of many colours. Trends Cell Biol. *8*, 282–288.

Oh, C.-S., Toke, D. A., Mandala, S., and Martin, C. E. (1997). ELO2 and ELO3, Homologues of theSaccharomyces cerevisiae ELO1 Gene, Function in Fatty Acid Elongation and Are Required for Sphingolipid Formation. J. Biol. Chem. *272*, 17376–17384.

Olesen, C., Picard, M., Winther, A.-M. L., Gyrup, C., Morth, J. P., Oxvig, C., Møller, J. V., and Nissen, P. (2007). The structural basis of calcium transport by the calcium pump. Nature *450*, 1036–1042.

Olivera-Couto, A., and Aguilar, P. S. (2012). Eisosomes and plasma membrane organization. Mol. Genet. Genomics *287*, 607–620.

Opekarová, M., Malínská, K., Nováková, L., and Tanner, W. (2005). Differential effect of phosphatidylethanolamine depletion on raft proteins: Further evidence for diversity of rafts in Saccharomyces cerevisiae. Biochim. Biophys. Acta BBA - Biomembr. *1711*, 87–95.

Orci, L., Amherdt, M., Montesano, R., Vassalli, P., and Perrelet, A. (1981a). Topology of Morphologically Detectable Protein and Cholesterol in Membranes of Polypeptide-Secreting Cells. Philos. Trans. R. Soc. Lond. B Biol. Sci. *296*, 47–54.

Orci, L., Miller, R. G., Montesano, R., Perrelet, A., Amherdt, M., and Vassalli, P. (1980). Opposite Polarity of Filipin-Induced Deformations in the Membrane of Condensing Vacuoles and Zymogen Granules. Science *210*, 1019–1021.

Orci, L., Montesano, R., Meda, P., Malaisse-Lagae, F., Brown, D., Perrelet, A., and Vassalli, P. (1981b). Heterogeneous distribution of filipin--cholesterol complexes across the cisternae of the Golgi apparatus. Proc. Natl. Acad. Sci. U. S. A. *78*, 293–297.

Orcl, L., Tagaya, M., Amherdt, M., Perrelet, A., Donaldson, J. G., Lippincott-Schwartz, J., Klausner, R. D., and Rothman, J. E. (1991). Brefeldin A, a drug that blocks secretion, prevents the assembly of non-clathrin-coated buds on Golgi cisternae. Cell *64*, 1183–1195.

Palmgren, M. G., and Nissen, P. (2011). P-type ATPases. Annu. Rev. Biophys. *40*, 243–266.

Panek, H. R., Stepp, J. D., Engle, H. M., Marks, K. M., Tan, P. K., Lemmon, S. K., and Robinson, L. C. (1997). Suppressors of YCK-encoded yeast casein kinase 1 deficiency define the four subunits of a novel clathrin AP-like complex. EMBO J. *16*, 4194–4204.

Papanikou, E., and Glick, B. S. (2014). Golgi compartmentation and identity. Curr. Opin. Cell Biol. *29*, 74–81.

Pashkova, N., Gakhar, L., Winistorfer, S. C., Yu, L., Ramaswamy, S., and Piper, R. C. (2010). WD40 Repeat Propellers Define a Ubiquitin-Binding Domain that Regulates Turnover of F Box Proteins. Mol. Cell *40*, 433–443.

Paulusma, C. C. *et al.* (2006). Atp8b1 deficiency in mice reduces resistance of the canalicular membrane to hydrophobic bile salts and impairs bile salt transport. Hepatol. Baltim. Md *44*, 195–204.

Paulusma, C. C., Elferink, R. P. J. O., and Jansen, P. L. M. (2010). Progressive familial intrahepatic cholestasis type 1. Semin. Liver Dis. *30*, 117–124.

Paulusma, C. C., Folmer, D. E., Ho-Mok, K. S., de Waart, D. R., Hilarius, P. M., Verhoeven, A. J., and Oude Elferink, R. P. J. (2008). ATP8B1 requires an accessory protein for endoplasmic reticulum exit and plasma membrane lipid flippase activity. Hepatol. Baltim. Md *47*, 268–278.

Pawlikowska, L. *et al.* (2004). A mouse genetic model for familial cholestasis caused by ATP8B1 mutations reveals perturbed bile salt homeostasis but no impairment in bile secretion. Hum. Mol. Genet. *13*, 881–892.

Peng, J., Schwartz, D., Elias, J. E., Thoreen, C. C., Cheng, D., Marsischky, G., Roelofs, J., Finley, D., and Gygi, S. P. (2003). A proteomics approach to understanding protein ubiquitination. Nat. Biotechnol. *21*, 921–926.

Peyroche, A., Paris, S., and Jackson, C. L. (1996). Nucleotide exchange on ARF mediated by yeast Gea1 protein. Nature *384*, 479–481.

Pickart, C. M., and Fushman, D. (2004). Polyubiquitin chains: polymeric protein signals. Curr. Opin. Chem. Biol. *8*, 610–616.

Pokrzywa, W., Guerriat, B., Dodzian, J., and Morsomme, P. (2009). Dual Sorting of the Saccharomyces cerevisiae Vacuolar Protein Sna4p. Eukaryot. Cell *8*, 278–286.

Pomorski, T., Hrafnsdóttir, S., Devaux, P. F., and Meer, G. van (2001). Lipid distribution and transport across cellular membranes. Semin. Cell Dev. Biol. *12*, 139–148.

Pomorski, T., Lombardi, R., Riezman, H., Devaux, P. F., van Meer, G., and Holthuis, J. C. M. (2003). Drs2p-related P-type ATPases Dnf1p and Dnf2p Are Required for Phospholipid Translocation across the Yeast Plasma Membrane and Serve a Role in Endocytosis. Mol. Biol. Cell *14*, 1240–1254.

Popoff, V., Adolf, F., Brügger, B., and Wieland, F. (2011). COPI Budding within the Golgi Stack. Cold Spring Harb. Perspect. Biol.

Post, R. L., Kume, S., Tobin, T., Orcutt, B., and Sen, A. K. (1969). Flexibility of an Active Center in Sodium-Plus-Potassium Adenosine Triphosphatase. J. Gen. Physiol. *54*, 306–326.

Poulsen, L. R., López-Marqués, R. L., McDowell, S. C., Okkeri, J., Licht, D., Schulz, A., Pomorski, T., Harper, J. F., and Palmgren, M. G. (2008). The Arabidopsis P4-ATPase ALA3 localizes to the golgi and requires a beta-subunit to function in lipid translocation and secretory vesicle formation. Plant Cell *20*, 658–676.

Prosser, D. C., Whitworth, K., and Wendland, B. (2010). Quantitative Analysis of Endocytosis with Cytoplasmic pHluorin Chimeras. Traffic *11*, 1141–1150.

Proszynski, T. J. *et al.* (2005). A genome-wide visual screen reveals a role for sphingolipids and ergosterol in cell surface delivery in yeast. Proc. Natl. Acad. Sci. U. S. A. *102*, 17981–17986.

Protopopov, V., Govindan, B., Novick, P., and Gerst, J. E. (1993). Homologs of the synaptobrevin/VAMP family of synaptic vesicle proteins function on the late secretory pathway in S. cerevisiae. Cell *74*, 855–861.

Quazi, F., Lenevich, S., and Molday, R. S. (2012). ABCA4 is an N-retinylidene-phosphatidylethanolamine and phosphatidylethanolamine importer. Nat. Commun. *3*, 925.

Quazi, F., and Molday, R. S. (2013). Differential Phospholipid Substrates and Directional Transport by ATP-binding Cassette Proteins ABCA1, ABCA7, and ABCA4 and Disease-causing Mutants. J. Biol. Chem. *288*, 34414–34426.

Raghupathy, R. *et al.* (2015). Transbilayer Lipid Interactions Mediate Nanoclustering of Lipid-Anchored Proteins. Cell *161*, 581–594.

Ren, J., Pashkova, N., Winistorfer, S., and Piper, R. C. (2008). DOA1/UFD3 Plays a Role in Sorting Ubiquitinated Membrane Proteins into Multivesicular Bodies. J. Biol. Chem. *283*, 21599–21611.

Riekhof, W. R., Wu, J., Gijón, M. A., Zarini, S., Murphy, R. C., and Voelker, D. R. (2007). Lysophosphatidylcholine Metabolism in Saccharomyces cerevisiae THE ROLE OF P-TYPE ATPases IN TRANSPORT AND A BROAD SPECIFICITY ACYLTRANSFERASE IN ACYLATION. J. Biol. Chem. *282*, 36853–36861.

Riezman, H. (2006). Organization and functions of sphingolipid biosynthesis in yeast. Biochem. Soc. Trans. *34*, 367–369.

Robinson, M. S. (2004). Adaptable adaptors for coated vesicles. Trends Cell Biol. *14*, 167–174.

Rodríguez-Vargas, S., Sánchez-García, A., Martínez-Rivas, J. M., Prieto, J. A., and Randez-Gil, F. (2007). Fluidization of Membrane Lipids Enhances the Tolerance of Saccharomyces cerevisiae to Freezing and Salt Stress. Appl. Environ. Microbiol. *73*, 110–116.

Roux, A., Cuvelier, D., Nassoy, P., Prost, J., Bassereau, P., and Goud, B. (2005). Role of curvature and phase transition in lipid sorting and fission of membrane tubules. EMBO J. *24*, 1537–1545.

Ryu, Y.-S. *et al.* (2014). Reconstituting ring-rafts in bud-mimicking topography of model membranes. Nat. Commun. *5*, 4507.

Sahu, S. K., Gummadi, S. N., Manoj, N., and Aradhyam, G. K. (2007). Phospholipid scramblases: An overview. Arch. Biochem. Biophys. *462*, 103–114.

Saint-Jean, M. de, Delfosse, V., Douguet, D., Chicanne, G., Payrastre, B., Bourguet, W., Antonny, B., and Drin, G. (2011). Osh4p exchanges sterols for phosphatidylinositol 4-phosphate between lipid bilayers. J. Cell Biol. *195*, 965–978.

Saito, K., Fujimura-Kamada, K., Furuta, N., Kato, U., Umeda, M., and Tanaka, K. (2004). Cdc50p, a Protein Required for Polarized Growth, Associates with the Drs2p P-Type ATPase Implicated in Phospholipid Translocation in Saccharomyces cerevisiae. Mol. Biol. Cell *15*, 3418–3432.

Santos, A. X. da S. dos, Riezman, I., Aguilera-Romero, M.-A., David, F., Piccolis, M., Loewith, R., Schaad, O., and Riezman, H. (2014). Systematic lipidomic analysis of yeast protein kinase and phosphatase mutants reveals novel insights into regulation of lipid homeostasis. Mol. Biol. Cell *25*, 3234–3246.

Santos, A. X. S., and Riezman, H. (2012). Yeast as a model system for studying lipid homeostasis and function. FEBS Lett. *586*, 2858–2867.

Sanyal, S., Frank, C. G., and Menon, A. K. (2008). Distinct Flippases Translocate Glycerophospholipids and Oligosaccharide Diphosphate Dolichols across the Endoplasmic Reticulum†. Biochemistry (Mosc.) *47*, 7937–7946.

Saraste, J., Palade, G. E., and Farquhar, M. G. (1986). Temperature-sensitive steps in the transport of secretory proteins through the Golgi complex in exocrine pancreatic cells. Proc. Natl. Acad. Sci. U. S. A. *83*, 6425–6429.

Sato, K., Sato, M., and Nakano, A. (2001). Rer1p, a Retrieval Receptor for Endoplasmic Reticulum Membrane Proteins, Is Dynamically Localized to the Golgi Apparatus by Coatomer. J. Cell Biol. *152*, 935–944.

Sato, Y., Yoshikawa, A., Yamashita, M., Yamagata, A., and Fukai, S. (2009). Structural basis for specific recognition of Lys 63-linked polyubiquitin chains by NZF domains of TAB2 and TAB3. EMBO J. *28*, 3903–3909.

Schekman, R. (2002). SEC mutants and the secretory apparatus. Nat. Med. *8*, 1055–1058.

Schorling, S., Vallée, B., Barz, W. P., Riezman, H., and Oesterhelt, D. (2001). Lag1p and Lac1p Are Essential for the Acyl-CoA–dependent Ceramide Synthase Reaction in Saccharomyces cerevisae. Mol. Biol. Cell *12*, 3417–3427.

Schröder, S., Schimmöller, F., Singer-Krüger, B., and Riezman, H. (1995). The Golgi-localization of yeast Emp47p depends on its di-lysine motif but is not affected by the ret1-1 mutation in alpha-COP. J. Cell Biol. *131*, 895–912.

Scott, P. M., Bilodeau, P. S., Zhdankina, O., Winistorfer, S. C., Hauglund, M. J., Allaman, M. M., Kearney, W. R., Robertson, A. D., Boman, A. L., and Piper, R. C. (2004). GGA proteins bind ubiquitin to facilitate sorting at the trans-Golgi network. Nat. Cell Biol. *6*, 252–259.

Sebastian, T. T., Baldridge, R. D., Xu, P., and Graham, T. R. (2012). Phospholipid flippases: building asymmetric membranes and transport vesicles. Biochim. Biophys. Acta *1821*, 1068–1077.

Seigneuret, M., and Devaux, P. F. (1984). ATP-dependent asymmetric distribution of spin-labeled phospholipids in the erythrocyte membrane: relation to shape changes. Proc. Natl. Acad. Sci. U. S. A. *81*, 3751–3755.

Sette, P., Nagashima, K., Piper, R. C., and Bouamr, F. (2013). Ubiquitin conjugation to Gag is essential for ESCRT-mediated HIV-1 budding. Retrovirology *10*, 79.

Shaw, J. A., Mol, P. C., Bowers, B., Silverman, S. J., Valdivieso, M. H., Durán, A., and Cabib, E. (1991). The function of chitin synthases 2 and 3 in the Saccharomyces cerevisiae cell cycle. J. Cell Biol. *114*, 111–123.

Sheetz, M. P., and Singer, S. J. (1974). Biological membranes as bilayer couples. A molecular mechanism of drug-erythrocyte interactions. Proc. Natl. Acad. Sci. U. S. A. *71*, 4457–4461.

Shih, S. C., Sloper-Mould, K. E., and Hicke, L. (2000). Monoubiquitin carries a novel internalization signal that is appended to activated receptors. EMBO J. *19*, 187–198.

Shindou, H., Hishikawa, D., Harayama, T., Yuki, K., and Shimizu, T. (2009). Recent progress on acyl CoA: lysophospholipid acyltransferase research. J. Lipid Res. *50*, S46–S51.

Shinoda, T., Ogawa, H., Cornelius, F., and Toyoshima, C. (2009). Crystal structure of the sodium–potassium pump at 2.4 Å resolution. Nature *459*, 446–450.

Sigal, C. T., Zhou, W., Buser, C. A., McLaughlin, S., and Resh, M. D. (1994). Amino-terminal basic residues of Src mediate membrane binding through electrostatic interaction with acidic phospholipids. Proc. Natl. Acad. Sci. U. S. A. *91*, 12253–12257.

Siggs, O. M., Arnold, C. N., Huber, C., Pirie, E., Xia, Y., Lin, P., Nemazee, D., and Beutler, B. (2011a). The P4-type ATPase ATP11C is essential for B lymphopoiesis in adult bone marrow. Nat. Immunol. *12*, 434–440.

Siggs, O. M., Schnabl, B., Webb, B., and Beutler, B. (2011b). X-linked cholestasis in mouse due to mutations of the P4-ATPase ATP11C. Proc. Natl. Acad. Sci. *108*, 7890–7895.

Sikorski, R. S., and Hieter, P. (1989). A system of shuttle vectors and yeast host strains designed for efficient manipulation of DNA in Saccharomyces cerevisiae. Genetics *122*, 19–27.

Silva, G. M., Finley, D., and Vogel, C. (2015). K63 polyubiquitination is a new modulator of the oxidative stress response. Nat. Struct. Mol. Biol. *22*, 116–123.

Simons, K., and Ikonen, E. (1997). Functional rafts in cell membranes. Nature *387*, 569–572.

Simons, K., and van Meer, G. (1988). Lipid sorting in epithelial cells. Biochemistry (Mosc.) *27*, 6197–6202.

Singer, S. J., and Nicolson, G. L. (1972). The fluid mosaic model of the structure of cell membranes. Science *175*, 720–731.

Skou, J. C. (1957). The influence of some cations on an adenosine triphosphatase from peripheral nerves. Biochim. Biophys. Acta *23*, 394–401.

Sorre, B., Callan-Jones, A., Manneville, J.-B., Nassoy, P., Joanny, J.-F., Prost, J., Goud, B., and Bassereau, P. (2009). Curvature-driven lipid sorting needs proximity to a demixing point and is aided by proteins. Proc. Natl. Acad. Sci. *106*, 5622–5626.

Spence, J., Sadis, S., Haas, A. L., and Finley, D. (1995). A ubiquitin mutant with specific defects in DNA repair and multiubiquitination. Mol. Cell. Biol. *15*, 1265–1273.

Spira, F., Mueller, N. S., Beck, G., von Olshausen, P., Beig, J., and Wedlich-Söldner, R. (2012). Patchwork organization of the yeast plasma membrane into numerous coexisting domains. Nat. Cell Biol. *14*, 640–648.

Stahelin, R. V., Scott, J. L., and Frick, C. T. (2014). CELLULAR AND MOLECULAR INTERACTIONS OF PHOSPHOINOSITIDES AND PERIPHERAL PROTEINS. Chem. Phys. Lipids *182*, 3–18.

Stapelbroek, J. M. *et al.* (2009). ATP8B1 is essential for maintaining normal hearing. Proc. Natl. Acad. Sci. U. S. A. *106*, 9709–9714.

Stefan, C. J., Manford, A. G., Baird, D., Yamada-Hanff, J., Mao, Y., and Emr, S. D. (2011). Osh Proteins Regulate Phosphoinositide Metabolism at ER-Plasma Membrane Contact Sites. Cell *144*, 389–401.

Stone, A., and Williamson, P. (2012). Outside of the box: recent news about phospholipid translocation by P4 ATPases. J. Chem. Biol. *5*, 131–136.

Strádalová, V., Stahlschmidt, W., Grossmann, G., Blažíková, M., Rachel, R., Tanner, W., and Malinsky, J. (2009). Furrow-like invaginations of the yeast plasma membrane correspond to membrane compartment of Can1. J. Cell Sci. *122*, 2887–2894.

Stringer, D. K., and Piper, R. C. (2011). A single ubiquitin is sufficient for cargo protein entry into MVBs in the absence of ESCRT ubiquitination. J. Cell Biol. *192*, 229–242.

Stukey, J. E., McDonough, V. M., and Martin, C. E. (1989). Isolation and characterization of OLE1, a gene affecting fatty acid desaturation from Saccharomyces cerevisiae. J. Biol. Chem. *264*, 16537–16544.

Surma, M. A., Klose, C., and Simons, K. (2012). Lipid-dependent protein sorting at the trans-Golgi network. Biochim. Biophys. Acta BBA - Mol. Cell Biol. Lipids *1821*, 1059–1067.

Suzuki, J., Denning, D. P., Imanishi, E., Horvitz, H. R., and Nagata, S. (2013). Xk-Related Protein 8 and CED-8 Promote Phosphatidylserine Exposure in Apoptotic Cells. Science *341*, 403–406.

Takahashi, Y., Fujimura-Kamada, K., Kondo, S., and Tanaka, K. (2011). Isolation and characterization of novel mutations in CDC50, the non-catalytic subunit of the Drs2p phospholipid flippase. J. Biochem. (Tokyo) *149*, 423–432.

Takatsu, H., Baba, K., Shima, T., Umino, H., Kato, U., Umeda, M., Nakayama, K., and Shin, H.-W. (2011). ATP9B, a P4-ATPase (a Putative Aminophospholipid Translocase), Localizes to the trans-Golgi Network in a CDC50 Protein-independent Manner. J. Biol. Chem. *286*, 38159–38167.

Tanaka, K., Fujimura-Kamada, K., and Yamamoto, T. (2011). Functions of phospholipid flippases. J. Biochem. (Tokyo) *149*, 131–143.

Tang, X., Halleck, M. S., Schlegel, R. A., and Williamson, P. (1996). A subfamily of P-type ATPases with aminophospholipid transporting activity. Science *272*, 1495–1497.

Tehlivets, O., Scheuringer, K., and Kohlwein, S. D. (2007). Fatty acid synthesis and elongation in yeast. Biochim. Biophys. Acta BBA - Mol. Cell Biol. Lipids *1771*, 255–270.

Toyoshima, C. (2008). Structural aspects of ion pumping by Ca2+-ATPase of sarcoplasmic reticulum. Arch. Biochem. Biophys. *476*, 3–11.

Toyoshima, C., Nakasako, M., Nomura, H., and Ogawa, H. (2000). Crystal structure of the calcium pump of sarcoplasmic reticulum at 2.6 |[angst]| resolution. Nature *405*, 647–655.

Umebayashi, K., and Nakano, A. (2003). Ergosterol is required for targeting of tryptophan permease to the yeast plasma membrane. J. Cell Biol. *161*, 1117–1131.

Valdivia, R. H., Baggott, D., Chuang, J. S., and Schekman, R. W. (2002). The Yeast Clathrin Adaptor Protein Complex 1 Is Required for the Efficient Retention of a Subset of Late Golgi Membrane Proteins. Dev. Cell *2*, 283–294.

Varadan, R., Assfalg, M., Haririnia, A., Raasi, S., Pickart, C., and Fushman, D. (2004). Solution Conformation of Lys63-linked Di-ubiquitin Chain Provides Clues to Functional Diversity of Polyubiquitin Signaling. J. Biol. Chem. *279*, 7055–7063.

Vestergaard, A. L., Coleman, J. A., Lemmin, T., Mikkelsen, S. A., Molday, L. L., Vilsen, B., Molday, R. S., Peraro, M. D., and Andersen, J. P. (2014). Critical roles of isoleucine-364 and adjacent residues in a hydrophobic gate control of phospholipid transport by the mammalian P4-ATPase ATP8A2. Proc. Natl. Acad. Sci., 201321165.

Vilsen, B., and Andersen, J. P. (1998). Mutation to the Glutamate in the Fourth Membrane Segment of Na+,K+-ATPase and Ca2+-ATPase Affects Cation Binding from Both Sides of the Membrane and Destabilizes the Occluded Enzyme Forms†. Biochemistry (Mosc.) *37*, 10961–10971.

Voelker, D. R. (1990). Lipid transport pathways in mammalian cells. Experientia *46*, 569–579.

Voelker, D. R. (2003). New perspectives on the regulation of intermembrane glycerophospholipid traffic. J. Lipid Res. *44*, 441–449.

Wang, L., Beserra, C., and Garbers, D. L. (2004). A novel aminophospholipid transporter exclusively expressed in spermatozoa is required for membrane lipid asymmetry and normal fertilization. Dev. Biol. *267*, 203–215.

Whitney, J. A., Gomez, M., Sheff, D., Kreis, T. E., and Mellman, I. (1995). Cytoplasmic coat proteins involved in endosome function. Cell *83*, 703–713.

Wiederkehr, A., Avaro, S., Prescianotto-Baschong, C., Haguenauer-Tsapis, R., and Riezman, H. (2000). The F-Box Protein Rcy1p Is Involved in Endocytic Membrane Traffic and Recycling Out of an Early Endosome in Saccharomyces cerevisiae. J. Cell Biol. *149*, 397–410.

Williamson, P., and Schlegel, R. A. (2002). Transbilayer phospholipid movement and the clearance of apoptotic cells. Biochim. Biophys. Acta *1585*, 53–63.

Xu, P., Baldridge, R. D., Chi, R. J., Burd, C. G., and Graham, T. R. (2013). Phosphatidylserine flipping enhances membrane curvature and negative charge required for vesicular transport. J. Cell Biol. *202*, 875–886.

Xu, P., Duong, D. M., Seyfried, N. T., Cheng, D., Xie, Y., Robert, J., Rush, J., Hochstrasser, M., Finley, D., and Peng, J. (2009). Quantitative proteomics reveals the function of unconventional ubiquitin chains in proteasomal degradation. Cell *137*, 133–145.

Yabas, M. *et al.* (2011). ATP11C is critical for the internalization of phosphatidylserine and differentiation of B lymphocytes. Nat. Immunol. *12*, 441–449.

Yetukuri, L., Ekroos, K., Vidal-Puig, A., and Orešič, M. (2008). Informatics and computational strategies for the study of lipids. Mol. Biosyst. *4*, 121–127.

Yeung, B. G., Phan, H. L., and Payne, G. S. (1999). Adaptor Complex-independent Clathrin Function in Yeast. Mol. Biol. Cell *10*, 3643–3659.

Yeung, T., Gilbert, G. E., Shi, J., Silvius, J., Kapus, A., and Grinstein, S. (2008). Membrane Phosphatidylserine Regulates Surface Charge and Protein Localization. Science *319*, 210–213.

Zachowski, A. (1993). Phospholipids in animal eukaryotic membranes: transverse asymmetry and movement. Biochem. J. *294*, 1–14.

Zhou, X., and Graham, T. R. (2009). Reconstitution of phospholipid translocase activity with purified Drs2p, a type-IV P-type ATPase from budding yeast. Proc. Natl. Acad. Sci. *106*, 16586–16591.

Zhou, X., Sebastian, T. T., and Graham, T. R. (2013). Auto-inhibition of Drs2p, a yeast phospholipid flippase, by its carboxyl-terminal tail. J. Biol. Chem. *288*, 31807–31815.

Zhu, X., Libby, R. T., de Vries, W. N., Smith, R. S., Wright, D. L., Bronson, R. T., Seburn, K. L., and John, S. W. M. (2012). Mutations in a P-type ATPase gene cause axonal degeneration. PLoS Genet. *8*, e1002853.

Zilversmit, D. B. (1983). Lipid transfer proteins: overview and applications. Methods Enzymol. *98*, 565–573.

Zinser, E., Paltauf, F., and Daum, G. (1993). Sterol composition of yeast organelle membranes and subcellular distribution of enzymes involved in sterol metabolism. J. Bacteriol. *175*, 2853–2858.

Zinser, E., Sperka-Gottlieb, C. D., Fasch, E. V., Kohlwein, S. D., Paltauf, F., and Daum, G. (1991). Phospholipid synthesis and lipid composition of subcellular membranes in the unicellular eukaryote Saccharomyces cerevisiae. J. Bacteriol. *173*, 2026–2034.

Ziółkowska, N. E., Christiano, R., and Walther, T. C. (2012). Organized living: formation mechanisms and functions of plasma membrane domains in yeast. Trends Cell Biol. *22*, 151–158.

Zwaal, R. F., and Schroit, A. J. (1997). Pathophysiologic implications of membrane phospholipid asymmetry in blood cells. Blood *89*, 1121–1132.

(2001). Phosphatidylserine, a death knell. Publ. Online 01 June 2001 Doi101038sjcdd4400817 *8*.